"Seasonal characterization of ablation, storage and drainage of melt runoff and simulation of streamflow for the Gangotri Glacier"

Project duration : January 2005 - March 2008

National Institute of Hydrology
Jalvigyan Bhawan
Roorkee - 247 667 (Uttarakhand)

PREFACE

Most of the large rivers of the world originate from the alpine and high mountainous areas. Upper catchments of these rivers are usually covered by snow and glaciers which supply at least one third of the water used for meeting irrigation and other demands in the world. In South Asia, snowmelt from the Himalayas provides a significant contribution to the Himalayan river system. In the northern part of India, the major river systems, namely Indus, Ganga and Brahamaputra which contribute a large part of India's water resources, originate from Himalayas. Over 600,000 km^2 area in the Himalayas is snowbound during winter season including the land of glaciers. During the ablation season, the snow and glacier melt provide main source of water for meeting the various demands. There is a tremendous pressure on the availability of the fresh water because of increasing demands in different sectors due to rapid increase in population. As the snow and glaciers are the major sources of fresh water, it is therefore required to carry out the scientific studies of the snow and glacier fed river systems to ensure the availability of fresh water for meeting the future demands.

National Institute of Hydrology, Roorkee has been actively involved in carrying out R & D studies in the area of snow and glacier hydrology. So far the Institute has carried out a number of scientific studies which includes the hydrological investigation & modelling studies for Dokriani Glacier and Gangotri Glacier. (U.A). The Dokriani Glacier was studied extensively for 4 years (1995-1998) under a research project funded by Department of Science and Technology (DST), Govt. of India, New Delhi. DST sponsored Gangotri Glacier project has been taken up by NIH in two different phases. During the first phase from the year 1999-2003, NIH monitored the hydrological and meteorological variables. However, in the second phase from the year December 2005 to March 2008, scope of the study has been extended to the hydrological modelling and applications of nuclear techniques in addition to the regular monitoring during the ablation season.

The project activities were planned under the guidance of Shri R. D. Singh Scientist F and Head, Surface water Hydrology Division and executed by Dr. Pratap Singh and Dr. Manohar Arora, Scientist Surface water hydrology division. During the first two years, Dr. Pratap Singh Scientist E II, Surface Water Hydrology Division was the Principal Investigator of the project. However, in the third year, Dr. Manohar Arora Scientist B, Surface Water Hydrology Division was nominated as the Principal

Investigator for the project as Dr. Pratap Singh resigned and left the Institute. The other scientists and staff of the Institute who have been actively involved during the project include Dr. S. P. Rai, Scientist C, Shri Naresh Kumar, PRA, Shri Yatveer Singh, SRA, Shri Hukam Singh SRA, Shri N K Bhatnagar SRA and Shri R K Nema SRA. In addition to this, project staff appointed under the project also participated in the field oriented R & D studies. I hope that the results of the project would be very much useful for the sustainable development and management of the water resources projects in the Himalayan region in general and for the Bhagirathi/Ganga River Basin in particular. There is a need to carry out the long-term studies which will enhance the knowledge about the melting pattern of the Himalayan glaciers and provide the capabilities of the hydrological models for simulating the runoff within the desirable accuracy.

April 30, 2008
Roorkee

(K. D. Sharma)
Director

SUMMARY

In the Indian territory of Himalayas, there are about 10,000 glaciers covering an area about 38,000 km^2. These glaciers contribute significantly to the flows of the rivers, originating from the Himalayas particularly during summer months. An accurate assessment of the flows resulting due to melt along with its distribution in time is vital for the planning and management of water resources projects. The present study deals with hydrological analysis of the hydrological and hydro-meteorological data of Gangotri Glacier under a project funded by Department of Science and Technology, Govt. of India, New Delhi for a period from December 2005 to March 2008. The Gangotri Glacier is one of the largest glaciers of Himalayas. The total catchment area of the study basin up to Bhojwasa gauging site is about 556 km^2, out of which 286 km^2 is usually covered by snow and ice. Bhagirathi River originates from the snout of Gangotri Glacier.

In order to achieve the objectives of the project, National Institute of Hydrology (NIH) established a meteorological observatory and a gauging site near the snout of the Gangotri Glacier and monitored the different types of hydrological and hydro-meteorological data during the ablation season. Rainfall, temperature, humidity, wind speed and direction, sunshine hours and evaporation data have been collected for three years during the ablation period (May-October). Gauge observations are taken round the clock at the gauging site with the help of automatic water level recorder. Wooden floats were used to compute the velocity of flow and the time travelled by the floats was recorded. The cross-section area of the channel was determined with the help of sounding rods in the beginning of the season and was rechecked at the end of the season before closing the investigations. For measurement of discharge, velocity-area method was used to estimate the flow in the river. Samples of suspended sediment were also collected at the gauging site and concentration of suspended sediment is determined.

The analysis of rainfall data shows that the temporal distribution and amount of rainfall varied significantly from year to year. Average ablation season rainfall (May-October) over three years is 260 mm. Most of the time light intensity rain (0.1-0.55 mm/hr) occurred in the study area. Mean monthly temperatures for May, June, July, August, September and October were 13.9, 16.3, 15.9, 15.7, 14.4 and 12.0°C, respectively, indicating that June is the warmest month. Average daily maximum and minimum temperatures over the ablation season are observed to be 14.9 °C

and 3.7 °C, respectively. Day-time wind speed is observed to be about 4 times stronger than the night-time wind speed. Mean daily sunshine hours is estimated to be 5.5 hours. Monthly pan evaporation values are 81.5, 119.0, 92.7, 91.4, 81.6 and 44.4 mm for the month of May, June, July, August, September and October, respectively. The total pan evaporation values during the ablation season vary between 492 and 521 mm. Observed meteorological conditions represent dry weather conditions in the study area.

The observed mean daily discharge ranged between 8 to 239 m^3/s. The mean monthly discharge observed for May, June, July, August, September and October are 28.7, 56.3, 110.9, 95.8, 34.8 and 12.7 m^3/s, respectively. From the temporal distribution of observed discharge, it is found that the maximum discharge is usually in the month of July followed by August. The months of July and August contributed about 63% to the total discharge of the ablation season. The strong storage characteristics of the Gangotri Glacier are reflected by the comparable magnitude of discharge observed during day-time and night-time. Mean monthly suspended sediment concentration for May, June, July, August, September and October during the study period are 1628, 1753, 3262, 2231, 892 and 225 ppm respectively. Mean monthly suspended sediment load for corresponding months are found to be 162, 220, 1016, 603, 81 and 5×10^3 tonnes respectively. The relationship between discharge and suspended sediment concentration/load has been investigated.

In order to simulate the streamflow, a simple conceptual hydrological model based on temperature index approach has been applied to simulate observed discharge at the gauging site of the Gangotri glacier. The routing of the melt water as well as rainfall contribution is carried out considering a cascade of linear reservoirs. The model has simulated daily streamflow satisfactorily for all the years. The average coefficient of determination (R^2) is about 0.92 and average difference in computed and observed volume of discharge is about 1.8%. Isotopic investigations of precipitation and stream water of Bhagirathi at Gomukh reveal the melting pattern of snow and glacier with time. The results also reveal the contribution of rain to stream at discharge measuring site.

CONTENTS

	List of Figures	iii
	List of Plates	vi
	List of Tables	vii
1.0	INTRODUCTION	1
	1.1 Importance of the Himalayas	2
2.0	HIMALAYAS	4
	2.1 Physical Features	4
	2.2 Himalayas Physiography	4
	2.3 Physical features of Himalayas	6
	2.4 Resources	9
3.0	OBJECTIVES OF THE PROJECT	11
4.0	STUDY AREA	12
	4.1 Location and Accessibility	12
	4.2 Gangotri Glacier System	12
	4.3 Geology	17
	4.4 Flora and Fauna	17
5.0	LITERATURE REVIEW	22
6.0	DATA COLLECTION PERIOD	25
7.0	MONITORING AND ANALYSIS OF METEROLOGICAL DATA	26
	7.1 Meteorological parameters monitoring	26
	7.2 Precipitation	29
	7.3 Air temperature	33
	7.4 Wind Speed and Direction	34
	7.5 Relative Humidity	40
	7.6 Sunshine Hour	41
	7.1 Evaporation	41
8.0	MONITORING OF RIVER GAUGE AND DISCHARGE DATA AND ITS ANALYSIS	43
8.1	Measurement of gauge and discharge data and development of stage discharge curve	43
8.2	Distribution of Streamflow and Water Yield	46
8.3	Melt Water Storage Drainage Characteristic of Gangotri Glacier	48
8.4	Diurnal Variations	50
8.5	Melt-Runoff Delaying Characteristics: time-lag and time to peak	51

9.0	SUSPENDED SEDIMENT DATA COLLECTION AND ANALYSIS	55
	9.1 Sources of Sediment	55
	9.2 Suspended Sediment Concentration (SSC)	56
	9.3 Suspended Sediment Load and Yield	58
	9.4 Diurnal Variations in SSC	60
	9.5 Particle Size Distribution	61
10.0	APPLICATION OF HYDROLOGICAL MODEL FOR THE GLACIERIZED BASIN	64
	10.1 Concept and Structure of the Model	64
	10.2 Input Data	65
	10.3 Division of Basin into Elevation Zones	65
	10.4 Precipitation	65
	10.5 Melt, Temperature and Degree-days	67
	10.6 Glaciated Area, Snow Covered Area and Snow Depletion Curves	68
	10.7 Rain on Snow / Ice	69
	10.8 Computation of Different Components of Runoff	70
	10.9 Routing of Different Components of Runoff	73
11.0	SIMULATION OF DAILY FLOW AT BHOJWASA SITE OF GANGOTRI GLACIER	78
	11.1 Data processing and data preparation	78
12.0	ISOTOPIC INVESTIGATION OF GANGOTRI GLACIER	85
	12.1 Introduction	85
	12.2 Basic Information about Isotopes	86
	12.3 Methodology	87
	12.4 Result and Discussion	91
13.0	DISCUSSION OF RESULTS AND CONCLUSIONS	103
14.0	RECOMMENDATIONS & SUGGESTIONS FOR FURTHER WORKS	107
15.0	PUBLICATIONS	109
16.0	REFERENCES	110
	ACKNOWLEDGEMENTS	114
	APPENDIX	115

LIST OF FIGURES

Figure1 : Location map of the study area.

Figure 2 : Satellite view of Gangotri Glacier captured from LISS-III- P6 images.

Figure 3 : (a) Daily rainfall, and (b) monthly rainfall observed for different months near the snout of Gangotri Glacier during different summer seasons.

Figure 4 : (a) Frequency distribution of hourly rainfall, and (b) range of hourly rainfall observed near the snout of Gangotri Glacier.

Figure 5 : Diurnal variation in mean rainfall intensity (bar and left side axis) and total number of rainfall events (continuous line and right side axis) for different months observed near the snout of the Gangotri Glacier.

Figure 6 : (a) Daily maximum and minimum air temperatures, and (b) daily mean temperature observed near the snout of Gangotri Glacier during different summer seasons.

Figure 7 : (a) Daily daytime (0830-1730 hours) and nighttime (1730-0830 hours) wind speeds, and (b) daily mean wind speed (0830-0830 hours) observed near the snout of Gangotri Glacier during different summer seasons.

Figure 8 : (a) Wind speed (km/hr) and direction observed at 08.30, 11.30, 14.30 and 17.30 hours near the snout of Gangotri Glacier during summer season 2000.

Figure 8 : (b) Wind speed (km/hr) and direction observed at 08.30, 11.30, 14.30 and 17.30 hours near the snout of Gangotri Glacier during summer season 2001.

Figure 8 : (c) Wind speed (km/hr) and direction observed at 08.30, 11.30, 14.30 and 17.30 hours near the snout of Gangotri Glacier during summer season 2002.

Figure 8 : (d) Wind speed (km/hr) and direction observed at 08.30, 11.30, 14.30 and 17.30 hours near the snout of Gangotri Glacier during summer season 2003.

Figure 9 : Diurnal variations in wind speed observed near the snout of Gangotri Glacier during different summer seasons.

Figure 10 : (a) Daily mean relative humidity (b) sunshine hours, and (c) evaporation observed for different months near the snout of

Gangotri Glacier during different summer seasons.

Figure 11 : Stage-discharge relationship established for the gauging site at Gangotri Glacier melt stream for the year 2003.

Figure 12 : (a) Daily mean discharge, and (b) monthly discharge observed for different months near the snout of Gangotri Glacier during different summer seasons.

Figure 13 : (a) Daily rainfall and (b) Daytime (0900-2000 hours) and nighttime (2100-0800 hours) mean discharge observed for different months near the snout of Gangotri Glacier during different summer seasons.

Figure 14 : Monthly distribution of daytime (0900-2000 hours) and nighttime (2100-0800 hours) discharge observed for different months near the snout of Gangotri Glacier during different summer seasons.

Figure 15 : Diurnal variations in the discharge observed near the snout of the Gangotri Glacier for selected clear weather days during ablation period 2005, 2006 and 2007.

Figure 16 : (a) Melt-runoff time-lag (b) time to peak, and (c) discharge ratio for selected clear weather days during summer 2005, 2006 and 2007 at the gauging site.

Figure 17 : (a) Daily mean suspended sediment concentration (SSC), and (b) mean monthly SSC observed for different months near the snout of Gangotri Glacier during different summer seasons.

Figure 18 : (a) Daily mean suspended sediment load (SSL), and (b) mean monthly total SSL observed for different months near the snout of Gangotri Glacier during different summer seasons.

Figure 19 : Diurnal variability in suspended sediment concentration (SSC) observed near the snout of the Gangotri Glacier for selected clear weather days during ablation period 2005, 2006 and 2007.

Figure 20 : Particle size distribution of the suspended sediment observed near the snout of Gangotri Glacier during summer season 2005, 2006 and 2007

Figure 21 : Particle size distribution of the suspended sediment observed near the snout of Gangotri Glacier during summer season three ablation seasons (2005-2007)

Figure 22 : Flow chart of the developed conceptual hydrological model for the Glacierized basin.

Figure 23 : Comparison of observed and simulated discharge for the calibration year 2005 for the Gangotri Glacier.
Figure 24 : Different components of simulated runoff for summer season 2005 for the Gangotri Glacier.
Figure 25 : Different components of simulated runoff for summer season 2006 for the Gangotri Glacier.
Figure 26 : Different components of simulated runoff for summer season 2007 for the Gangotri Glacier.
Figure 27 : Variation of $\delta^{18}O$ values in precipitation during ablation period in year 2004-2007.
Figure 28 : Isotopic composition of premonsoon and monsoon precipitation.
Figure 29 : Meteoric Water Line for Bhagirathi river at Gomukh based on 2004-2007 data.
Figure 30 : $\delta^{18}O$ and δD variations in Bhagirathi River stream and precipitation with time at Gomukh.
Figure 31 : Variation of δD vs $\delta^{18}O$ for stream discharge at site Gomukh.
Figure 32 : Composition of δD and $\delta^{18}O$ of Bhagirathi stream at Gomukh site.
Figure 33 : Variation of stream discharge and its $\delta^{18}O$ composition with rainfall during ablation period in the year 2005.
Figure 34 : a) Rainfall events and variation of $\delta^{18}O$ composition in precipitation at site Gomukh during the year 2004.
Figure 34 : b) Variation of $\delta^{18}O$ values in stream discharge due to rainfall of depleted $\delta^{18}O$ in year 2005
Figure 35 : Runoff component separated out using isotopic signatures of stream water and precipitation on the basis of daily sampling data during the year 2005 at site Gomukh.

LIST OF PLATES

Plate 1 : A view of the snout of the Gangotri Glacier (Gomukh, 4000 m).

Plate 2 : Deep crevasses as observed on the surface of the Gangotri Glacier.

Plate 3 : Snow-clad Shivling peak (~6500 m): a view from Tapoban.

Plate 4 : A view of the U shaped Bhagirathi valley as seen from the top of snout of the Gangotri Glacier. Meandering pattern of the proglacial stream can also be noted.

Plate 5 : A supraglacial lake (~4100 m) surrounded by supraglacial moraines as observed in the ablation zone of the Gangotri Glacier.

Plate 6 : Tillite hillocks on the right bank of the Bhagirathi River located between Chirwasa and Gomukh.

Plate 7 : A view of the snow has laden Bhagirathi peaks alongwith available vegetation at Chirwasa.

Plate 8 : Meteorological observatory established near the snot of Gangotri glacier.

Plate 9 : Meteorological observatory established by NIH near the snout of Gangotri Glacier.

Plate 10 : Gauging site established by NIH near the snout of the Gangotri Glacier.

Plate 11 : Cross section observations from the Gauging well at Bhagirathi River near the snout of Gangotri glacier.

Plate 12 : Debris covered ablation zone of the Gangotri Glacier.

LIST OF TABLES

Table 1 : Data collection period for different years.

Table 2 : Meteorological instruments installed and observations taken at the meteorological observatory.

Table 3 (a) : General statistics of the daily air temperature, T (°C); rainfall, R (mm); discharge, Q (m^3/s); suspended sediment concentration, S (ppm); relative humidity, RH (%); Sunshine hours, SH (hours); Evaporation, E (mm); and Wind speed, W (km/hr) for the summer 1999 on monthly basis.

Table 3 (b) : General statistics of the daily air temperature, T (°C); rainfall, R (mm); discharge, Q (m^3/s); suspended sediment concentration, S (ppm); relative humidity, RH (%); Sunshine hours, SH (hours); Evaporation, E (mm); and Wind speed, W (km/hr) for the summer 2000 on monthly basis.

Table 3 (c) : General statistics of the daily air temperature, T (°C); rainfall, R (mm); discharge, Q (m^3/s); suspended sediment concentration, S (ppm); relative humidity, RH (%); Sunshine hours, SH (hours); Evaporation, E (mm); and Wind speed, W (km/hr) for the summer 2001 on monthly basis.

Table 3 (d) : General statistics of the daily air temperature, T (°C); rainfall, R (mm); discharge, Q (m^3/s); suspended sediment concentration, S (ppm); relative humidity, RH (%); Sunshine hours, SH (hours); Evaporation, E (mm); and Wind speed, W (km/hr) for the summer 2002 on monthly basis.

Table 3 (e) : General statistics of the daily air temperature, T (°C); rainfall, R (mm); discharge, Q (m^3/s); suspended sediment concentration, S (ppm); relative humidity, RH (%); Sunshine hours, SH (hours); Evaporation, E (mm); and Wind speed, W (km/hr) for the summer 2003 on monthly basis.

Table 4 : Total seasonal volume of water observed during different melt seasons (10^{th} May - 11^{th} October).

Table 5 : Date of pass of maximum peak discharge during the melting seasons (2005-2007)

Table 6 : Diurnal variation in SSC of the selected clear weather days near the snout of Gangotri Glacier.

Table 7 : Distribution of total particle size in the proglacial melt water stream near the snout of Gangotri Glacier.

Table 8 : Area of elevation zone derived from Digital Elevation Model (DEM) for Gangotri Glacier up to Bhojwasa.

Table 9 : Output parameter of the model used in study.

1.0 INTRODUCTION

World's Mountain systems cover about one-fifth of the earth's continental areas and are all inhabited to a greater or lesser extent except for Antarctica. Because of their great altitudinal range, mountains such as the Himalayas, the Rockies, the Andes, and the Alps are also a key element of the hydrological cycle, being the source of many of the world's major river systems. Shifts in climatic regimes, particularly precipitation, in space or seasonally in a changing global climate, would impact heavily on the river systems originating in mountain areas, leading to disruptions of the existing socio-economic structures of populations living within the mountains and those living downstream. Glaciers store a substantial amount of water in the form of snow and ice. The seasonal, character and amount of runoff is closely linked to cryosphric processes. Glaciers, including the Antarctic and Greenland ice sheets, ice caps and valley glaciers in polar regions and in high mountains retain significant amount of water land, and they are the largest fresh water reservoir. They contain more than 75% of the total fresh water on the surface of the earth.

Hydrology of glaciers has been given by several investigators and important regulatory role exerted by the glaciers in a basin was illustrated (Meier 1973; Krimmel and Tangborn, 1974). Delayed response of the glacier melt water has been considered by Stenborg (1970) and Singh et al. (1995). Hodgkins (2001) studies the seasonal evolution of melt water generation, storage and discharge at a non-temperate glacier in Svalbard, Arctic region. A major difference in the melt water storage characteristics of the polar and temperate glacier was reported. Hannah and Gurpell (2001) have applied a conceptual model for simulation for a small glacier (Taillon Glacier) in France, Recently, Bollasina et al. (2002) in the Nepal Himalayas based on the records collected at Pyramid Meteorological Station (5050 m.a.s.l.) for a period of 5 years (1994-1998). The status of the studies clearly indicates that hydrological processes, modelling of melt runoff and separation of different components of using isotopic method are the important research areas and limited research work has been carried out these topics for the Himalayan region.Meltwater draining from outlet of the glacier causes erosion, and the development of complex drainage networks within all glacial environments (Menzies, 1995). Hydrology of glacierized basins, therefore, is an integral element in understanding all glacial environments and processes. Data published in the world Atlas of Snow and Ice (Kotyakov, 1997) there are about 30 million km^3 of Ice on our planet. In winter, snow

covers about 66% of the land surface. The total glacier-derived runoff, equal to 3,450 km^3 of water, accounts for about 8% of the total surface water runoff to the ocean (44,700 km^3) and for about 3% of the land precipitation (119,000 km^3). Of this amount, Antarctica and Arctic Islands contribute 3,010 km^3, and mountain glaciers 440 km^3, or 1.0 % of the land surface runoff. Nearly another 1% (370 km^3) is contributed by the seasonal runoff of glacier snow in summer periods in the absence of melt-water runoff from ice-free areas; the latter factor is very important in enhancing the value of glacier-derived runoff as a water resource (Kotyakov, 1996). . In Himalayas, it is possible to observe the distribution of runoff where the upper parts of the basins experience a meltwater runoff and at the same time in the lower parts of the basins is dominated by rainfall. In glaciated areas, much of the precipitation falls in solid form of throughout the year, so that it contributes to mass storage rather than directly to runoff. For example in the Alps, a minimum variation in annual runoff is observed from the river basin with 30-40% glacier cover (Kasser, 1959).In Himalayas the runoff generated from snow and glacier contribute 60% of the snow cover (Singh,2006).

1.1 Importance of the Himalayas

The Himalayas constitute the largest reservoir of snow and ice outside the Polar Regions. The Himalayan mountain, system is the source of one of the world's largest supplies of fresh water. All the major south Asian rivers originate in the Himalayan and their upper catchments are covered with snow and glaciers. The Indus, the Ganga and the Brahmaputra river systems originating in from the Himalayan region receive substantial amount of precipitation in the form of snow and glaciers in the mountains, like Himalayas, over a long period provides a large amount of water potentially available and also regulates the annual distribution of the water. The perennial nature of Himalayan Rivers and appropriate topographic setting of the region provide a substantial exploitable hydropower in this area. In the Himalayan range there are more than >10,000 glaciers (GSI, 2006) and feed a number of Himalayan rivers. The melting of glaciers starts after depletion of seasonal snow cumulated during winter over the glaciers. The melting of glaciers starts after depletion of seasonal snow exposes the ice surface of the glacier. This ice exposed surface of the glacier increases with time resulting in higher quantum of runoff. As the melt season advances, the melt water contribution from the glaciers increases. By the end of melt season, the melt runoff is reduced due to increases in air temperature and fresh snowfall on the higher reaches. Evidently, runoff generated

from the glaciers in the Himalayan basins have a significant influence on the streamflow of the river. The melt rate of the glacier is determined by the prevailing climatic conditions and, therefore, varies from year to year. The physical changes in the glacier, like trend of exposition of glacier surface, influence the melting and runoff pattern of the glacier. The runoff processes including the storage and drainage of melt water from the glaciers, which control the emerging outflow, are not well understood, and need investigations. Further, contribution of snow and ice melt to the total increase with altitude, but variation in the different components of runoff with season have not been quantified for any Himalayan rivers. There is need to carry out such hydrological investigation for the Himalayan glaciers. Similarly, major detrimental effects of suspended sediment, which include loss of storage capacity, damage to or impairment of hydro equipment have to be studied.

2.0 HIMALAYAS

Himalaya's the great mountain system of Asia forms a barrier between the Tibetan Plateau to the north and the alluvial plains of the Indian subcontinent to the south. The Himalayas include the highest mountains in the world, with more than 110 peaks rising to elevations of 7,300 metres or more above sea level. The great heights of the mountains rise above the line of perpetual snow. Forming the northern border of the Indian subcontinent and an almost impassable barrier between it and the lands to the north, the ranges are part of a great mountain belt that stretches halfway around the world from North Africa to the Pacific coast of Southeast Asia. The Himalayas themselves stretch uninterruptedly for about 2,500 kilometers from west to east between Nanga Parbat and Namcha Barwa, in Tibet. The Himalayas are bordered to the northwest by the mountain ranges of the Hindu Kush and Karakoram and to the north by the high Plateau of Tibet. The width of the Himalayas from south to north varies between 125 and 250 miles. Their total area amounts to about 229,500 square miles (594,400 square kilometres).

2.1 Physical features

The most characteristic features of the Himalayas are their soaring heights, steep-sided jagged peaks, valley and Alpine glaciers often of stupendous size, topography deeply cut by erosion, seemingly unfathomable river gorges, complex geologic structure, and series of elevational belts (or zones) that display different ecological associations of flora, fauna, and climate. The greater part of the Himalayas, however, lies below the snow line. The mountain-building process that created the range is still active and is accompanied by considerable stream erosion and by landslides of great dimension. The Himalayan ranges can be grouped into four parallel, longitudinal mountain belts of varying width, each having distinct physiographic features and its own geologic history. They are designated, from south to north, as the Outer, or Sub, Himalayas; the Lesser, or Lower, Himalayas; the Great, or Higher, Himalayas; and the Tethys, or Tibetan, Himalayas.

2.2 Himalayas Physiography

The Outer Himalayas comprise flat-floored structural valleys and the

Shiwalik Hills, which border the Himalayan mountain system to the south. Except for small gaps in the east, the Shiwalik run for the entire length of the Himalayas in the Indian state of Himachal Pradesh. The main Shiwalik range has steeper southern slopes facing the Indian plains and descends gently northward to flat-floored basins, called duns. To the north the Shiwalik range abuts a 50-mile-wide massive mountainous tract, the Lesser Himalayas, where mountains rising to 15,000 feet and valleys with altitudes of 3,000 feet run in different directions. There is a general conformity of altitude among neighboring summits, which creates the appearance of a highly dissected plateau. The three principal ranges of the Lesser Himalayas—the Nag Tibba, the Dhaola Dhar, and the Pir Panjal—have branched off from the Great Himalayan Range lying farther north. The Nag Tibba, the most easterly of the three ranges, is some 26,800 feet high near its eastern end, in Nepal, and forms the watershed between the Ganges and Yamuna rivers, in the Uttarakhand. To the west the picturesque Vale of Kashmir, a structural basin (i.e., an elliptical basin in which the rock strata are inclined toward a central point), forms an important section of the Lesser Himalayas. It extends from southeast to northwest for 100 miles, with a width of 50 miles, and has an average elevation of 5,100 feet; the basin is traversed by the meandering Jhelum River, which runs through Wular Lake, a large freshwater lake in the Indian-held portion of Jammu and Kashmir. The backbone of the entire mountain system is the Great Himalayan Range, rising above the line of perpetual snow. The range reaches its maximum height in Nepal; among the peaks are 9 of the 14 highest in the world, each of which exceeds 26,000 feet in elevation. From west to east they are Dhaulagiri 1, Annapurna 1, Manaslu 1, Cho Oyu, Gyachung Kang 1, Mount Everest, Lhotse, Makalu 1, and Kanchenjunga 1.Farther east the range changes from a southeasterly to an easterly direction as it enters Sikkim, an old Himalayan kingdom now a part of India. After this, it runs eastward for another 260 miles through Bhutan and the eastern part of Arunachal Pradesh as far as the peak of Kangto (23,260 feet) and finally turns northeast, terminating in Namcha Barwa. There is no sharp boundary between the Great Himalayas and the ranges, plateaus, and basins lying to the north of the Great Himalayas, generally grouped together under the name of the Tethys Himalayas and extending far northward into Tibet. In Kashmir and in the Indian state of Himachal Pradesh, the Tethys are at their widest,

forming the Spiti Basin and the Zaskar Mountains, the highest peaks of which, to the southeast, are Leo Pargial (22,280 feet), rising north of the Sutlej River opposite Shipki Pass, and Shilla.

2.3 Physical features of the Himalayas

1) Drainage

The Himalayas are drained by 19 major rivers, of which the Indus and the Brahmaputra are the largest, each having catchment basins in the mountains of about 100,000 square miles in extent. Of the other rivers, five belong to the Indus system—Jhelum, Chenab, Ravi, Beas, and Sutlej—with a total catchment area of about 51,000 square miles; nine belong to the Ganges system—the Ganges, Yamuna, Ramganga, Kali (Sarda), Karnali, Rapti, Gandak, Baghmati, and Kosi-draining another 84,000 square miles; and three belong to the Brahmaputra system-the Tista, Raidak, and Manas—draining another 71,000 square miles. The major Himalayan rivers rise north of the mountain ranges and flow through deep gorges that generally reflect some geologic structural control. The rivers of the Indus system as a rule follow northwesterly courses, whereas most of those of the Ganges-Brahmaputra systems take easterly courses while flowing through the mountain region. To the north of India, the Karakoram Range, with the Hindu Kush range on the west and the Ladakh Range on the east, forms the great water divide, shutting off the Indus system from the rivers of Central Asia. The counterpart of this divide on the east is formed by the Kailas Range and its eastward continuation, the Nien-ch'ingt'ang-ku-la (Nyenchen Tangla) Mountains, which prevent the Brahmaputra from flowing northward. South of this divide, the Brahmaputra flows to the east for about 900 miles before cutting across the Great Himalayan Range in a transverse gorge, although many of its Tibetan tributaries flow in an opposite direction, as the Brahmaputra may once have done.

The Great Himalayas, which normally would form the main water divide throughout its entire length, functions as such only in limited areas. This situation exists because the major Himalayan rivers, such as the Indus, Brahmaputra, Sutlej, and at least two headwaters of the Ganges—the Alaknanda and Bhagirathi—are older than the mountains they traverse. It is believed that the Himalayas were uplifted so slowly that the old rivers had no difficulty in continuing

to flow through their channels and, with the rise of the Himalayas, even acquired a greater momentum, which enabled them to cut their valleys more rapidly. The elevation of the Himalayas and the deepening of the valleys thus proceeded simultaneously, with the result that the mountain ranges emerged with a completely developed river system cut into deep transverse gorges that range in depth from 5,000 to 16,000 feet and in width from 6 to 30 miles. The earlier origin of the drainage system explains the peculiarity that the major rivers drain not only the southern slopes of the Great Himalayas but, to a large extent, its northern slopes as well, the water divide being north of the crest line.

The role of the Great Himalayan Range as a watershed, nevertheless, can be seen between the Sutlej and Indus valleys for 360 miles; the drainage of the northern slopes is carried by the north-flowing Zaskar and Dras rivers, which drain into the Indus. Glaciers also play an important role in draining the higher altitudes and in feeding the Himalayan rivers. Several glaciers occur in Uttarakhand, of which the largest, Gangotri, is 20 miles long and is one of the sources of the Ganges. The Khumbu Glacier drains the Everest region in Nepal and is one of the most popular routes for the ascent of the mountain. The rate of movement of the Himalayan region glaciers varies considerably; in the neighboring Karakoram Range, for example, the Baltoro Glacier moves about six feet per day, while others, such as the Khumbu, move only about one foot daily. Most of the Himalayan glacier in retreat.

2) Soils

Not much is known about the Himalayan soils. The north-facing slopes generally have a fairly thick soil cover, supporting dense forests at lower altitudes and grasses higher up. The forest soils are dark brown in colour and silt loam in texture and occur mainly in Uttarakhand; they are ideally suited for growing fruit trees. The mountain meadow soils are well developed but vary in thickness and in their chemical properties. Of the soils that are not restricted to any particular area, alluvial soils (deposited by running water) are the most productive, though they occur in limited areas, such as the Valley of Kashmir, the Dehradun, and the high terraces flanking the Himalayan valleys. Lithosols, consisting of imperfectly weathered rock fragments that are deficient in humus content, cover many large areas at high altitudes and are the least productive soils.

3) Climate

The Himalayas, as a great climatic divide affecting large systems of air and water circulation, exercise a dominating influence upon meteorological conditions in the Indian subcontinent to the south and in the Central Asian highlands to the north. By virtue of its location and stupendous height, the Great Himalayan Range obstructs the passage of cold continental air from the north into India in winter and also forces the southwestern monsoonal (rain-bearing) winds to give up most of their moisture before crossing the range northward, thus causing heavy amounts of precipitation (both rain and snow) on the Indian side but arid conditions in Tibet. Most important factors controlling the climate and weather conditions in the Himalayas are altitude and aspect. Largely due to variation in the altitude, the climate varies from hot and moist tropical in the lower valleys, to cool temperate at about 2000 m and tends towards polar as the altitude increases beyond 2000 m. Altitude controls not only temperature but also the type and amount of precipitation. Maximum rainfall occurs in the outer Himalayan ranges. Beyond the Great Himalayas the rainfall is very little. The second factor cotrolling the climate is aspect. Looking at the cyclic process of the seasons throughout the year, the snow is least during August. In the high altitude region of the Himalayas, the fresh snowfall starts at the end of September and continues till the end of March. Especially during February and March the Western Himalayas get maximum snowfall due to 'western disturbances'. At the lower altitudes, the seasonal snow starts melting around beginning of March. During June, vast amount of snowmelt results in heavy runoffs in snowfed rivers (Ramamoorthi et al., 1991). During peak winters, area covered by seasonal snow is 30-50 times more than permanent ice cover (Upadhyay et al., 1991). The total catchment area of the Ganga in the Indian part of the sub-continent covers an area of about 861404 km2 of which, roughly 2500 km2 remains under perennial snow cover (Oberoi et al., 1999).There are two periods of wet weather: the winter rains and the rains brought by the southwestern monsoon winds. Winter precipitation results from low-pressure weather systems advancing into India from the west, which cause heavy snowfall. Within the regions where western disturbances are felt, condensation occurs in upper air levels at a height of 10,000 feet from the surface; as a result, precipitation is much greater over the high mountains. It is during this season that snow accumulates around the Himalayan high peaks and that the western Himalayas receive more

precipitation than the eastern Himalayas. In January, for example, Mussoorie in the west receives almost 3 inches, while Darjiling to the east receives less than an inch. By the end of May the meteorological conditions are reversed. Southwestern monsoon currents passing over the eastern Himalayas drop precipitation to elevations of 18,000 feet; in June, therefore, Darjiling receives about 24 inches and Mussoorie less than 8 inches. The rains cease in September, after which the finest weather in the Himalayas prevails until the beginning of winter in December.

2.4 Resources

Economic conditions in the Himalayas are fitted to the limited resources available in this expansive and heterogeneous region of varied ecological zones. The principal activity is animal husbandry, but the exploitation of the wild biota and trade are also important. The Himalayas abound in economic resources. These include rich arable land, extensive grassland and forest, workable mineral deposits, and easily harnessable waterpower. The most productive arable lands in the western Himalayas are in the Vale of Kashmir, the Kangra Valley, the Sutlej River basin, and the terraces flanking the Ganges and Yamuna rivers in Uttarakhand. The Himalayan rivers have a tremendous potential for hydroelectric generation, which has been harnessed intensively in India since the 1950s. A giant multipurpose project is located at Bhakra-Nangal on the Sutlej River in the Outer Himalayas; completed in 1963, its reservoir has a storage capacity of some 348 billion cubic feet (10 billion cubic metres) of water and a total installed generating capacity of 1,050 megawatts. Three other Himalayan rivers, the Kosi, Gandak (Narayani), and Jaldhaka, have been harnessed by India, which then supplies electric power to Nepal and Bhutan. Major river system the Indus, Ganga, Brahmaputra and their tributaries have significant contribution from melting of snow and ice. During summer season the melt runoff is of vital importance for hydroelectric power generation, irrigation and drinking water supply. Important multipurpose projects like Bhakra on Satluj River depend heavily on snow and glacier melt runoff since about 50 to 60% of the annual flows of Satluj River at Bhakra are generated from the snow and glacier melt runoff (Singh and Jain, 2003, Jain et al., 2003). Therefore, correct and timely information on the snow cover extent, glaciated area in the basin and about the volume of snow and glacier melt runoff likely to occur, is of great importance for

the water resources managers, especially to those who are dealing with multipurpose reservoir operations. To forecast the discharge, a lot of information about terrain, snowpack, glaciated area and meteorological parameters are required. Such information is not available in sufficient quantity from the ground data collection network due to many reasons such as difficult, inaccessible and hazardous terrain.

3.0 OBJECTIVES OF THE PROJECT

In order to carry out hydrological investigations on the Gangotri Glacier, Department of Science and Technology (DST) sanctioned a project entitled "Seasonal characterization of ablation, storage and drainage of melt runoff and simulation of streamflow for the Gangotri Glacier" to National Institute of Hydrology in the month of December 2005 for a period of 3 years, i.e., till December 2007. It was extended for a period of 3 months until March 2008.

The main objectives of the project are given below:

(i) Installation and monitoring of the hydrometeorological instruments for the continuous observations of meteorological and hydrological data. This data would provide monthly and seasonal specific water yield, which can be studied for its variability from the year to year.

(ii) To study the melt water storage and drainage characteristics of the glacier.

(iii) To simulate daily streamflow using a conceptual hydrological model using observed meteorological and hydrological data. Degree-day approach would be used for the modelling of runoff.

(iv) To identify the contribution of snow melt, ice melt, rain and groundwater into the total streamflow using isotopic method and to study the changes in each component of runoff during the ablation period. Different components of runoff obtained using isotopic method would also be compared with simulated components through modelling approach.

(v) Estimation of suspended sediment concentration and load from the Gangotri Glacier and its relationship with discharge.

4.0 STUDY AREA

4.1 Location and Accessibility

The present study was carried out for the Gangotri Glacier, which is one of the largest glaciers of Himalayas. This glacier is located in the Uttarkashi District of Uttarakhand State (U.A.) falling in the Garhwal Himalayan region. The location of Gangotri Glacier is shown in Figure 1. The study area lies within the latitudes 3043'N - 30°01'N and longitudes 79°0'E - 7917'E. The proglacial melt water stream, known as Bhagirathi River, emerges out from the snout of the Gangotri Glacier at an elevation of 4000 m. The snout of the Gangotri Glacier is known as "Gomukh". A view of the Gomukh is shown in Plate 1. The approach to the snout of the Glacier includes a trekking of about 18 km distance starting from the Gangotri town. The major part of the trekking is along the Bhagirathi River. There is no information available on the depth of the glacier but rough estimates based on the topography of the area and some field observations suggest the depth of glacier to be about 200 m (Dutta et. al., 2003). Crevasses are very common and prominent surface features from any small glaciers to the large ice sheets. Gangotri Glacier also contains a large number of crevasses spread all over the ablation zone (Plate 2). These crevasses are well exposed when seasonal snow accumulated in the ablation zone is depleted.

The Survey of India topographic sheet no. 53 M/4, N/1, N/2, N/5 and N/6 on 1:50,000 scales were used to delineate the catchment boundary. Contours, snow covered and snow free area, drainage and the benchmarks were digitized using GIS software ILWIS 3.0. Satellite images of LISS-III P-6 sensor of the Gangotri Glacier are shown in Figure 2 during different dates of ablation season 2005. For very preliminary information, Indian Remote Sensing Satellite (IRS) imageries were also acquired for mapping of the area. IRS 1C and 1D LISS III images were used for this purpose.

4.2 Gangotri Glacier Systems

The Gangotri Glacier system most commonly known as Gangotri Glacier, is a cluster of many glaciers comprising of main Gangotri Glacier (length: 30.20 km; width: 0.20 - 2.35 km; area: 86.32 km^2) as trunk part of the system. It flows in the northwest direction. The major glacier tributaries of the Gangotri Glacier system are Raktvarn Glacier (55.30 km^2), Chaturangi Glacier (67.70 km^2), Kirti Glacier (33.14

km^2), Swachand Glacier (16.71 km^2), Ghanohim Glacier (12.97 km^2), Meru Glacier (6.11 km^2), Maindi Glacier (4.76 km^2) and few others having glacierised area of about 3.08 km^2. The Raktvarn, Chaturangi, Swachand and Maindi glaciers are merging with trunk glacier from north-east while the Meru, Kirti and Ghanohim glaciers are meeting the trunk glacier from south-west. The Gangotri Glacier is a valley type glacier system with total glacierized area of about 286 km^2. Total catchment area of the Gangotri Glacier and melt stream up to the discharge-gauging site established downstream of the snout by NIH is about 556 km^2. The elevation range of the Gangotri Glacier varies from 4000 to 7000 m, whereas elevation of the study area up to the gauging site lies between 3800-7000 m. The Gangotri Glacier area also has several high peaks around it. Plate 3 shows the majestic snow clad Shivling peak (~6500 m) in the study area.

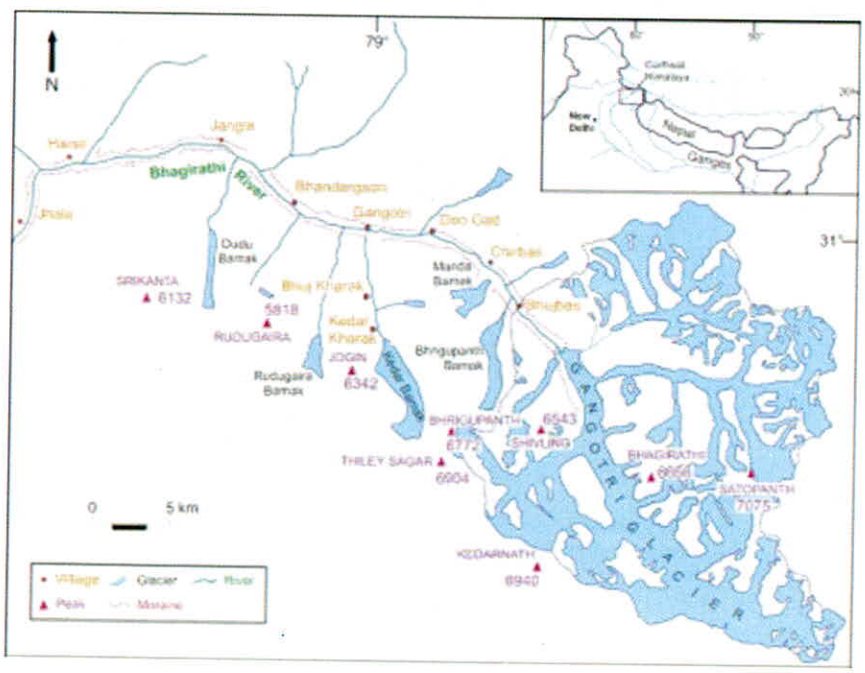

Figure1: Location map of the study area.

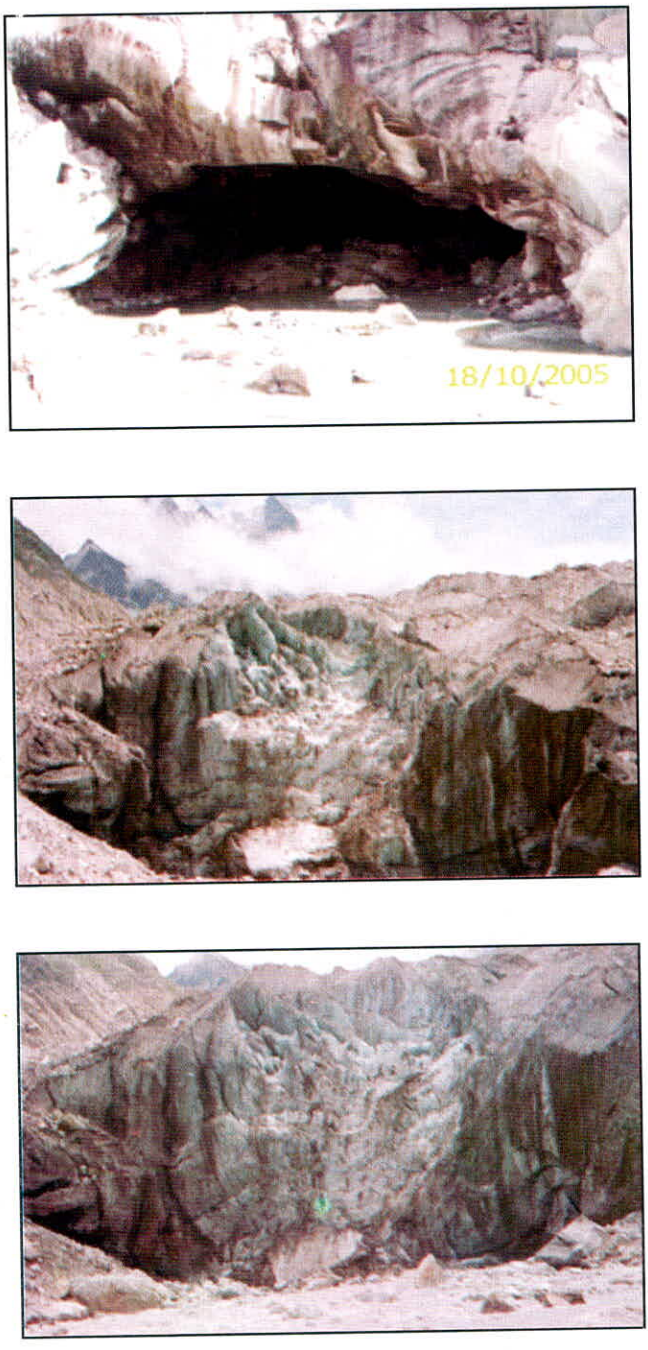

Plate 1: Different views of Gomukh are shown during the observation time near the snout of Gangotri Glacier.

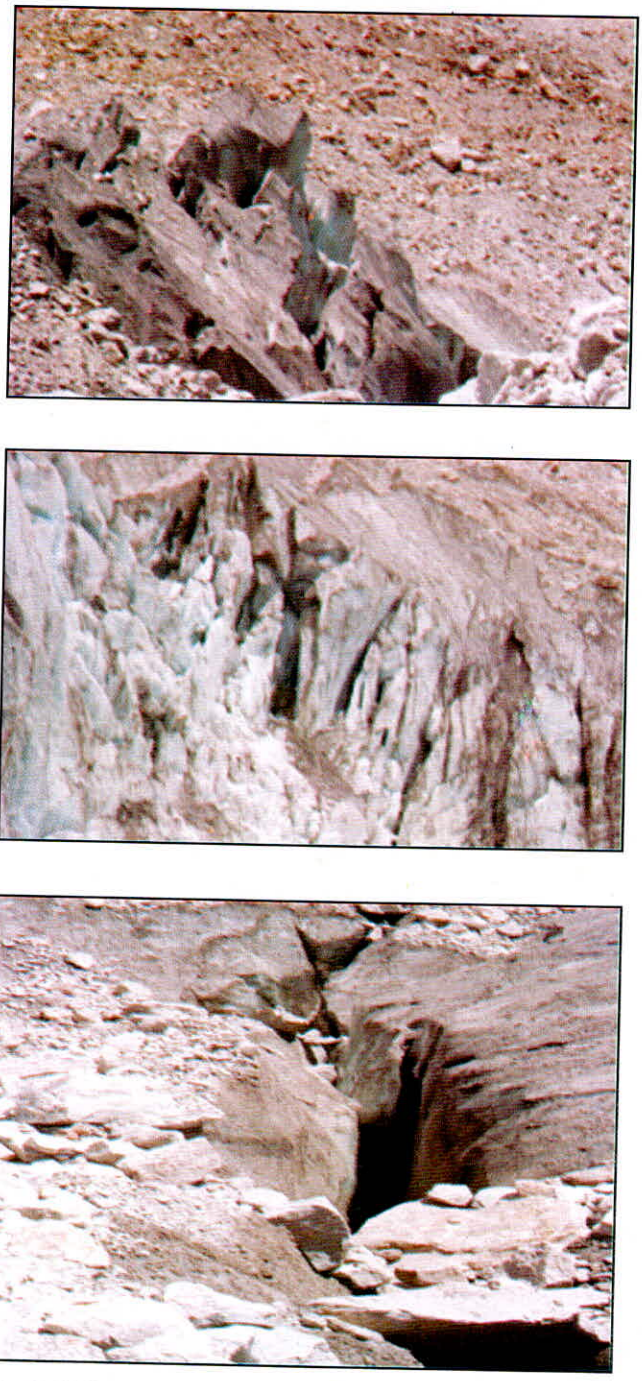

Plate 2: Different views of ice exposed and crevasses over the Gangotri Glacier.

Figure 2: Satellite view of Gangotri Glacier captured from LISS-III- P6 images.

4.3 Geology

The Gangotri Glacier lies in the central crystalline zone. The Himalayan crystallines along the Bhagirathi valley is composed of Pelitic and semi-pelitic metasediments with acid and basic intrusive. The area is situated north of Main Central Thrust (MCT) which separates the metamorphic from the underlying very low grades of unmetamorphosed sedimentary sequence of the lesser Himalaya. Mica schists are the predominant rock found over the MCT. Further, northeast of Gangotri these schists are intruded by hard and massive granite known as Gangotri granite. From Gangotri town towards Gomukh, the Gangotri granite gradually changes into fine grained, well-foliated, garnetiferrous gneiss and augen gneiss intruded by fine-grained aplitic veins.

The Bhagirathi river valley is a broad U-shaped with high sidewalls, which is a characteristic of its glacial origin (Plate 4). The lower part of the ablation zone of the glacier is covered with thick supraglacial moraine and shows development of few lakes (Plate 5). Due to the recession, the location of Gomukh has also moved upstream with time. Morainic material present between Chirwasa and Gomukh in the form of tillite hillocks are considered as evidences of the extent of Gangotri Glacier (Plate 6). It is NW-SE trending valley within the granitic terrain. The prominent geomorphic landforms formed by the glacial environment are different levels of lateral and recessional moraines, U-shaped glacial troughs, kame terraces and outwash plains.

4.4 Flora and Fauna

Thick vegetation is found from Gangotri town to Deo Gad. Deo Gad, located about 5 km upstream to the Gangotri town, is a tributary to the Bhagirathi River. The vegetation gradually reduces beyond Deo Gad. There is little vegetation around Chirwasa, a place between Deo Gad and Gomukh, but beyond Chirwasa, the vegetation is significantly reduced up to Gomukh. Plate 7 shows the view of snow-laden Bhagirathi peaks and vegetation around Chirwasa. As such there is very little vegetation between Chirwasa and Gomukh. Common flora found in the area are Himalayan cedar (*Botanical name: Cedrus deodara*) which dominate on the slopes along with few Spruce (*Picea smitbiana*), Silver fir (*Abies pindrow*) and Blue pine (*Pinus wallichiana*). The Indian birch (*Betula utilis*) is the only tree found in and around the Bhojwasa. The important faunas include leopard, musk deer and varau deer. Different varieties of species of birds also found in the area.

Plate 3: Snow-clad Bhagirathi peaks: a view from Bhojwasa.

Plate 4: A views of the U shaped Bhagirathi valley as seen from the top of snout of Gangotri Glacier.

Plate 5: Supraglacial lakes over the ablation zone of the Gangotri Glacier surrounded by morainic debris

Plate 6: Tillite hillocks on the right bank of the Bhagirathi River located between Chirwasa and Gomukh.

Plate7: A view of the snow laden Bhagirathi valley during the summer seasons.

5.0 LITERATURE REVIEW

Glaciology was thus fairly launched in India by nineteenth century. The pattern of occasional and incidental observation of Himalayan Glaciers was basically altered in 1907-10 when the Geological Survey of India (GSI) made a concerted effort at systematized glacier observations as a part of International Programme to study glaciers. A second effort for glacier observations was organized during International Geophysical Year (1957-58) when many glaciers were revisited to study their fluctuations. In 1945 a on the role of glaciers and snow hydrology of Punjab rivers was presented at the Annual Research Committee meeting of Central Board of Irrigation and Power (Kanwar Sain, 1946). The Indian National Committee on International Hydrological Programme (1965-74) under CSIR, appointed another high level committee on Snow, Ice and Glaciers. Under the guidance of this High Level Committee, Inter-Departmental Glaciological Expeditions were organized to various Himalayan Glaciers. The studies included hydrometeorological observations, glacier dynamics, mass balance, geomorphological and isotopic investigations, ice drilling and experiments for artificial melting of snow and ice. Geological Survey of India undertook the preparation of glacier inventory on 1:50,000 scale with cooperation from Survey of India. A UNESCO regional workshop on snow, ice and avalanches was organized at the Snow and Avalanche Study Establishment (SASE), Manali in 1977 followed by a training seminar in 1978. Government of India established separate units/divisions and organisation to undertake studies of Himalayan snow and ice. Predominant organizations are:

SASE (Snow and Avalanche Study Establishment) was established in late sixties by the Ministry of Defence with the sole objective to study snow cover and meteorology, snow-mechanics and avalanche dynamics"snow physics, artificial triggering of avalanches, available technology and control structures along with field trials with a view to facilitate movement over high altitude roads constructed by Border Road Organisation. Geological Survey of India (GS]), Calcutta Systematic glaciological studies in GSI was initiated in 1974 with the creation of Glaciology Division. Present studies cover glacier inventory; glacier regimen, glacier and snow hydrology, suspended sediment transport, seasonal snow cover assessment, ice flow movement and other specialized studies. India Meteorological Department (IMD), New Delhi established a Glaciological Study and Research Unit during 1972-73 for taking active participation in national glacier expeditions. Activities include

meteorological observations, such as precipitation, temperature, wind speed and direction, short wave, long wave radiation for energy budget and mass balance studies on Himalayan glaciers. Central Water Commission (CWC), New Delhi Central Water Commission (CWC) was the first organization to initiate snow surveys for stream flow studies. In 1985, CWC established a Snow Hydrology Unit at Shimla for flood forecasting of Upper Yamuna Catchment. Recently, National Institute of Hydrology (NIH), Roorkee has been actively involved for mountain hydrology of the snowy and glaciated Himalayas. Being the nodal organization for water resources exploration and management, CWC has yet to establish a suitable network of observation stations for evalauation of meltwater contributions from Himalayan snow and ice.

Survey of India (Sol), Dehradun Survey of India (Sol) has always been associated for topographical surveys and preparation of large scale maps of glaciers and its surroundings including snow and moraine features, rock fall, ice walls, crevasses, snouts, dead moraines, caves, glacier movements. These studies are coordinated by the Geodetic and Research Branch of Survey of India. Wadia Institute of Himalayan Geology (WIHG), Dehradun Wadia Institute of Himalayan Geology (WIHG), Dehradun under the department of Science and Technology has played a lead role since 1986 for multidisciplinary scientific expeditions under the Himalayan Glaciology Programme. The Institute established a semi-permanent field research station near Dokriani Glacier at an altitude of 3750 m in 1992. Field laboratory facilities for sedimentological, melt water discharge and meteorological studies. Physical Research Laboratory (PRL), Ahmedabad Physical Research Laboratory (PRL), Ahmedabad under the Department of Space has been studying snow and ice problems Using Isotopic studies. Glacier dynamics (using ^{32}Bi, ^{210}Pb and ^{137}Cs) and climatic variations (^{18}O, ^{2}H) and chemical composition of snow and ice. Studies for deep ice core from glacier Ice for climatic variations and chemical composition have been identified as the future thrust area. National Remote Sensing Agency (NRSA), Hyderabad National Remote Sensing Agency (NRSA), Hyderabad, under Department of Space has been providing seasonal and short-term snow melt run-off forecasts for various Himalayan river basins on an operational basis for last two decades. Space Application Centre (SAC), Ahmedabad Space Application Centre (SAC), Ahmedabad under the Department of Space has initiated remote sensing studies from satellite imageries, the thrust area identified by the organization are snow mapping and snow hydrology; inventory of glaciers and mass balance of

glaciers. Hazards from glacier dammed lakes of Sikkim are being monitored.

In respect of Gangotri glacier area, proposed surveyed map of entire basin along with the position of the snout has been first published by survey of India in 1937. Hodgson and Herbert in 1842, Griesbach and J.B. Auden of Geological Survey of India in 1889 and 1934, respectively, visited the glacier and started the scientific study of the glacier. Addition to the inventory of Himalayan glaciers various investigators (Karpov and Kirmani, 1968; Muller, 1970; Vohra, 1978; GSI, 1999) made there efforts time to time. The most recent inventory of the Himalayan glaciers has been published by GSI (2006). Glacier geomorphology of the area has been studied by number of workers (Tangri, 2000; Naithani et al., 2001; Nainwal et al., 2003; Sharma, 2003). All along the mass balance and glacier hydrology are the two most difficult tasks as far as glaciology is concerned because it is corroborated with extensive field investigations and needs regular monitoring in order to collect the data. Large size, treacherous terrain and harsh weather conditions make this work even more difficult for the Gangotri Glacier. GSI has done some preliminary work on the mass balance of Gangotri Glacier from 1974-1977. U.P. Remote Sensing Application Centre, U.P. (RSACUP) monitored the melt runoff from the Gangotri Glacier between 1993 and 1998. Recently, G.B. Pant Institute for Himalayan Environment and Development, Almora and Jawahar Lal Nehru University, New Delhi are started working on the Gangotri Glacier.

6.0 DATA COLLECTION PERIOD

This data collection is for the period of 2005 to 2007, observations were made for the whole ablation period (May to October). Table 1 shows the period of data collection in different years.

Table 1: Data collection period for different years

Year	Period	Days
2005	01st May-20th October	173
2006	01st May-20th October	173
2007	07th May-13th October	160

7.0 MONITORING AND ANALYSIS OF METEOROLOGICAL DATA

7.1 Meteorological parameters monitoring

The meteorological data such as rainfall, maximum and minimum temperature, humidity, evaporation, wind speed and direction, sunshine hours and solar radiation are measured to provide the data base for the ablation season. These data are utilized to characterize the climate of that location and to supply meteorological input for simulating the hydrological process. Precipitation contributes to river runoff and is considered to be a key component for the hydrologic modeling of any glaciated catchment. Wind speed and wind direction are at least partial determinants of rain or snow distribution over a basin, and temperature data are vital to parameters such as snow melt. The hydrologic regime of the glaciated catchment is intimately related to climactic factors. The meteorological variables are the important input to the hydrological modeling studies.

Now extensive networks of the meteorological stations are found at high altitude all over the developed countries. Most of these are simple observing stations. However, in Indian Himalayas the network of meteorological stations is sparse. In order to monitor the meteorological variables for the Gangotri glacier, a standard meteorological observatory (30 m $\times$ 30 m) was set up at about 3800 m altitude near the gauging site at Bhojwasa (Plate 9). While selecting the site proper care was taken to consider the criteria laid down by India Meteorological Department (IMD) for establishing an observatory. As per the conditions the site chosen should be well exposed levelled plot of size 25 m NS x 15 m EW. The key meteorological parameters observed with the different kinds of meteorological instruments are given in Table 2.

Table 2: Meteorological instruments installed and observations taken at the meteorological observatory

S. No.	Instrument	Observations
1	Ordinary raingauge	Rainfall
2	Self recording raingauge	Continuous rainfall/rain intensity
3	Thermograph	Continuous temperature
4	Max. & min. thermometers	Max. & Min. temperatures
5	Dry & wet bulb thermometers	Dry & wet bulb temperatures
6	Hygrograph	Relative humidity
7	Pan evaporimeter	Pan evaporation
8	Anemometer	Wind speed
9	Wind vane	Wind direction
10	Sunshine recorder	Sunshine hours
11	Pyranometer	Solar radiation

Some of the observations were made round the clock using automated instruments, while some were observed manually at a standard frequency during the daytime. Observation for dry and wet bulb temperatures, wind speed and wind directions were made at 0830, 1130, 1430 and 1730 hours, whereas observation for maximum and minimum temperatures, rainfall and evaporation were made at 0830 and 1730 hours. Continuous records of temperature, relative humidity, rainfall and sunshine hours were collected using thermograph, hygrograph, self recording rain gauge and sunshine recorder respectively. A detailed analysis on various meteorological and hydrological observations are presented in the following section. The statistical characteristics of the hydrometeorological data provides the basic information about their frequency distributions and variabilities. Tables 3 (a)-(e) given in Appendix-II presents the basic statistical features of the hydrometeorological records collected for four different ablation seasons (May-October).

Plate 8 : Meteorological Instruments: Thermometers, Pan –evaporimeter, Pyrenometer, Self recording rain gauge.

Plate 9 : Meteorological observatory at the Gangotri Glacier Project site near the snout of the Gangotri Glacier.

7.2 Precipitation

The precipitation received in the catchment of Gangotri glacier up to Bhojwasa varies in time and space. During the accumulation season the form of precipitation received in the catchment is snowfall whereas during the ablation season the rainfall occurs in the lower part of the catchment. However, during the ablation season in addition to the rainfall contribution the glacier melt contributes significantly to the river runoff. In order to get the temporal pattern of the rainfall at the Bhojwasa site, ordinary rain gauge as well as a self recording rain gauge are installed at the site.

A team of NIH Scientist and staff has monitored the daily rainfall data at the NIH site of the Gangotri glacier. The temporal variation in the daily observed rainfall, observed during the ablation season is shown in Figure 3(a) for the years 2005 - 2007. These observations indicate that daily rainfall hardly exceeds 15 mm in the study area. From the rainfall records it is observed that out of the total rain events about 78.74 % events provided daily rainfall less than or equal to 5 mm, 15.75 % in the range of 5-10 mm and only 2.36 % between 10-15 mm. These results suggest that during the summer season mostly light rain occurred in the study region, except some unusual heavy rainfall events.

The observed daily rainfall values have been aggregated in order to get the monthly values. The distribution of monthly rainfall for different years is shown in Figure 3(b). A significant variation was observed in monthly rainfall from year to year, particularly in July, August and September, and total seasonal rainfall varied accordingly. For example, the total rainfall for the whole summer season (May - October) for 2005, 2006, and 2007 was found to be 380.5, 208.1 and 237.6 mm. Based on available rainfall records, average monthly rainfall for May, June, July, August, September and October has been computed to be 24, 20.8, 94.8, 53, 80.3 and 2.4 mm, respectively. It shows that July and September experienced relatively higher rainfall during summer period.

The self recording rain gauge installed at the NIH site was utilized for having the rainfall at shorter time interval. In this regard the NIH staff monitored the self recording rain gauge data replacing the SRRG charts daily. From these charts, hourly rainfall values were derived. These hourly rainfall values were used to study

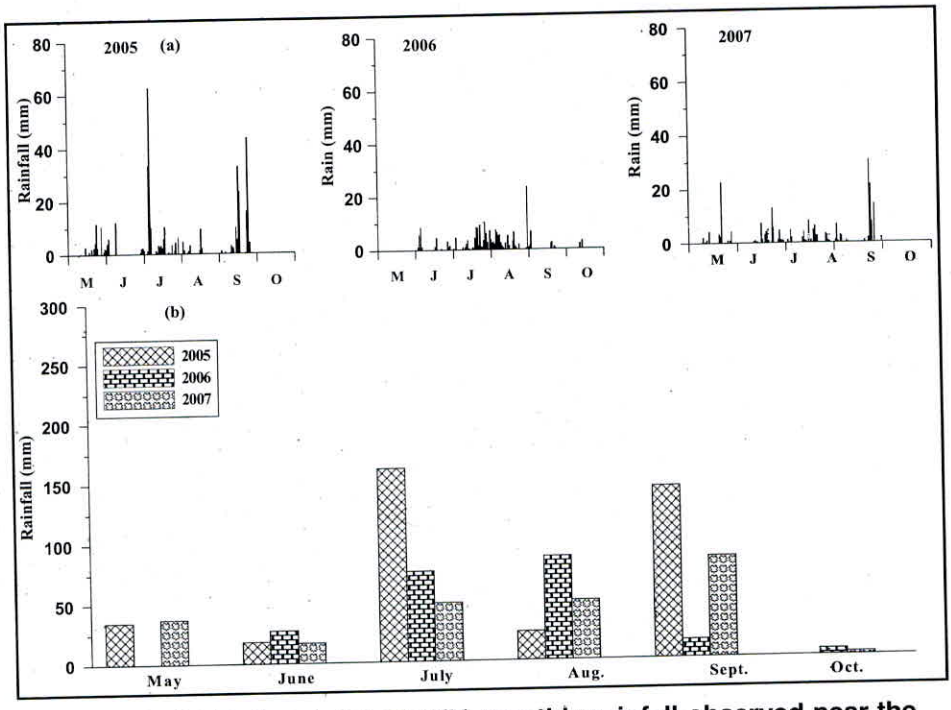

Figure 3 : (a) Daily rainfall and (b) monthly rainfall observed near the snout of Gangotri Glacier during the different summer season (2005-2007)

the rainfall intensity and its variation with time. The frequency distribution of hourly rainfall for the Gangotri Glacier area is shown in Figure 4(a) for the years 2005-2007. It is found that about 41% hourly rainfall events represented the rainfall intensity between 0.1 and 0.5 mm/hr and 23% events between 0.5 to 1.0 mm/hr. The total rainfall at hourly interval for the ablation season was computed and its variation with time (hour) is shown in Figure 4(b).

Diurnal pattern of rainfall provides information on the timing of occurrence of rainfall and can also be used to study the influence of monsoon on occurrence of rainfall in the study area. Month wise average rainfall intensity and corresponding number of rainfall events at hourly interval are shown in Figure 5. These observations clearly indicate that although the intensity was in general higher in May as compared to June, but the numbers of rainy events were more or less similar during these two months. However, during July, because of monsoon rain, the total number of rain events increased throughout the day. Figure 5 shows the variation of the average

rainfall intensity at hourly interval within 24 hours for the different months of the ablation season. From these figures it is observed that the timings of the different events varied over the entire ablation season. Maximum rainfall events occurred either in the evening or early morning and, generally, the least rainfall events were recorded between 0800 hours to 1400 hours, except in August and September. At the start of the melt season the rainfall occurs mostly due to formation of convective clouds. As the melting season advances and monsoon season (July, August and September) approaches, the frequency of rainfall increased due to combination of local convective activity and a partial influence of monsoon. It resulted in possibility of rainfall any time during the day and night. However, still the trend of rainfall occurrence shows that late evening or early morning was the most probable time for the occurrence of rainfall. It is to be pointed out that most of the moisture of monsoon clouds precipitates before they reach at high altitude region beyond 4000 m, like the present study area and, therefore, has only limited influence of rainfall.

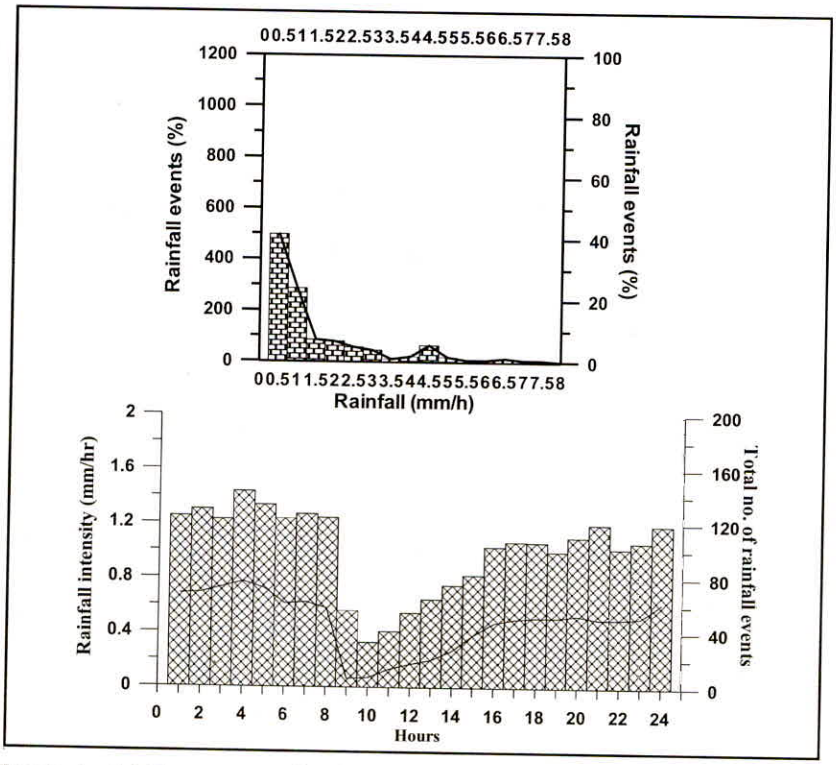

Figure 4 : (a) Frequency distribution of hourly rainfall, and (b) range of hourly rainfall observed near the snout of Gangotri Glacier.

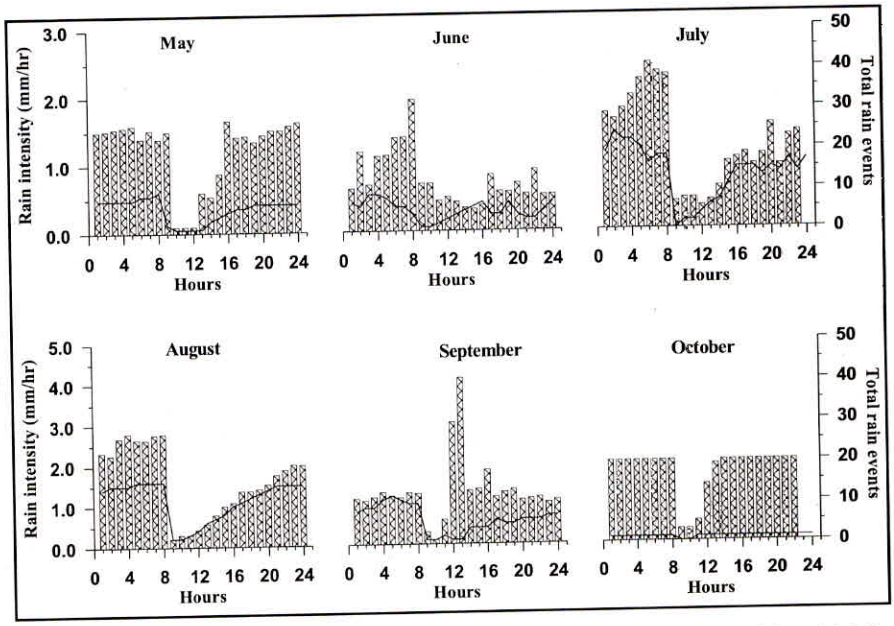

Figure 5 : (a) Diurnal variation in mean rainfall intensity (bar and left side axis) and total number of rainfall events (continuous line and right side axis) for different months observed near the snout of the Gangotri Glacier during summer season 2006 and 2007.

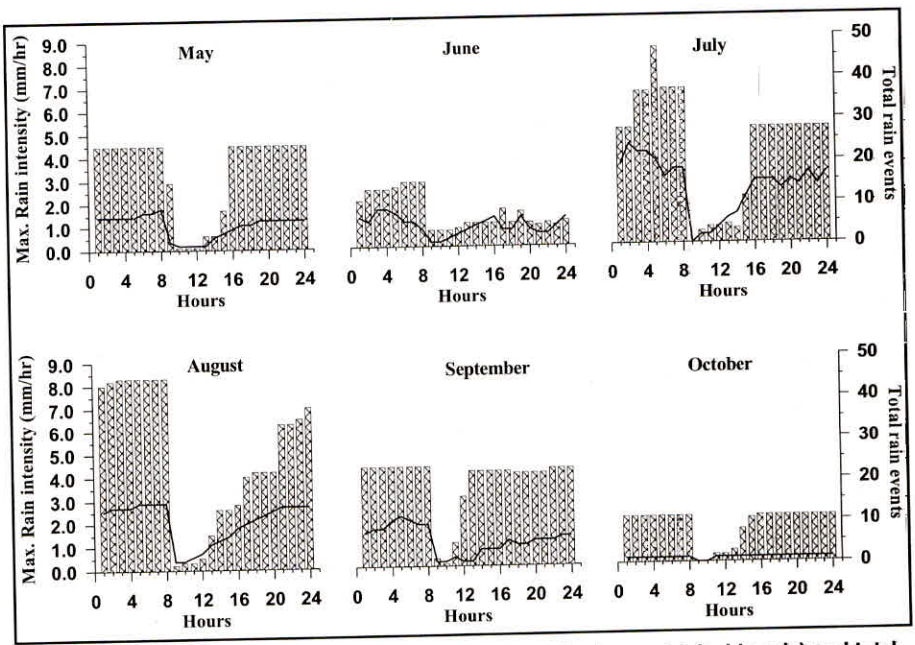

Figure 5 : (b) Diurnal variation in maximum rainfall intensity (bar and left side axis) and total number of rainfall events (continuous line and right side axis) for different months observed near the snout of the Gangotri Glacier during summer season 2006 and 2007.

7.3 Air Temperatures

In order to estimate the melting of the snow and glacier, the air temperature is the one of the most important variables. Normally the air temperatures are measured using daily thermographs located at limited number of sites within the basin. However, the temperature values are extrapolated at different altitudes using temperature lapse rate method. In this study area the thermograph has been installed at Bhojwasa site and the temperature at the higher altitude have been extrapolated using the lapse rate method during the hydrological modeling.

Daily maximum, minimum and mean air temperatures observed near the snout of Gangotri Glacier for different years are shown in Figure 6(a) and 6(b). In order to eliminate aberrations and reveal the real trend of data series, a 7-day running mean is also shown in this figure. Broadly, the trend of changes in temperatures over the summer season is found to be almost similar for all the years, i.e., it follows increasing trend till July and then starts decreasing. It is observed that the changes in minimum temperature are more significant than the changes in maximum temperature. Diurnal variations in temperature indicate that, generally, maximum temperature is observed around 1400 hours, while the minimum is observed in the early morning. Over the ablation season for the years 2005, 2006 and 2007, average daily maximum and minimum temperatures were computed to be 14.9 °C and 3.7 °C, respectively, whereas average mean temperature was 9.3 °C for the same period.

The distribution of temperature over the ablation season has been studied. The mean monthly maximum temperatures for May, June, July, August, September and October were 13.9, 16.3, 15.9, 15.7, 14.4 and 12.0°C, respectively, whereas mean monthly minimum temperatures for these months were 1.2, 3.9, 6.6, 6.2, 3.5 and -0.4°C respectively. The corresponding mean monthly temperatures for these months were computed to be 7.5, 10.1, 11.2, 10.9, 8.9 and 5.8 °C, respectively. Based on the mean monthly temperature data, it is observed that the July was the warmest month of ablation season in the study area for three years.

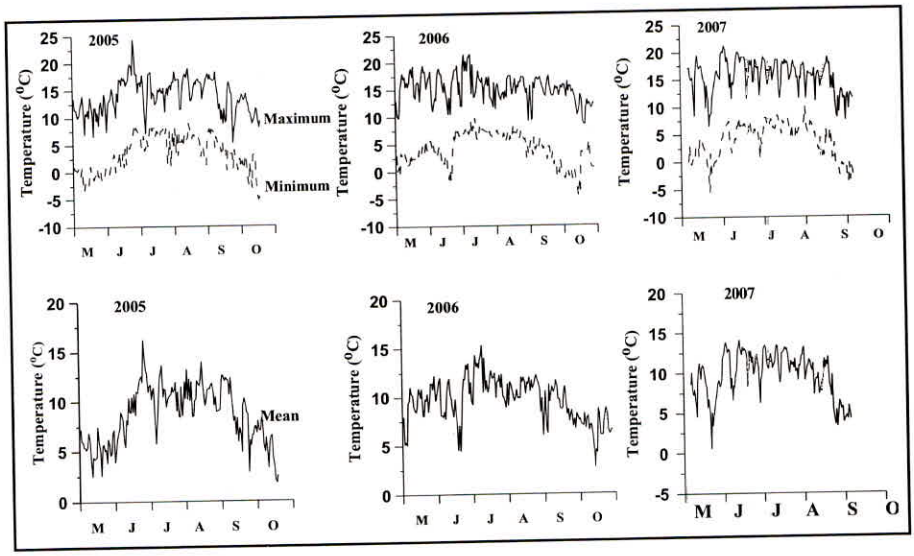

Figure 6 : (a) Daily maximum and minimum air temperatures and (b) daily mean temperature observed during different summer seasons (2005-2007) near the snout of Gangotri Glacier

7.4 Wind Speed and Direction

The wind speed and direction is an important parameter to support weather prediction in a basin. Also wind speed and direction can encourage the initiation of precipitation thunderstorms with a number of physical processes. The wind regime of the high altitude regions is one of the decisive factors affecting the transport of moisture, formation of clouds, occurrence of precipitation and melting of glaciers. In the mountain regions, during daytime the slopes of the mountains heat up rapidly because of intense insolation and warm air moves up along the slope, while nocturnal radiation brings a rapid cooling of the mountain slopes resulting into the cooler air blows into the down valley. The daytime wind blowing from the valley towards mountain is also known as up valley wind and the nighttime wind blowing from the mountains towards valley is known as down valley mountain wind. The upslope valley wind in the mountain areas accelerates the cloud formation processes.

In the present study, the wind speed and directions in the study area were observed using the anemometer at the Bhojwasa site for four times a day: 0830, 1130, 1430 and 1730 hours. Availability of wind data at different time intervals made it possible to study the changes in wind speed and direction on different time scales

and also helped in determining the daytime and nighttime wind regimes. Daytime (0830-1730 hours), nighttime (1730-0830 hours) and mean daily wind speeds (0830-0830 hours) observed for different years are shown in Figure 7. The monthly mean wind speeds for May, June, July, August, September and October were 7.8, 7.2, 6.3, 6.1, 5.9 and 7.3 km/hr, respectively. Average wind speed for the whole season was found to be 6.6 km/hr. Wind directions observed over the melt period for different seasons have been depicted through wind roses (Figure 8 (a)-(e)). It shows that during the ablation season most of the time wind blew from northwest direction, i.e., from valley towards mountain. A change in the wind direction was noted after sunrise and late evening.

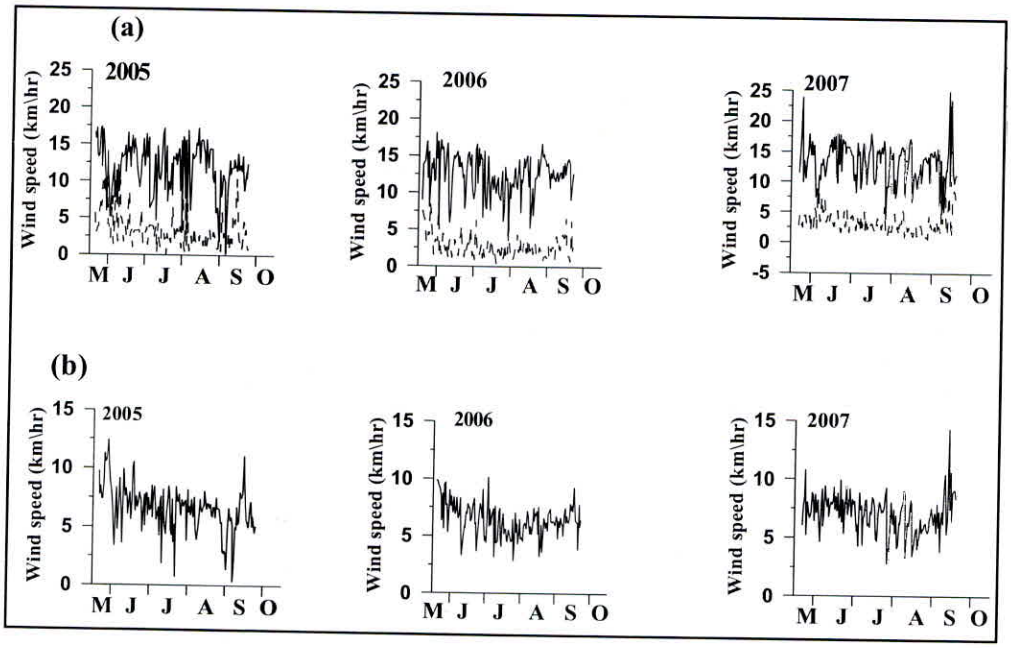

Figure 7 : (a) Daily daytime (0830-1730 hours) and night time (1730-0830 hours) (b) daily mean wind speed (0830-0830 hours) observed near the snout of Gangotri Glacier during summer season 2005, 2006 and 2007.

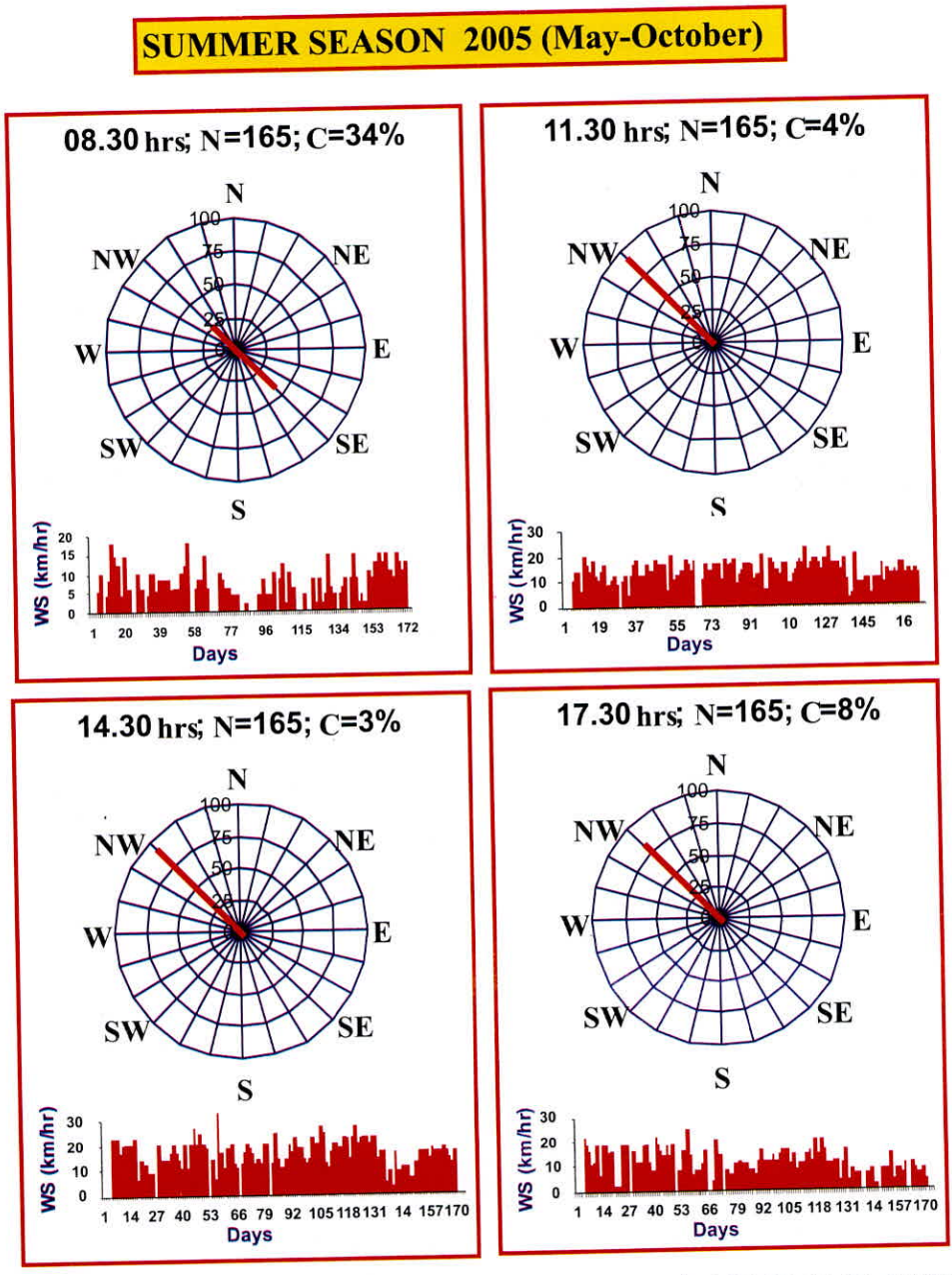

Figure 8 : (a) Wind speed (WS) and direction observed at 08.30, 11.30, 14.30 and 17.30 hours near the snout of Gangotri Glacier during 2005.

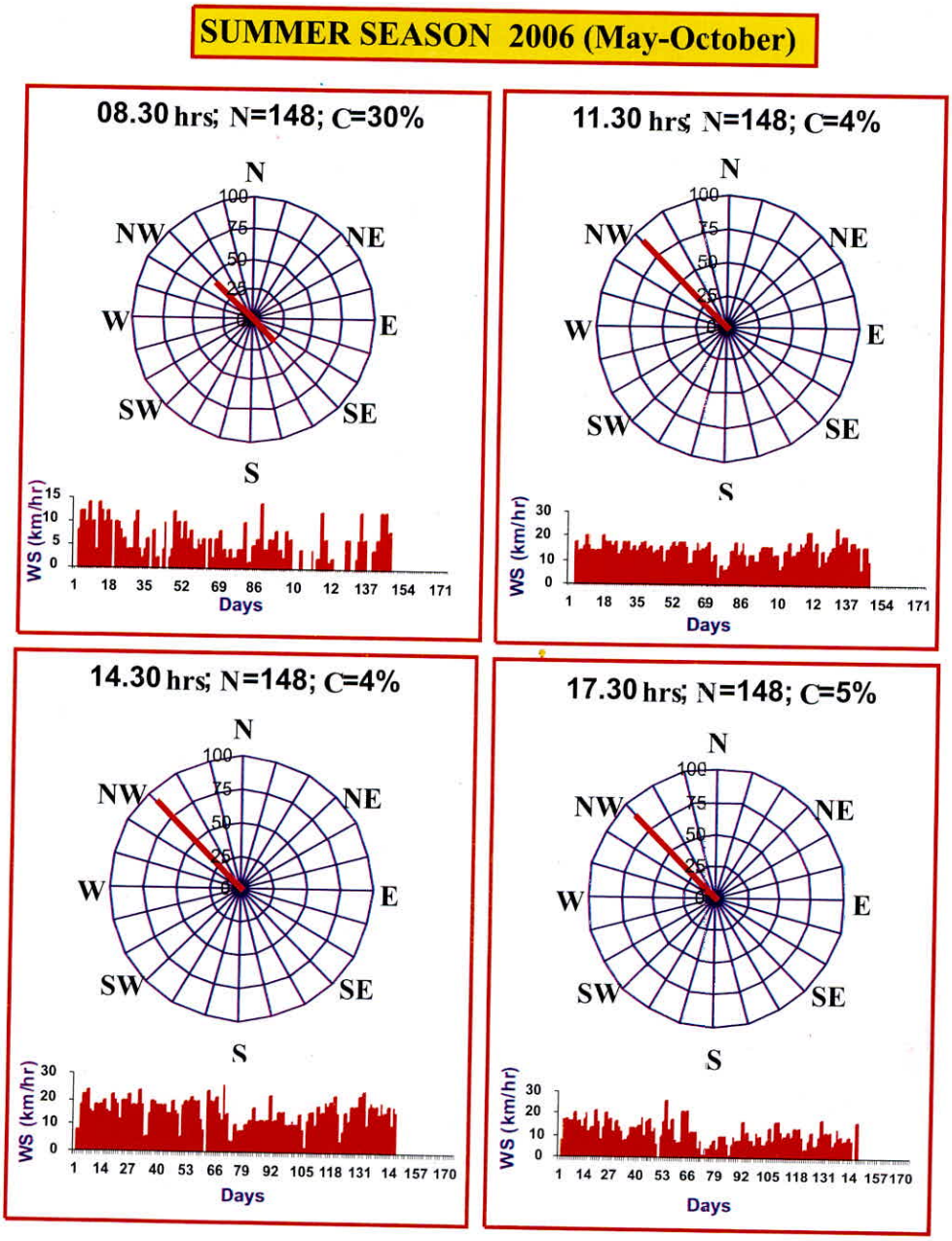

Figure 8 : (b) Wind speed (WS) and direction observed at 08.30, 11.30, 14.30 and 17.30 hours near the snout of Gangotri Glacier during 2005.

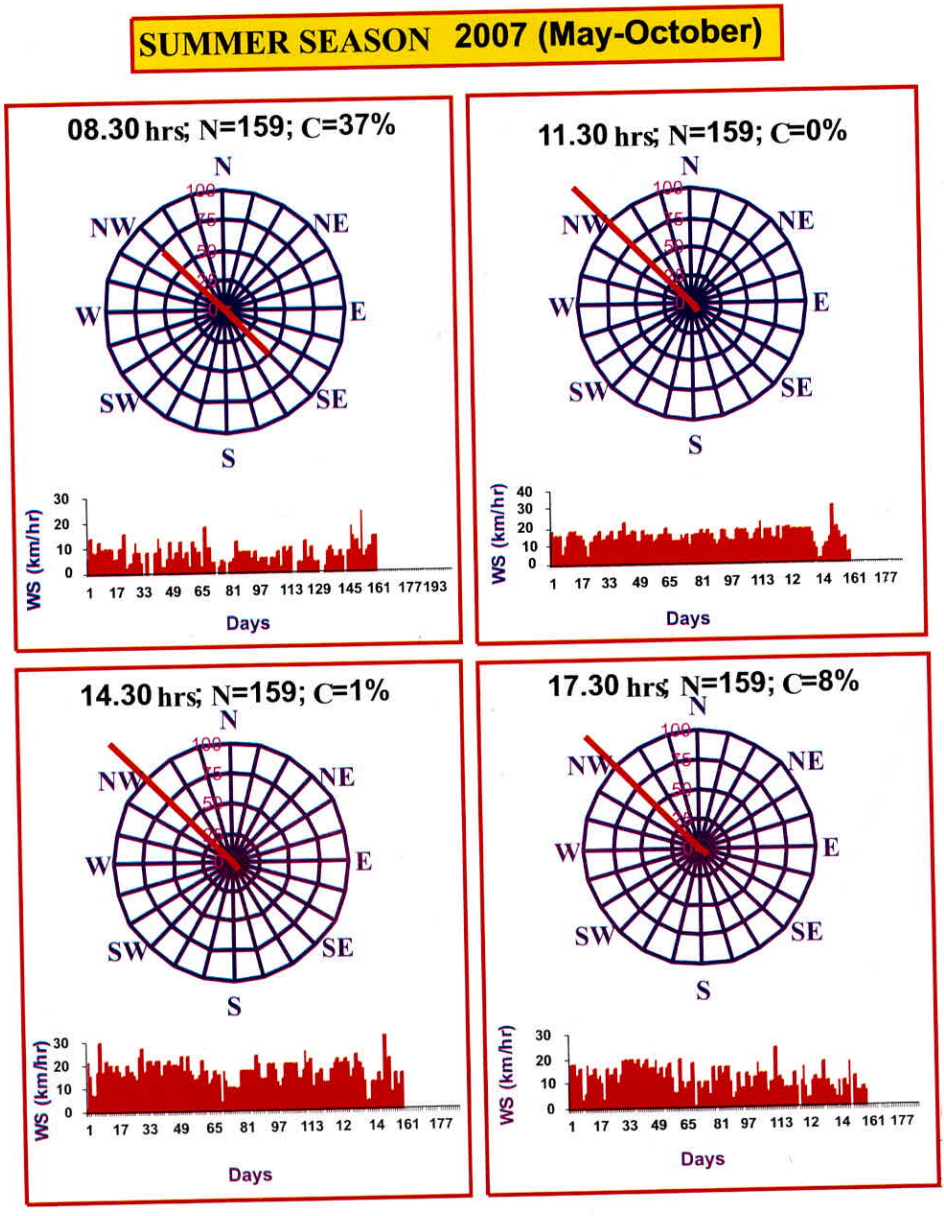

Figure 8 : (c) Wind speed (km/hr) and direction observed at 08.30, 11.30, 14.30 and 17.30 hours near the snout of Gangotri Glacier (Bhojwasa, 3800m) during Summer Season 2007.

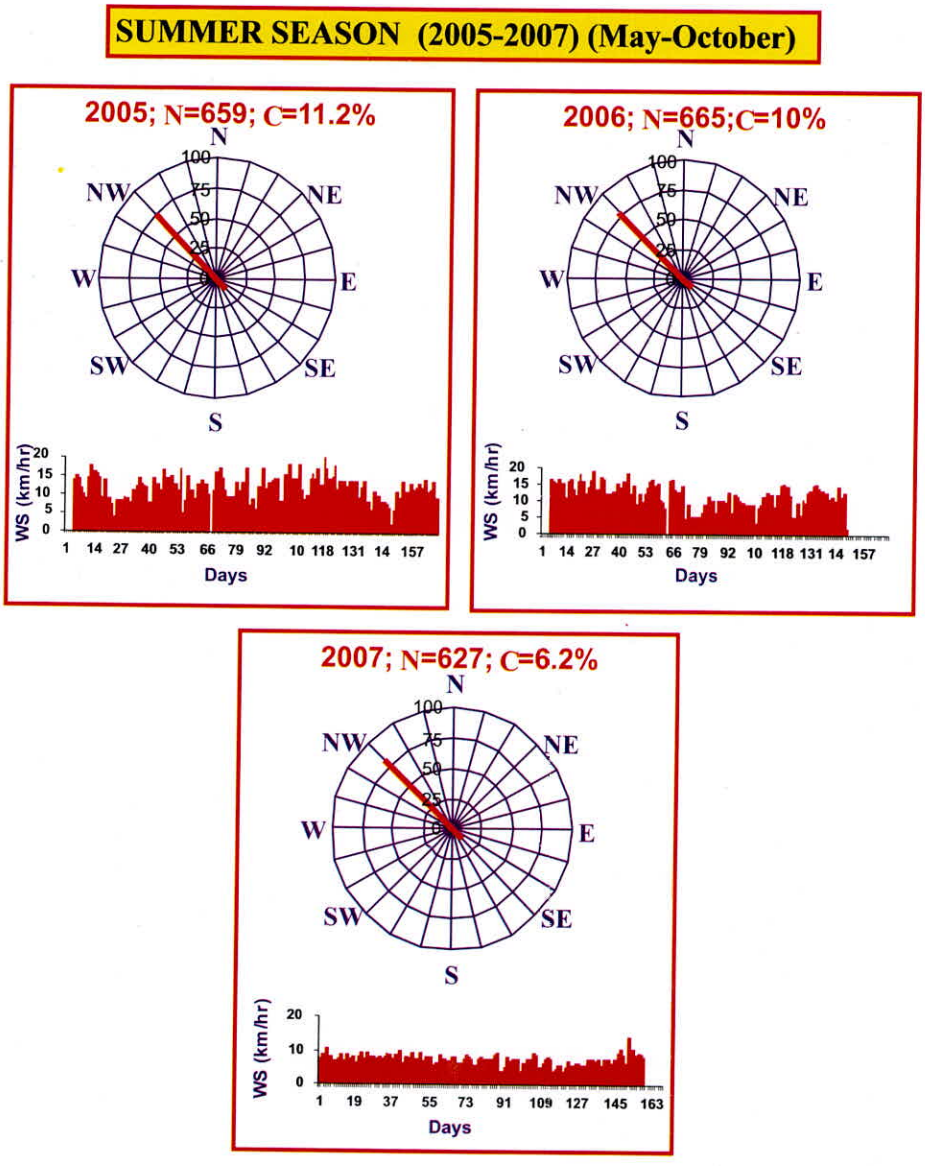

Figure 8 : (d) Average daily wind speed (WS) and direction observed near the snout of Gangotri Glacier during different summer seasons.

On the seasonal scale for three years, mean daytime and nighttime winds were 12.5 and 3.2 km/hr, respectively. In other words, average daytime wind speed was about 4 times higher than the nighttime wind speed. The diurnal variation in dayime wind speed shows that strong winds (>10 km/hr) blew during the daytime, being at maximum about 15 km/h at 1430 hours (Figure 9)

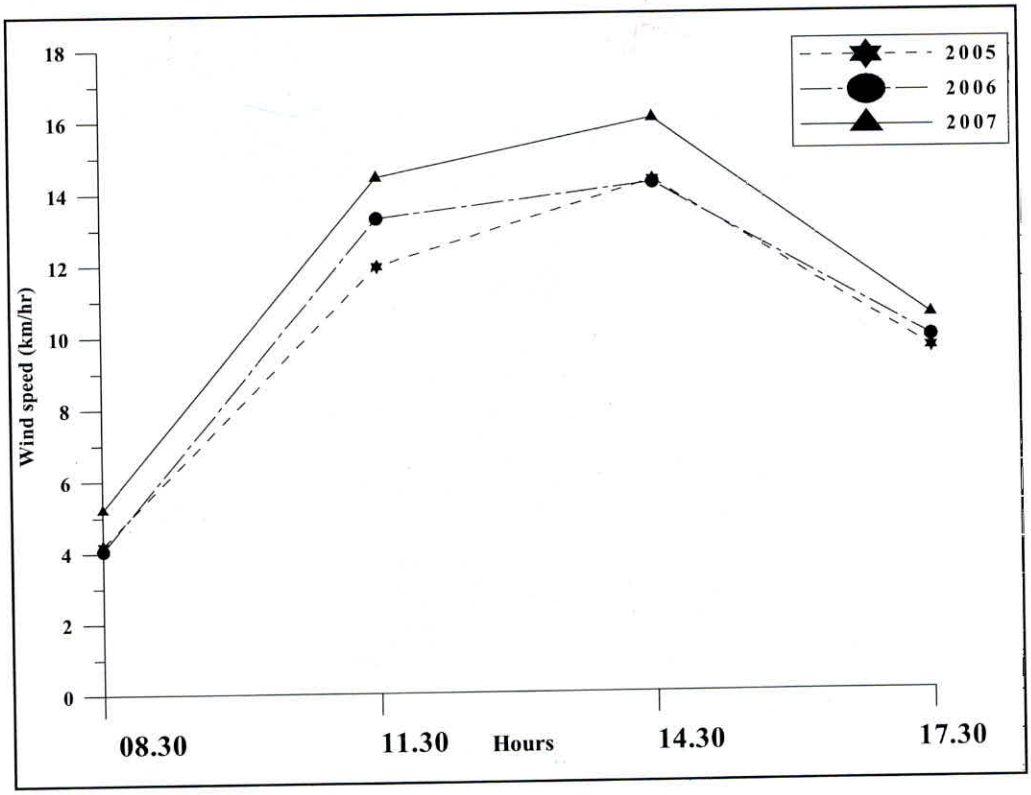

Figure 9 : Diurnal variation in wind speed at different hours observed near the snout of Gangotri Glacier during 2005, 2006 and 2007 summer seasons.

7.5 Relative Humidity

Relative humidity is a function of temperature because the vapour pressure that determines relative humidity is a function of temperature. Cooling of air during night increases the relative humidity providing usually a maximum value in the morning when air temperature is minimum.

Relative humidity data were measured using hygrograph at the Bhojwasa site round the clock and then mean daily values were computed. Figure 10 (a) shows the daily mean relative humidity for different summer seasons. There were no significant changes in relative humidity from the year to year. Over the study period, daily values of relative humidity ranged between 22-100%. Maximum humidity was always associated with the low air temperature and high rainfall and *vice-versa* was true for the minimum humidity. Mean monthly relative humidity was 70, 75, 89, 88, 79 and 65% for the months of May, June, July, August, September and October, respectively. As compared to the mean monthly relative humidity for the month of July and August, their values are lower for the month of May and June whereas, its value is minimum in the month of October. These results suggest lower moisture content in the air (low relative humidity) in the beginning (May) and end (October) of the ablation season. But for the monsoon months (June-September) relative humidity was quite high suggesting high moisture content in the air. Average relative humidity over different summer seasons varied between 77-83%, respectively.

7.6 Sunshine Hours

Sunshine duration with temperature data is used in snowmelt and evaporation computations in few hydrological models. Total bright sunshine hours are a useful extra parameter against which to interpret other climate statistics. Daily sunshine hours were recorded at Bhojwasa site using the sunshine recorder. The sunshine hours for the ablation season for the years 2005, 2006 and 2007 are presented in Figure 10 (b) On average, for May, June, July, August, September and October, the sunshine hours were observed to be 5.7, 5.8, 4.5, 4.8, 5.3 and 6.8 respectively. Results indicate that study area experienced maximum sunshine hours in October when the rainfall is either negligible or nil.

7.7 Evaporation

Estimates of evaporation are of great importance to hydrological modeling and hydro meteorological studies. Factors affecting the rate of evaporation from any basin can be broadly divided into two groups, meteorological factors and surface factors. Atmospheric temperature, wind velocity, wind direction and relative humidity are the main meteorological factors that control evaporation from the basin.

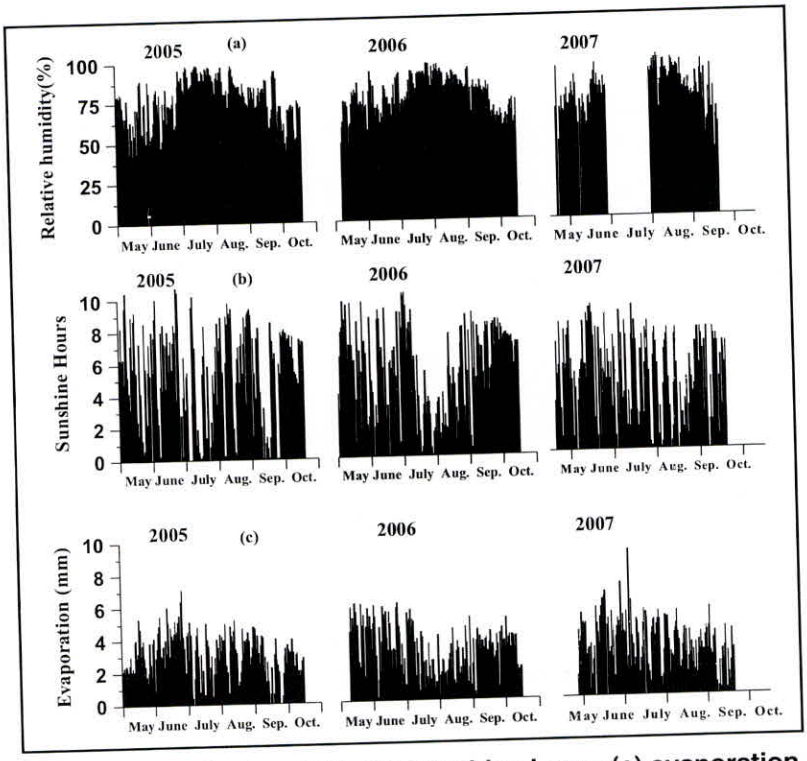

Figure 10 : Daily (a) relative humidity (b) sunshine hours (c) evaporation observed for different months near the snout of Gangotri Glacier during summer season 2005, 2006 and 2007.

Perhaps the simplest way of measuring evaporation is with an evaporation pan. A pan evaporimeter was installed at the meteorological observatory located at Bhojwasa. Daily pan evaporation records over the ablation season near Gangotri Glacier are shown in Figure 10 (c). Mean daily pan evaporation observed is 3.5, 4.1, 3.0, 3.0, 2.7 and 2.8 mm for the month of May, June, July, August, September and October, respectively. Evaporation was maximum in May and minimum in the month of August. The lower relative humidity, high sunshine hours and high wind speed are responsible for higher evaporation observed for May, while low evaporation in August is possible due to less number of sunshine hours. Mean monthly total evaporation during 4 ablation period was 81.5, 119.0, 92.7, 91.4, 81.6 and 44.4 mm for the month of May, June, July, August, September and October, respectively. The total pan evaporation during the summer season 2005, 2006 and 2007 was 244.6, 357.1, 278.1, 274.3, 244.9 and 133.3 mm, respectively. Based on the total records, mean daily evaporation for the ablation season as a whole was recorded to be 3.2 mm.

8.0 MONITORING OF RIVER GAUGE AND DISCHARGE DATA AND ITS ANALYSIS

8.1 Measurement of gauge and discharge data and development of stage discharge curve.

A Gauge and Discharge site has been estabilished at River Bhagirathi near Bhojwasa. In order to measure the water level data, an automatic water level recorder was installed on the stilling well installed near the river bank has been utilised. The chart daily mounted on the stilling well is utilised for deriving the hourly gauge values for each day. Due to high rate of suspended sediment in the flowing water, sediment was deposited in the stilling well and needed its cleaning time to time. The frequency of cleaning of sediment was about once in 15 days, except peak melt period. During peak melt period, sediment was removed from the well at least once a week. The description about the establishment of the gauging site and stilling well are given in (NIH-ES/91/12/97). A view of gauging site is shown in Plate 10.

A graduated staff gauge was also installed on the gauging site near the stilling well for manual observations of water level. A calibration was made between water levels observed at the staff gauge and water levels in the well. Manual observations of water levels were made during day and night time. This manual data set was used for cross checking of recorded level fluctuations in the river flow. Wooden floats were used to compute the velocity of flow and the time travelled by the floats was recorded. The float travelling length at the gauging site was about 20 m. For accuracy in velocity, the readings were repeated at least three times and an average value was adopted for further computations. The surface velocity of streamflow was observed in the range of 0.5 to 4.5 m/s, being maximum during peak melt period. For the measurement of water velocity the channel was divided into four segments. Further, because surface velocity of flow is higher than the mean flow velocity, therefore, the mean flow velocity was determined by multiplying the surface velocity by a factor of 0.90. The cross-section area of the channel was determined with the help of sounding rods in the beginning of the season and was rechecked at the end of the season before closing the investigations. A typical Cross section observed at the gauging site on 18th October 2005 is shown in Plate 11. For measurement of discharge, velocity-area method was used to estimate the flow in the river.

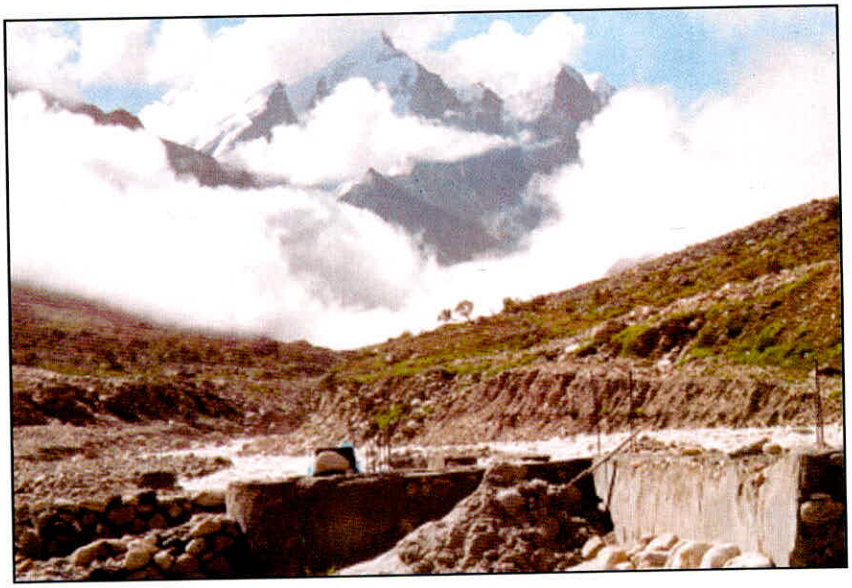

Plate10: Gauging site established by NIH near the snout of the Gangotri Glacier

Plate11: Cross section observations from the Gauging well at Bhagirathi River near Bhojwasa.

A stage-discharge relationship for the gauging site was developed analysing the observed gauge and corresponding discharge data. This relationship was used to compute the hourly discharge values corresponding to the hourly gauge values for which no discharge observation were made. Figure 11 shows a stage-discharge relationship developed for ablation periods (2005-2007). Such relationships were developed for each summer season separately and used to convert water levels into discharges. The computed hourly discharge values for a day are averaged in order to estimate the daily average discharge values. Figure 12 (a) illustrates the daily average discharge hydrograph at the gauging site for the ablation seasons of the year 2005 to 2007. Monthly mean values of the discharge were computed from the daily mean values for each month of the ablation season. Figure 12 (b) shows the bar chart of the monthly mean values for the ablation seasons of the year 2005 to 2007.

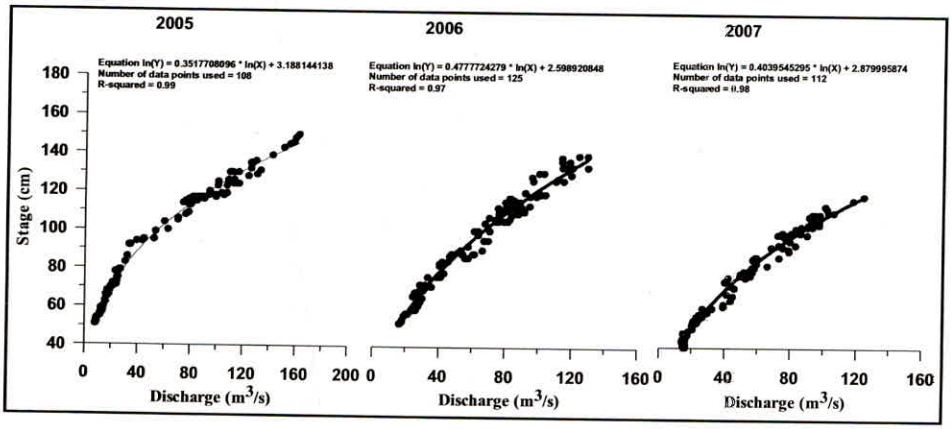

Figure 11 : Stage-Discharge relationship curve for different summer seasons 2005 2005, 2006 & 2007 near the snout of Gangotri Glacier.

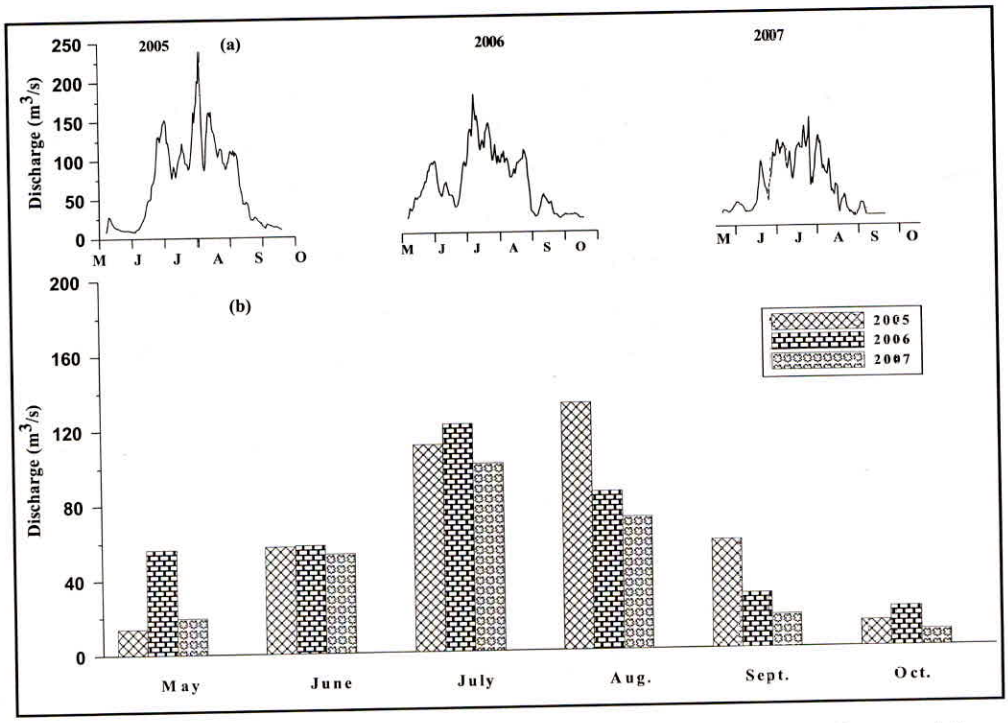

Figure 12 : (a) Daily mean discharge and (b) monthly discharge observed for different months near the snout of Gangotri Glacier during different summer seasons (2005-2007).

8.2 Distribution of Streamflow and Water Yield

The main sources of runoff from the Gangotri Glacier area are: (i) melting of ice and snow, and (ii) rainfall. In the study area, the contribution of the rainfall is less than the contribution of the melting of ice and snow during the ablation season. Melt water hydraulic systems of the glacier include supraglacial system, englacial and subglacial system. The first two systems exhibit considerable fragility, being easily susceptible to rapid change, whereas the third system is more resistant to alteration unless ice conditions are dramatically transformed. Finally total melt water emerges out as integrated runoff through the snout of the glacier. In the present case, the runoff drained from the glacier into a single melt stream.

From the figure 12 (a) it is observed that the daily mean discharge shows increasing trend from May onward and reaches to its maximum value sometimes in the month of July/August during the years 2005 to 2007. Subsequently it shows

the decreasing trend till the end of the ablation season.

Table 4: Total seasonal volume of discharge observed during different melt seasons (10th May - 11th October).

Year	V = Seasonal Volume MCM	Date of peak
2005	999	**4.08.05**
2006	931	**8.07.06**
2007	689	**1.08.07**
Mean	**873**	-
SD	**162.94**	-
CV	**0.2**	-

Table 5: Date of pass of maximum peak discharge during the melting seasons.

Year	Dis cumecs	Value of Centre of Gravity	Centre of Gravity pass on date	Values of Gravity on date of pass
2005	11447.9	**83**	31/07/05	166.81
2006	10610.2	**70**	18/07/06	108.38
2007	7970.83	**72**	20/07/07	107.50

Based on the three years (2005 to 2007), the average monthly discharge computed for May, June, July, August, September and October (upto 10th of October) are 28.7, 56.3, 110.9, 95.8, 34.8 and 12.7 m^3/s, respectively. The average monthly volume of water flowing from the gauging site are 69.2, 142.7, 290.8, 256.6, 90.3 and 21.3 MCM for May, June, July, August, September and October are, respectively. Distribution of runoff volume indicates maximum runoff in July (33.39%) followed by August (29.46%). As such, July and August contribute about 62.85% to the total melt runoff. High melt rate is observed due to dry weather conditions in the study area.

Over the whole ablation season, daily mean discharge varied from 8 to 239 m^3/s. Maximum mean daily runoff from the basin in 2005, 2006 and 2007 was observed to be 238.5, 177.6 and 149.0 m^3/s, respectively. Estimations were also made in terms of water yield from the study basin. Monthly water yield was estimated

to be 0.12, 0.26, 0.52, 0.46, 0.16 and 0.04 m for May, June, July, August, September and October, respectively. The total melt water yield for 2005, 2006 and 2007 was 1.77, 1.68 and 1.25 m, respectively, whereas melt water yield during the complete study period is about 1.56 m.

In terms of volume, the total melt water from the Gangotri Glacier for the ablation period was estimated to be 999, 931 and 689 MCM for 2005, 2006 and 2007. Results indicate that out of three ablation periods, maximum total and minimum total runoff was generated during summer 2005 and summer 2007, respectively, whereas maximum daily and minimum daily flow was generated during summer 2005 and summer 2007, respectively. The respective date of peak volume discharge were found to be in August for the ablation periods of 2005 and 2007, July was the peak discharge month for the year 2006 (Table 4).

In order to understand the runoff generation trends and its variability from the year to year, a long-term discharge series is required. It is suggested that a broader database must be established for the Gangotri Glacier, which contributes a substantial quantum of runoff in the Bhagirathi River.

8.3 Melt Water Storage Characteristics of Gangotri Glacier

In the glacierized basins only a portion of the melt water produced each day emerges as runoff from the snout on the same day. The remaining melt water is stored within the glacier and this stored water drains out gradually on subsequent days. Thus runoff observed at particular time is generated by a combination of melting occurred on the same day and on previous days. The occurrence of maximum streamflow in the glacierized rivers in the late afternoon or evening clearly suggests that a major part of the melt water produced during the day period reaches the snout after few hours. The storage characteristics of the glaciers are responsible for delayed response of melt water generated over the glacier surface into runoff. The size of the glacier including ablation and accumulation area of the basin, extent of snow cover, depth of snow over the glacier and drainage network of the glacier are the important factors which control the magnitude of the water runoff.

Melt-water storage characteristics of the glacier have direct impact on the distribution of runoff. To determine the storage characteristics of the Gangotri Glacier,

continuous monitoring (24 hours) of the glacier melt runoff was made. Daily streamflow records were divided into daytime flow (0900-2000 hours) and nighttime flow (2100-0800 hours), respectively. Daily rainfall and daily mean daytime and nighttime flow for different years are shown in Figure 13(a), and Figure 13 (b) respectively, whereas monthly discharges for the respective periods are presented in Figure 14. The magnitude of the streamflow during daytime and nighttime indicates that in the beginning and at the end of the melt season, volume of the nighttime flow is very close to the daytime flow, but during the peak melting season, nighttime flow reduces in comparison to the daytime flow. As shown in Figure 14, similar trends of daytime and nighttime flows were observed for all the years. As such, very little or no melting takes place during the nighttime, but still there was significant flow observed from the glacier during the nighttime. This may be attributed to the storage characteristics of the Gangotri Glacier because of which the melt water of the glacier generated during the day time appears in the night at the gauging site. However, further investigations are needed to properly understand the variations in the storage characteristics over the melt season for this glacier.

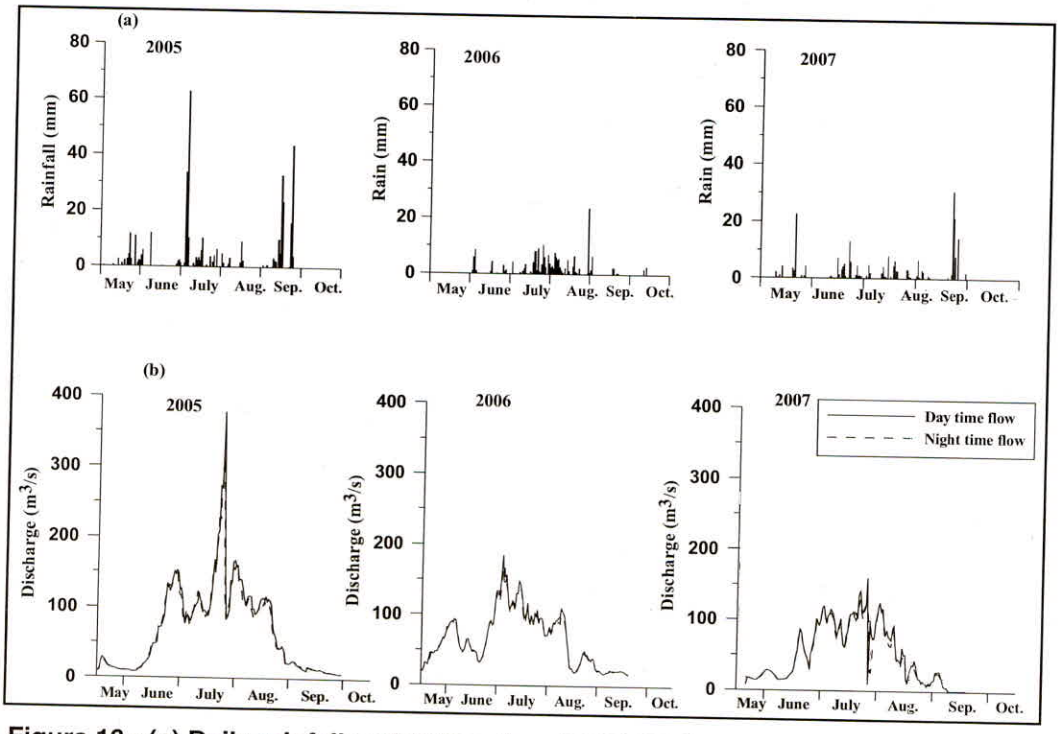

Figure 13 : (a) Daily rainfall and (b) Daytime (0900-2000) and nighttime (2100-0800 hours) mean discharge observed for different months near the snout of Gangotri during different summer seasons (2005-2007).

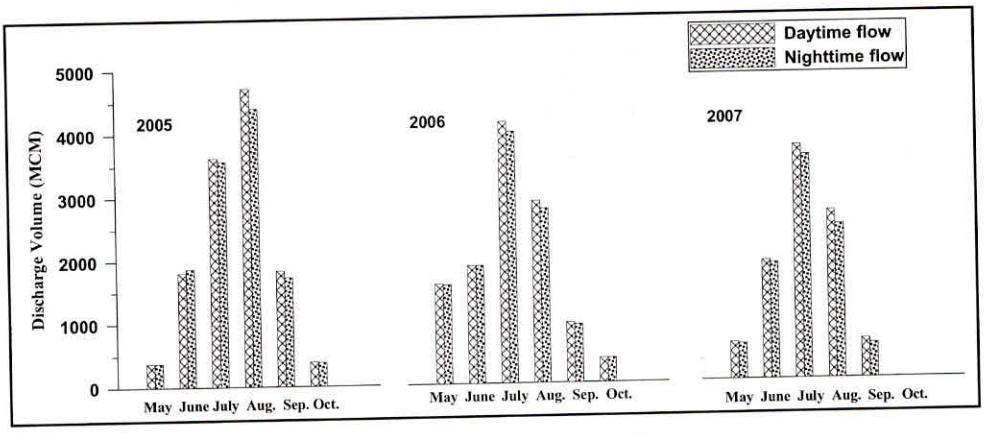

Figure 14 : Monthly distribution of daytime (0900-2000 hours) and nighttime (2100-0800 hours) discharge observed for different months near the snout of Gangotri during different summer seasons.

8.4 Diurnal Variations

For each month the average values of the flow are computed at a specified time. These average values provide the diurnal variations in discharge for the respective months. Figure 15 shows such variations for the ablation season during the year 2005-2007. The average flow starts rising in June and attains its maximum value in July and then subsequently starts declining. However, in the early and later part of the day, the average flows are almost flat as observed from the Figure 16. It indicates that there is no significant variation in runoff during these periods. The average flow shows the fluctuations with advancement of the ablation season.

Based on the distinct variations in the runoff characteristics, the ablation season can be divided into 3 parts: beginning of the melt season (May - June); peak melt season (July - August) and end of the melt season (September - October). Results suggest that during early part of the melt season the shape of the hydrograph is very much controlled by the depth and extent of snow cover in the basin. Presence of large extent of seasonal snow over the glacier causes dampening effect on the melt runoff. It results in a much delayed response of the melt because melt water passes through the snowpack and flows as interflow after reaching the ground surface. Consequently, in the early and later part of the season, both limbs of hydrograph are almost flat. The flatness of the hydrograph representing no significant

changes in the later part of seasons is because of little or no melting due to cold temperatures during this period. As the ablation season advances intense melting takes place due to availability of higher radiation and larger extent of exposed glacier ice. The extent of ice exposed area increases on the expense of depletion of snow cover as the melt season progresses. The distribution of average flows at hourly interval indicates that maximum discharge, $Q_{max,}$ was recorded between 1800 and 2100 hours, whereas minimum flow, $Q_{min,}$ occurred between 0700 and 1000 hours (Figure 15). It shows a trend of early occurrence of Q_{min} and Q_{max} during the peak melt season, while these are delayed during early and later part of the melt season.

8.5 Melt-Runoff Delaying Characteristics: time-lag and time to peak

The melt water generated in the glacierized basin appears as runoff at the snout of glacier with a time-lag. Changes in delaying characteristics of the runoff over the melt season can be understood by studying the variations in time to peak (t_p) and time-lag (t_l) between melt generation and its emergence as runoff from the data observed during 2005-2007. The time to peak is the time elapsed from the beginning of the rising limb to the peak discharge whereas time lag is the difference between maximum temperature and maximum discharge. The magnitude of t_p and t_l depends on the melt water storage and drainage characteristics of the glacier. As a first approximation it can be safely assumed that maximum melting occurs when solar radiation is maximum. Following this approximation, the time-lag between maximum melting and maximum runoff can be determined. For each month of an ablation season during the period 2005 to 2007, clear days have been identified considering the bright sunshine hours more than 5 hours and clear sky. For each clear day during a month tp and tl values are computed. Average values of tp and tl for each month are obtained averaging the tp and tl values computed for the clear days in the respective months. Figure 16 (a & b) illustrates the variation of tl and tp over different months during the ablation season. As shown in these figures, both t_l and t_p follow the similar trend of changes over the ablation period. They are higher in the beginning and in the end of ablation season as compared to the middle of the ablation season. Depending upon the melting conditions, t_l varied between 4 to 8 hours, whereas t_p varied between 10 to 12 hours over the entire ablation season.

In the early stages of the ablation period, poor drainage network and stronger storage characteristics of the glaciers due to the presence of seasonal snow cover

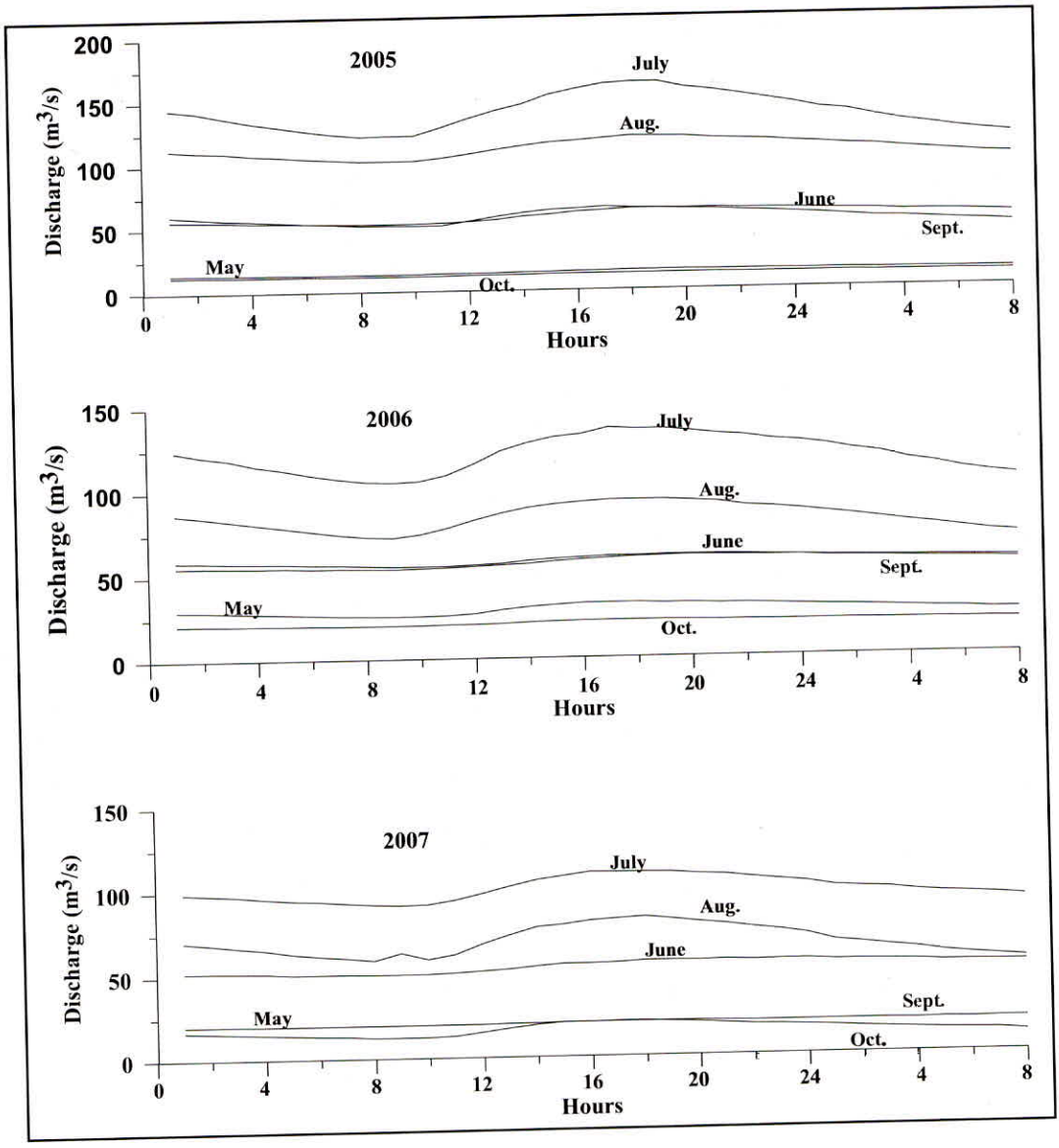

Figure 15 : Diurnal variations in the discharge observed near the snout of Gangotri Glacier during the ablation season 2005, 2006 and 2007.

results in a much delayed response of melt water, providing a higher t_l and t_p. The reduction in these parameters with advancement of melt season is possible because of depletion of snow (or exposing of glacier ice) and strengthening of drainage network of the glacier. As discussed above, Gangotri is a large glacier and stronger delaying response or higher time-lag for the Gangotri Glacier is very much likely

because of its large size. In the later part of melt season, as such very little or no melting takes place and water already stored in the accumulation area drains slowly providing again higher t_l and t_p.

In order to investigate the inter relationship between the variation in runoff and delaying characteristics of the glacierized basin, changes in the discharge ratio, i.e., Q_{max}/Q_{min} were computed over the ablation season. Here Qmax is the maximum flow derived from the flows on the clear days in a month during the period 2005 to 2007 whereas Qmin is the corresponding minimum flow. Figure 16 (c) shows the variation of this ratio over the months during the ablation season. As illustrated in Figure 16(c), this discharge ratio for the Gangotri Glacier varied between 1.0 and 1.5, indicating a large variation in the runoff over the melt period. A comparison of runoff delaying parameters with discharge ratio clearly indicates that changes in t_l and t_p during the melt season are inversely correlated with variations in discharge.

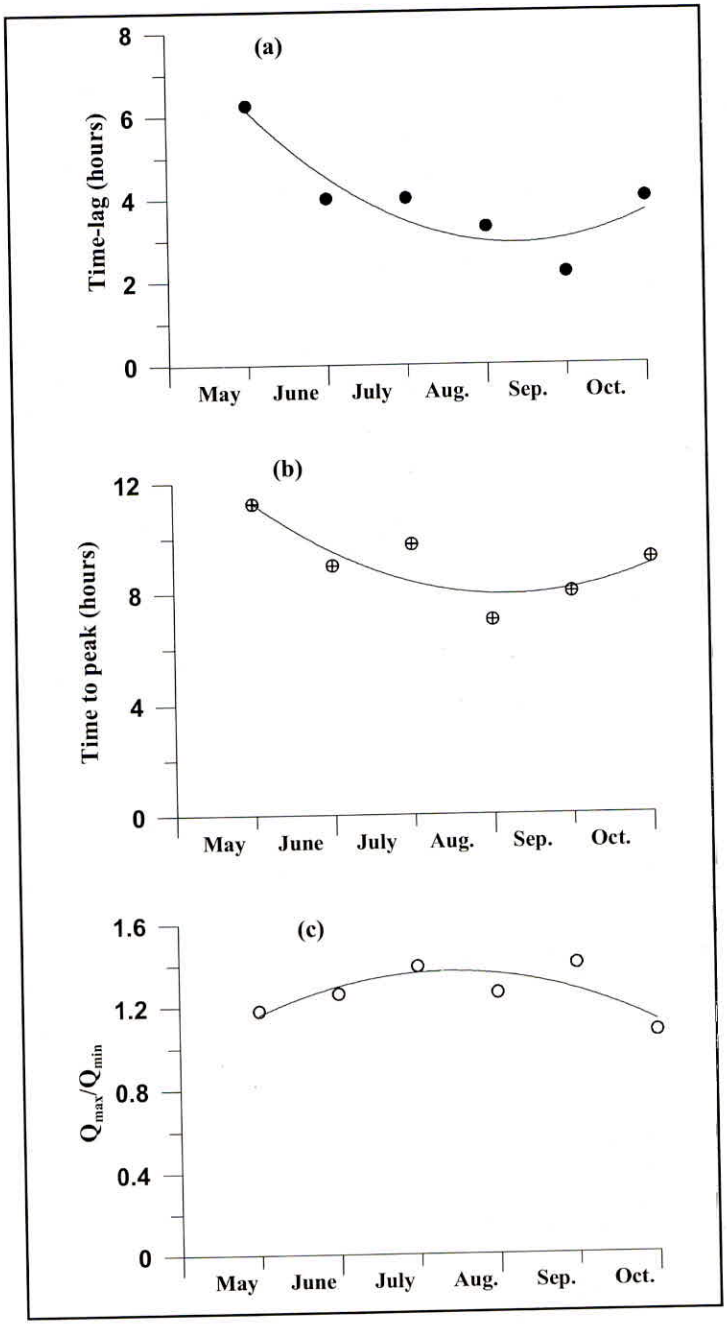

Figure 16 : Average value of (a) melt-runoff time-lag, (b) time to peak, and (c) discharge ratios for different summer seasons observed near the snout of Gangotri Glacier.

9.0 SUSPENDED SEDIMENT DATA COLLECTION AND ANALYSIS

The sedimentary system of the glacier can be defined in the terms of sediment sources, processes of erosion and entrainment, modes and medium of transport, sediment concentration and load in the melt water. Glacier melt streams transport a significant amount of sediment in the form of silt, gravel and boulders into the rivers and then to the reservoirs located in the downstream. Due to their own movement, glaciers transport enormous debris material in the form of moraines, which becomes the source of fine sediment and silt. Assessment of these sediments transported by the melt stream is important because it has direct influence on the capacity of the reservoirs. The glaciers melt water carries sediment as suspended sediment or bed load. Suspended sediment refers to the grains flow with water above the bed of channel and is considered as a characteristic of the turbulent flows. Suspended sediment concentration in the glacial streams reflects the availability of sediments. Bed load, which are bigger in size, refers to the grains swept along with the bed of a stream, in continuous or intermittent contact with the bed. In the present case, sediments transported as bed load are much less in comparison to the suspended sediment at the gauging site.

9.1 Sources of Sediment

The main sources of sediment production in the glacier fed channels are the glacier system, bedrock system and channel system. The glacier system includes sedimentation from different parts of the glacier such as the accumulation zone, ablation zone, snout and the lateral moraines, whereas bedrock system deals with glacier bottom ice and bedrock. These sediments transported by the glacier follow three basic routes: supraglacial, englacial and subglacial. Processes like sliding of rocks and debris, snow and glacier avalanches accelerate the transport of moraines and sediment. Over wide areas in the glaciated regions the bedrock is markedly abraded and becomes the important source of sediment transport.

Like all other Himalayan glaciers, Gangotri Glacier is also covered with boulders, moraines. Obviously, one of the important sources of sediment from the study glacier becomes the presence of sediment material like boulders, debris and moraines over the glacier surface (Plate 12). During the active melting period supraglacial material remains in contact with melt water and becomes a regular

source of sediment. The ablation zone of the glacier contributes a large amount of sediment because a large quantity of such material is found in this area and water travels by surface pathways in the ablation zone of the glacier. A part of the sediment material available on the glacier surface is also transported down through extensive longitudinal and transverse crevasses into englacial and subglacial tunnels. From the features of the surface texture of the lateral moraines, it could be expected that chemical and mechanical processes might also mobilise the lateral moraines sediment into the glacier melt stream.

9.2 Suspended Sediment Concentration

To determine the mean suspended sediment concentration, load, yield and particle size in the Gangotri Glacier melt stream, two water samples at 0830 and 1730 hours were directly scooped from the channel at the gauging site in a cleaned polyethylene bottle (500 ml). A sample was collected from the stream at about mid depth and filtered at the site itself using Whatman-40 ashless filter paper. The suspended sediment samples thus collected on the filter papers were properly packed in the self locking small polythene bags and details such as, time and date of sample collection, were marked on it. These packed samples were brought to the laboratory at the National Institute of Hydrology (NIH), Roorkee for further analysis. In the laboratory these sediment samples were dried. in an oven at 200°C for a period of 24 hours and then suspended sediment concentration (SSC) for each sample was determined by weighing the individual sample.

Suspended sediment concentration in the melt runoff from the study area was very high. Daily mean suspended sediment concentrations in the melt stream varied from 34 to 11093 ppm. Distribution of sediment transport over the ablation season was found almost like the distribution of streamflow. It begins to increase with discharge from May onwards, as the melting season advances, attains its maximum in July and then again it starts reducing. Daily mean suspended sediment concentration recorded at gauging site near the snout of the Gangotri Glacier for 2005, 2006 and 2007 are given in Figure 17(a). Mean monthly suspended sediment concentration, as shown in Figure 17(b), for May, June, July, August, September and October during the study period was 1628, 1753, 3262, 2231, 892 and 225 ppm, respectively. Maximum daily mean suspended sediment concentrations observed in May, June, July, August, September and October were 10200, 6096,

Plate 12: Debris covered ablation zone of the Gangotri Glacier

8590, 5286, 2513 and 807 ppm, respectively. For the entire melt season, the mean daily suspended sediment concentration was computed to be 1802 ppm. Data presented in the table 3 (a)-(e) in appendix – II indicate that discharge in the melt stream was less variable than suspended sediment concentration.

9.3 Suspended Sediment Load and Yield

Suspended sediment load (SSL) can be determined by multiplying SSC with discharge and changing the unit into tonnes. The variation in daily suspended sediment load and daily mean discharge during the ablation period is shown in Figure 18(a). Daily suspended sediment loads ranged between 22 and 120946 tonnes. The monthly distribution of suspended sediment loads for the different years is shown in Figure 18(b). Mean monthly total suspended sediment loads for May, June, July, August, September and October during the study period was found to be 162, 220, 1016, 603, 81 and 5×10^3 tonnes respectively. The total suspended sediment from the Gangotri Glacier was estimated to be 2.11, 2.53, and 1.96 $\times10^6$ tonnes for 2005, 2006, and 2007. The average total suspended sediment load for the melt season was computed to be 2.2×10^6 tonnes.

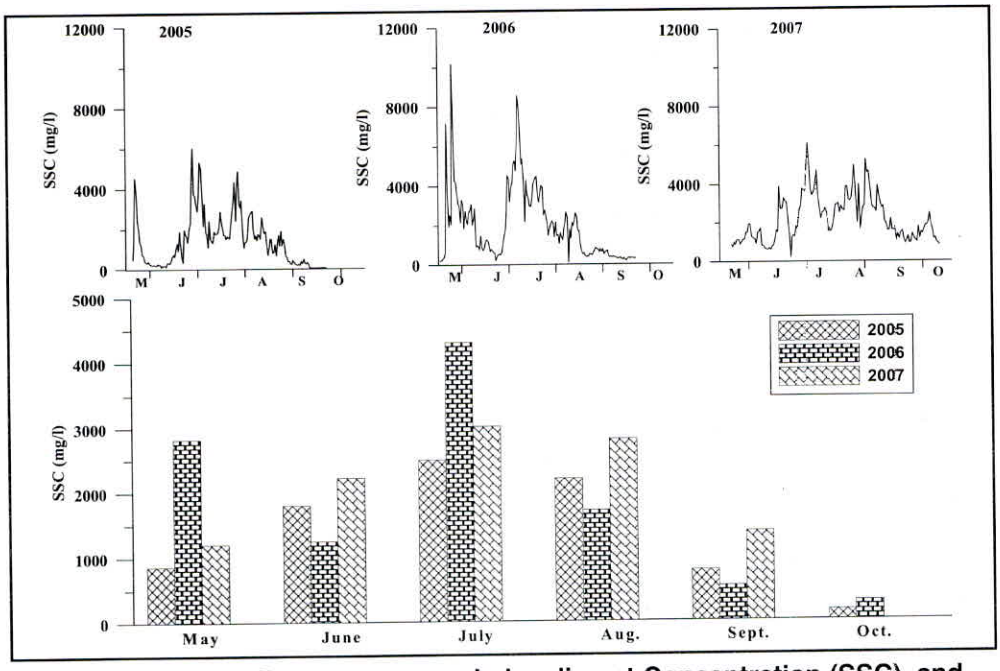

Figure 17 : (a) Daily mean suspended sediment Concentration (SSC), and (b) mean monthly SSC observed for different months near the snout of Gangotri Glacier during different summer seasons.

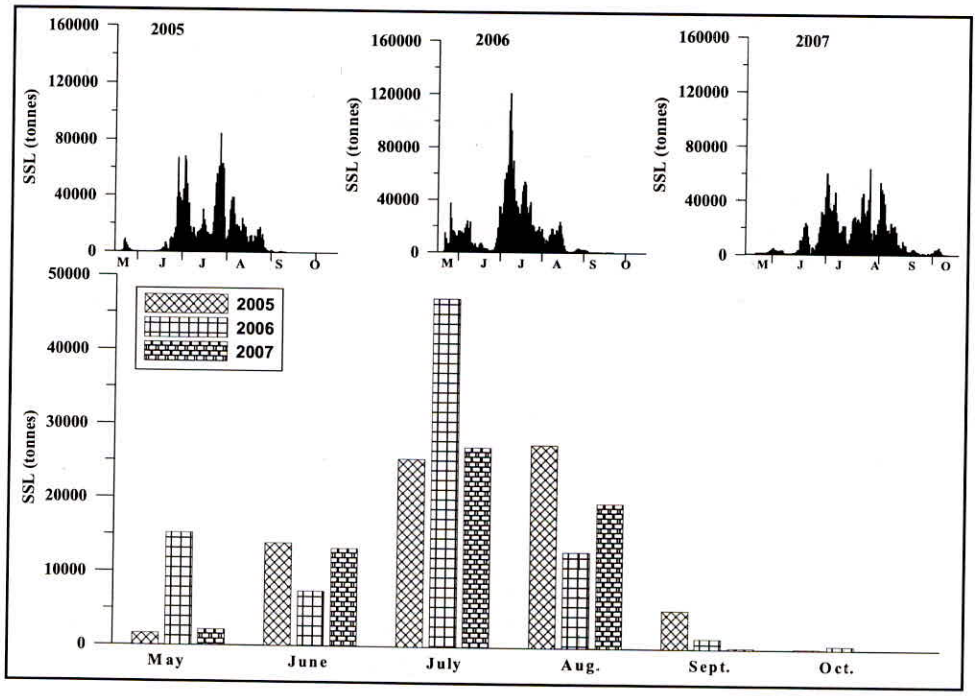

Figure 18 : (a) Daily mean suspended sediment Load (SSL) and (b) mean monthly SSL observed for different months near the snout of Gangotri Glacier during different summer seasons (2005-2007).

Proglacial meltwater has very high sediment yield in response to glacial and fluvioglacial erosion within the source catchment. The high sediment yields recorded from glacial meltwaters to some extent mask the high temporal variability that characterizes these inputs of sediment to the proglacial channel system. It shows wide seasonal and interannual variations, which are partly due to switches in the subglacial drainage system. Sediment yield can be affected by five factors, (1) basin geology and thus the erodibility of materials beneath the glacier, (2) climate and its effects on mass balance and runoff (3) glacier dynamics and thermal regime and their effects on erosion and sediment entrainment by ice (4) the percentage of glacier cover and its state of change, and (5) the type and extent of the subglacial drainage system in relation to the location and quantity of sediment available for transport. Sediment yields can be used to estimate long-term erosion rates. Assuming that the suspended sediment yield during the melt season can be used to represent the annual yield, the average suspended sediment yield for the Gangotri Glacier basin was computed to be about 4834 tonnes/km^2/yr.

9.4 Diurnal Variations in SSC

Changes in hourly SSC for different dates observed during ablation seasons 2005-2007 are shown in Figure 19. It can be noted that SSC is much more variable than streamflow. Variability in SSC increases with melt period, being maximum during the peak melt period. Figure 20 shows that even on non-rainy days or days having negligible rainfall, SSC varied significantly on the diurnal scale. A combination of intense melting and rainfall further provide higher variability in SSC. Maximum variations in SSC were recorded during the intense melt period, i.e., on 15th July 2005, 15th May 2006 and 15th August 2007 with respective value of SSC 2300 (mg/l), 5640 (mg/l) and 4008 (mg/l) whereas minimum variations were found during the end of the melt season, i.e., September and October each of the melting seasons 2005-2007. It is expected that large variations in SSC during the peak melt period perturbed relationship between SSC and discharge. It appears that local phenomena, like bed erosion due to development of sub-glacial channels, slumping of the heavily sediment laden portal ice into the stream, occurrence of rain, landslides and rockslides in the ablation zone attribute to the sudden increase in SSC. High variations in SSC from the glacierized basins have also been reported by several investigators (Collins, 1979; Østrem, 1975; Singh et al, 2005).

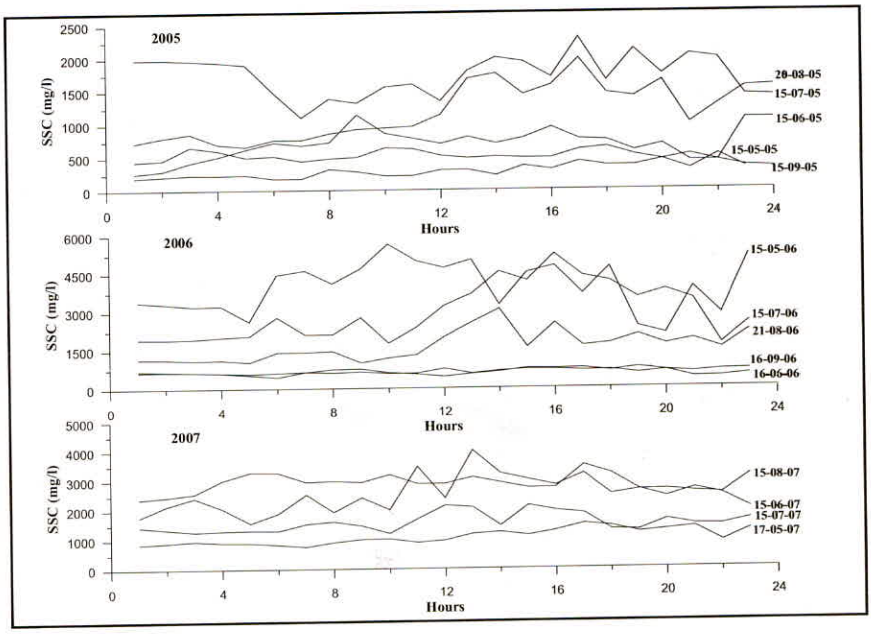

Figure 19 : Diurnal variability in SSC observed near the snout of Gangotri Glacier for selected clear weather days during different summer seasons (2005-2007).

Table 6: Diurnal variation in SSC of the selected clear weather days near the snout of the Gangotri Glacier during different summer seasons (2005-2007).

Year with Dates	Max. Value of SSC (mg/l)	Range (Peak hours)
15-07-2005	2300	1600-2000 Hrs.
20-08-2005	1980	1600-2000 Hrs.
15-05-2006	5640	0800-1200 Hrs.
15-07-2006	5220	1600-2000 Hrs.
15-06-2007	3488	0800-1200 Hrs.
15-08-2007	4008	1200-1600 Hrs.

9.5 Particle Size Distribution

The mineralogical compositions, accessibility for weathering, erosion and transport play perhaps the most important role in the grain size distribution of the suspended sediment. The analysis of the composition of suspended sediment in proglacial streams becomes important because this water is used for hydropower generation. The efficiency of these hydropower schemes is affected by the type and size of suspended particles and has also an impact on the trap efficiency of reservoirs. Less consideration has been given to grain size distributions of sediments transported or settled in glacial melt water streams. The variation in the particle size, collected near the snout of Gangotri Glacier shown in Figure 20 during the ablation periods 2005-2007.

In the present study, the particle size analysis was made using Malvern Mastersizer E Instrument which gives results in 32 size classes, ranging from 0.5 μm to 600 μm (0.0005 – 0.600 mm).Seasonal values of particle size classes are shown in Figure 22. The particle size analysis for entire ablation seasons 2005-2007 has been shown in Figure 21. The particle size analysis indicates that the suspended sediment load from the study area is predominately by the silt-sized (0.002 – 0.060 mm) grains (Table 7).

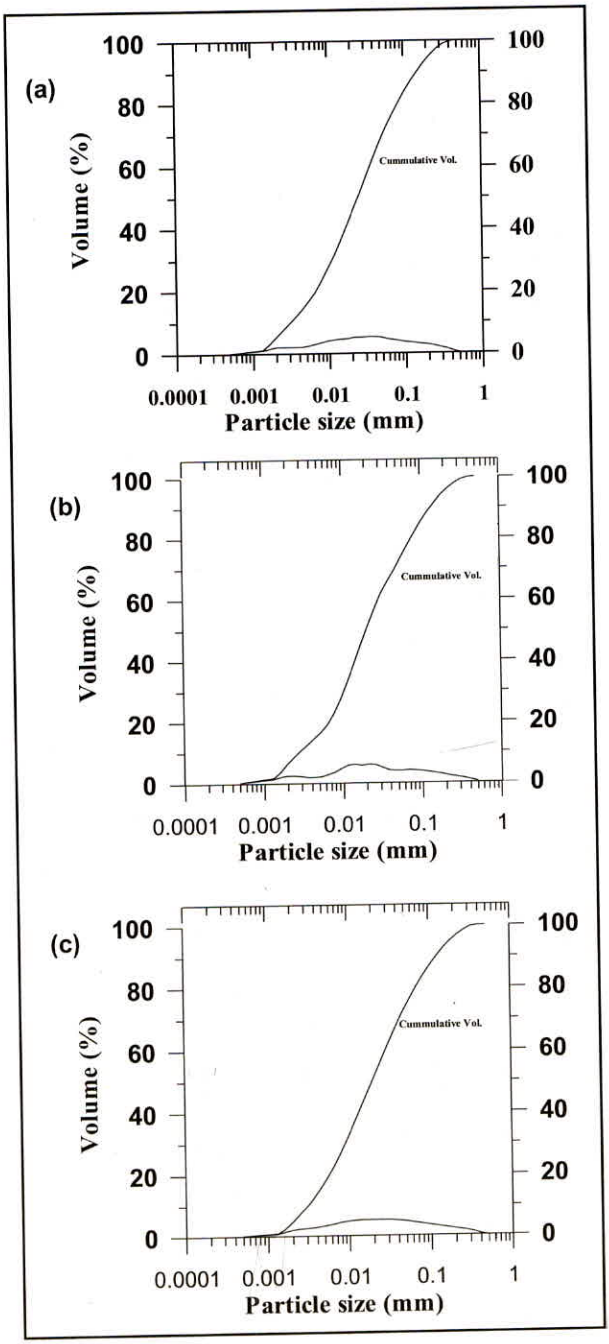

Figure 20 : Particle size distribution of the suspended sediment (a), (b) and (c) observed near the snout of Gangotri Glacier during different summer seasons 2005, 2006, 2007 respectively

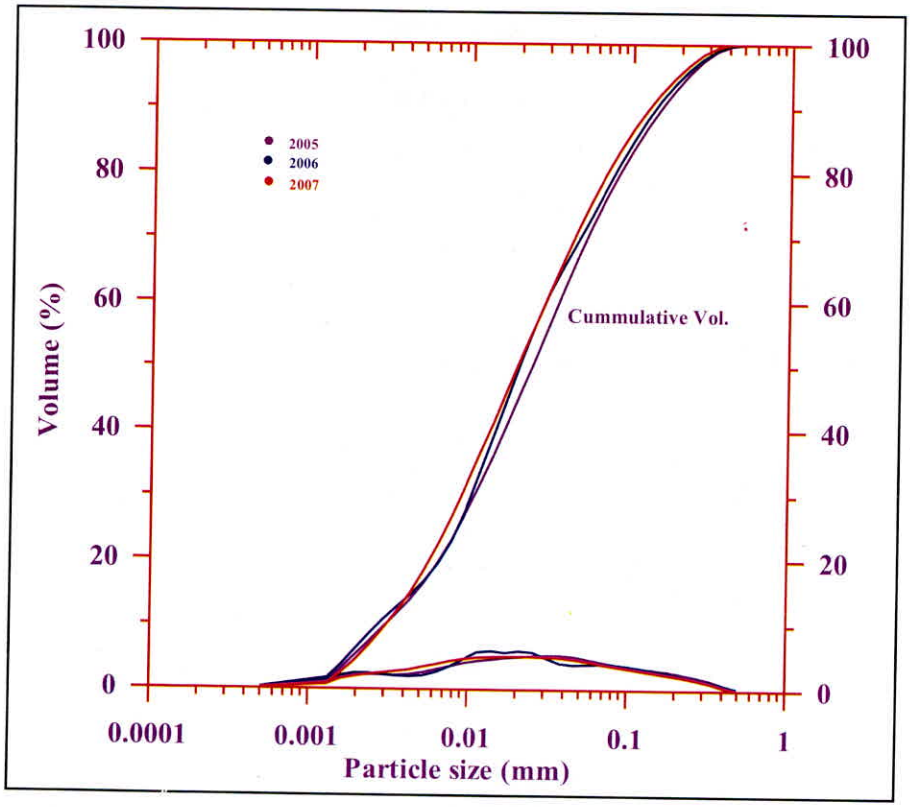

Figure 21 : Particle size distribution of the suspended sediment observed near the snout of Gangotri Glacier during different summer seasons (2005-2007).

Table7: Distribution of total particle size in the proglacial melt water stream near the snout of Gangotri glacier as a percentage of clay, total sand and total silt.

Range of Particle size	2005	2006	2007	Avg.(2005-2007)
(0.002-0.06mm) Total Silt	73.08	73.80	77.48	74.79
(0.06-0.6mm) Total sand	23.90	22.51	20.11	22.17
<0.002mm Clay	3.01	3.68	2.40	3.03

10.0 APPLICATION OF HYDROLOGICAL MODEL (SNOWMOD) FOR THE SIMULATION OF DAILY FLOW OF THE GLACIERIZED BASIN

The Himalayan river basins receive the flow contributions resulting due to snow melt, glacier melt and rainfall. The existing model structures for the rainfed river basins, as such, cannot be applied to simulate the flows for such basins. Hence a suitable structure of a hydrological model, capable of representing the various hydrological processes prevailing in the Himalayan region together with their interactions, is needed for simulating the flows of Himalayan rivers systems within the desirable accuracy. The Himalayan region has huge hydropower potential. In order to tap the hydropower potential, various minor, medium and major water resources projects are either already constructed or being planned for the near future. For better planning, designing and operation of these projects, the simulation of river flows using an appropriate hydrological model provides one of the important inputs. A hydrological model SNOWMOD developed at National Institute of Hydrology is capable of simulating the flows from the rain, snow and glacier fed river basins. One of the major objectives of the project is to simulate the flow from the glacierised basin utilizing suitable hydrological model. In order to achieve this objective SNOWMOD model has been selected considering the data availability and the objectives. This model has been applied for simulating the daily flow of the Gangotri glacier utilizing the spatial as well as temporal data. The temporal data has been monitored by the Institute during the ablation season whereas the spatial data have been derived analyzing the satellite imagery procured from NRSA. The concept and the structure of the SNOWMOD model are briefly described hereunder.

10.1 Concept and Structure of the Model

The hydrological model has been developed for daily streamflow for the mountainous basins having contribution from both melt and rainfall. The process of generation of streamflow from such basins involves primarily the determination of the input derived from the melt and rain, and its transformation into runoff. For simulating the streamflow, the basin is divided into a number of elevation zones and various hydrologic processes relevant to the melt and rainfall runoff are evaluated for each zone. The model deals with melt and rainfall runoff by performing the following three operations at each time step:

(I) extrapolate available meteorological data to the different elevation zones,

(ii) calculate rates of melt and/or rainfall at different points, and

(iii) Integrate melt runoff from snow and glacier covered area (SCA) and rainfall runoff from snow free area (SFA), and route these components separately with proper accounting of baseflow to the outlet of the basin. The model optimises the parameters used in routing of the melt runoff and rainfall-runoff. The structure of the model is shown through flow chart in Figure 22. Details of data requirement, computation of melt runoff and generation of streamflow from the basin are discussed below.

10.2 Input Data

The following physiographical and hydro meteorological data are required for computing the streamflow from the glacierized basin:

(i) Physiographical data: This data represents physical features of the basin, which includes total area of the basin, its altitudinal distribution through elevation zones and their areas, altitude of precipitation and temperature stations.

(ii) Hydrometeorological data: Daily precipitation, means air temperature, snow covered area/glaciated area and streamflow data.

The handling of physiographical and meteorological data has been discussed below

10.3 Division of Basin into Elevation Zones

In a mountainous basin, temperature and precipitation vary with elevation. In order to distribute the temperature in the basin, the study basin is divided into a number of elevation zones depending upon the topographic relief of the basin. For the purpose of computation of different components of runoff, each elevation zone is treated as a separate watershed with its own characteristics. Total streamflow for the whole basin is obtained by synthesizing the runoff from all elevation zones. In the present study, the digital elevation model (DEM) of the study basin was prepared and used for preparing the area-elevation curve of the basin. The basin was divided into 9 elevation zones with an elevation difference of 500 m.

10.4 Precipitation

The distinction between rain and snow for each elevation zone is important

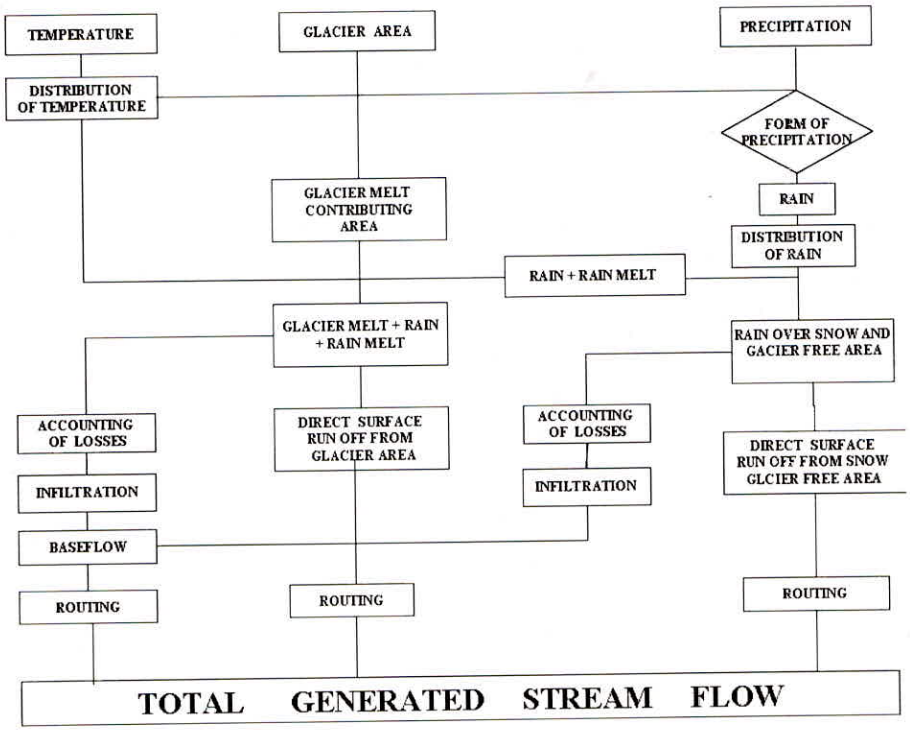

Figure 22: Flow chart of the developed conceptual hydrological model for the glacerized basin.

for all the snowmelt models because precipitation falling in the form of rain and snow behaves differently in terms of contribution to the streamflow. The contribution of rain to the streamflow is faster than that of snow because snow is stored in the basin until it melts, whereas rain almost immediately contributes to streamflow. The temperature in a particular elevation zone decides the form of precipitation and model handles it accordingly. A critical temperature, $T_{c,}$ is specified in the model to determine whether the measured precipitation was rain or snow. Therefore, value of T_c is usually selected slightly above the freezing point. In the present study, T_c = 2°C is considered. The algorithm used in the model to determine the form of precipitation is given below.

if $T_m \geq T_c$, all precipitation is considered as rain,
if $T_m \leq$ 0°C, all precipitation is considered as snow,

where T_m is the daily mean temperature. In case, $T_m \geq 0°C$ and $T_m \leq T_c$, the precipitation is considered as a mixture of rain and snow and their proportion is determined as follows

$$Rain = (T_m / T_c) \times P \quad (1)$$

$$Snow = P - Rain \quad (2)$$

where P is the total observed precipitation. The distribution of precipitation with altitude was not considered in the present study simply because information on precipitation distribution is not available.

10.5 Melt, Temperature and Degree-days

For the Himalayan basins, availability of limited data has to be taken into consideration when approach for computing melt is adopted. Estimation of melt using energy balance approach requires much climatic data such as radiation, cloudiness, wind speed etc and such meteorological data are hardly available in the Himalayan region. There is very sparse network of measurement stations in the high altitude region of the Himalayas and only temperature and precipitation data are collected at most stations. Therefore, for the development of a conceptual model, temperature index or degree-day approach is considered as a suitable approach for the melt computation for such basins. The simplest and most common expression relating snowmelt to temperature index is,

$$M = D (T_i - T_b) \quad (3)$$

where M is the depth of melt water (mm) produced in a unit time (one day in present case), D = degree-day factor (mm $°C^{-1}$ d^{-1}), T_i = index air temperature (°C), T_b = base temperature (usually, 0°C). Clearly, D is used to convert the degree-days to the melt expressed in depth of water. Singh and Kumar (1996) and Singh et al. (2000) have computed value of D for Himalayan basin for a specific time and compared those with available information.

Daily mean temperature is the most commonly used index of temperature for the melt computation. Where only maximum, $T_{max,}$ and minimum temperatures, T_{min}, are available, T_{mean} or the number of degree-days are computed as

$$T_i = T_{mean} = (T_{max}+T_{min})/2 \quad (4)$$

However, in the present study the streamflow computed using mean daily

temperature was underestimated, while using maximum temperature flows were overestimated. The same trend was found all the years. Then streamflow computations were made by providing different weights for the maximum and minimum temperatures. Finally, weights for maximum temperature and minimum temperature were adopted 0.75 and 0.25, respectively and used for all the years of computation.

In general, air temperatures are available at few locations in the basin. These point values are extrapolated or interpolated to mid elevation of each elevation zone using a predefined temperature lapse, as given below.

$$T_{i,j} = T_{i,base} - \delta (h_j - h_{base}) \qquad (5)$$

where $T_{i,j}$ is daily mean temperature on i^{th} day in j^{th} zone (°C), $T_{i,base}$ is daily mean temperature (°C) on i^{th} day at base station, h_j is zonal hypsometric mean elevation (m), h_{base} is elevation of base station (m) and δ is temperature lapse rate (°C/100m). Generally, the mean temperature is lapsed at 0.60°C/100 m or at a specified rate to the mean hypsometric elevation of each elevation zone.

10.6 Glaciated Area, Snow Covered Area and Snow Depletion Curves

Keeping in view the scope of the future work to handle the melting the snow and ice melt separately, an option has been made in the model so that it can make separate calculation for snow covered area, glaciated area and snow free area. The information on SCA can be easily obtained from the satellite imageries/digital data. These days there are a number of satellites available and provide SCA data with a reasonably high frequency. SCA for each elevation zone was plotted against the elapsed time to construct the depletion curves for the various elevation zones in the basin. In order to simulate daily runoff, daily SCA for each zone is required as input to the model. Daily values of SCA can be obtained by interpolating/extrapolating the derived depletion curves. It is to be pointed out that the depletion of snow covered area is controlled by the accumulated snow during preceding winter and patterns of the temperature during the melt period. Because amount of snowfall/snow covered area and temperature conditions fluctuate from year to year, therefore, snow covered area and depletion trends also vary from year to year. A seasonal snow cover will disappear at a faster rate during warmer climatic conditions, while it will follow slow

depletion under a colder temperature regime. The amount of melt water produced from each altitude zone indicates the total amount of solid precipitation in that zone. However, in the present study, differentiations in melting from SCA and glaciated area were not considered because information on SCA not available and it was not included in the budget of the project. Glaciated area in each elevation zone was determined using toposheets and satellite data.

10.7 Rain on Snow / Ice

For snow or ice, which is isothermal at 0°C, the release of heat results in snowmelt, while for the colder snow/ice this heat tends to raise the temperature of snow/ice to 0 °C. In case the snow/ice is isothermal at 0°C, the melt occurring due to rain is computed by (Singh and Singh, 2001)

$$Q_p = \rho C_p (T_r - T_s) P_r / 1000 \qquad (6)$$

where,

Q_p = energy supplied to the pack by rain (kJ $m^{-2}d^{-1}$)
ρ = density of water (1000 kg m^{-3})
C_p = specific heat of water (4.20 kJ kg^{-1} $^0C^{-1}$)
T_r = temperature of rain (°C)
T_s = temperature of snow/ice (°C)
P_r = depth of rain (mm d^{-1})

Substituting the values of various parameters in the above equation, it reduces to

$$Q_p = 4.2\ T_r\ P_r \qquad (7)$$

Usually, rain temperature is considered equal to the air temperature on that day. The melt caused by this energy is computed as

$$M_r = Q_p / (\rho\ h_f B) = Q_p / 325 \qquad (8)$$

Or

$$M_r = 4.2\ T_r\ P_r / 325 \qquad (9)$$

where, M_r is the melt caused by the energy supplied by rain (mm d^{-1}), h_f is the latent heat of fusion of water (335 kJ kg^{-1}), and B is the thermal quality of snow (0.95-

0.97). It is to be noted that only high rainfall events occurring at higher temperatures would cause the melting due to rain, otherwise this component would not be so significant (Singh et al., 1997).

10.8 Computation of Different Components of Runoff

The computation of runoff for each component was made for each elevation zone separately and then output from all the zones was integrated to provide the total runoff from the basin. Computations of different runoff components of streamflow are discussed below.

(i) Surface runoff from glaciated area

The runoff from glaciated area consists of:

(i) melt caused due to prevailing air temperature,

(ii) under rainy conditions, melt due to heat transferred to the snow/ice from rain, and

(iii) runoff from rain itself falls over SCA. Runoff from these three sources of runoff from glaciated area can be computed as

(a) Melt runoff for each elevation zone of the basin was computed using degree-day approach and extent of SCA in that zone.

$$M_{s,i,j} = C_{s,i,j}\ D_{i,j}\ T_{i,j}\ S_{c,i,j} \qquad (10)$$

where,

$M_{s,i,j}$ = snowmelt in terms of depth of water on i^{th} day for j^{th} zone (mm d^{-1})

$C_{s,i,,j}$ = runoff coefficient for snow melt on i^{th} day for j^{th} zone

$D_{i,j}$ = degree-day factor on i^{th} day for j^{th} zone ($mm^{o}C^{-1}d^{-1}$)

$T_{i,j}$ = temperature on i^{th} day for j^{th} zone (^{o}C)

$S_{c,i,,j}$ = ratio of SCA to the total area of j^{th} zone on i^{th} day.

(b) Runoff depth due to snowmelt from the heat transferred to snow/ice by the rain falling on SCA. The depth of snowmelt caused by rain in a elevation zone is given by

$$M_{r,i,j} = 4.2\ T_{i,j}\ P_{i,j}\ S_{c,i,j} / 325 \qquad (11)$$

where,

$M_{r,i,j}$ = melt in terms of depth of water due to rain on snow on i^{th} day for j^{th} zone (mm d^{-1})

$P_{i,j}$ = rainfall on snow/ice on i^{th} day for j^{th} zone (mm d^{-1})

(c) Runoff depth from rain itself falling over snow and glacier covered area is given by

$$R_{s,i,j} = C_{s,i,j}\ P_{i,j}\ S_{c,i,j} \qquad (12)$$

It is to be noted that for the computation of runoff from rain, the coefficient C_s is used (not C_r), because the runoff from the rainfall falling on SCA behaves like the runoff from the melting of snow.

The daily total discharge from the SCA is computed by adding contribution from each elevation zone. Thus, discharge from the SCA for all the zones is given by

$$Q_{sca} = \alpha \sum_{j=1}^{n} a \quad (M_{s,i,j} + M_{r,i,,j} + R_{s,i,j})\ A_{sca,i,j} \qquad (13)$$

where, n is the total number of zones, $A_{sca,i,j}$ is snow covered area in the j^{th} zone on the i^{th} day (km^2) and α is a factor (1000/86400 or 0.0116) used to convert the runoff depth (mm d^{-1}) into discharge ($m^3 s^{-1}$). This discharge is routed to outlet of the basin following the procedure described in the next section.

(ii) Surface runoff from snow/ice free area

The source of surface runoff from the SFA is only rainfall. Like melt runoff computations, runoff from the SFA was also computed for each zone using the following expression.

$$R_{f,i,j} = C_{r,i,j}\ P_{i,j}\ S_{f,i,j} \qquad (14)$$

where,

$P_{i,j}$ = rainfall on snow on i^{th} day for j^{th} zone (mm d^{-1})

$C_{r,i,j}$ = coefficient of runoff for rain on i^{th} day for j^{th} zone

$S_{f,i,j}$ = ratio of SFA to the total area of j^{th} zone on i^{th} day.

Because SCA and SFA are complimentary to each other, therefore, $S_{f,i,j}$ can be directly calculated as (1- $S_{c,i,j}$). The total runoff from SFA for all the zones is thus given by

$$Q_{sfa} = \alpha \sum_{j=1}^{n} R_{f,i,j} \quad A_{sfa,i,j} \qquad (15)$$

Where $A_{sfa,i,j}$ is snow free area in the j^{th} zone on the i^{th} day. The discharge from the SFA was also routed to the outlet of the basin before adding it to the other components of discharge.

(iii) Estimation of subsurface runoff

The subsurface flow or the baseflow represents the runoff from the unsaturated zone of the basin to the streamflow. After accounting for the direct surface runoff from the melt and rainfall, the remaining water contributes to the groundwater storage through infiltration and appears at the outlet of the basin with much delayed effect as subsurface flow or baseflow. The depletion of this groundwater storage also takes place due to evapotranspiration and percolation of water to deep groundwater zone. It is assumed that a part of the water percolates down to shallow groundwater and contributes to baseflow, while remaining water accounts for the loss from the basin in the from of evapotranspiration and percolation to deep groundwater aquifer, which may appear further downstream or becomes part of deep inactive groundwater storage. The depth of runoff contributing to baseflow from each zone is given by

$$R_{b,i,j} = \beta[(1-C_{r,i,j}) \quad R_{f,i,j} + (1-C_{s,i,j}) \; M_{t,i,j}] \qquad (16)$$

where $M_{t,i,j} = M_{s,i,j} + M_{r,i,j} + R_{s,i,j.,}$ and β is a coefficient (=0.50). The subsurface runoff was computed by multiplying the depth with conversion factor α and area, and given as follows:

$$Q_b = \alpha \sum_{j=1}^{n} R_{b,i,j} \, Ai, j \qquad (17)$$

where, $A_{i,j}$ is the total area (km^2) of zone j on i^{th} day and represents the sum of $A_{sca,i,j}$ and $A_{sfa,i,j}$. This component is also routed separately before adding to the other components of discharge from snow melt and rainfall.

(iv)Total streamflow

The daily total streamflow emerging out from the basin is calculated by adding the different routed components of discharge for each day, as given below:

$$Q = Q_{sca} + Q_{sfa} + Q_b \qquad (18)$$

As discussed above, the direct surface runoff results from the overland or near surface flow, while the baseflow is regarded as the contribution from the water stored in the groundwater reservoir to the streamflow. In order to consider the soil moisture deficit, soil moisture index (SMI) has been considered. It represents the soil moisture deficit in the basin in the beginning of simulation. The contribution to baseflow starts only after saturation of topsoil. In the present study, initial value of SMI was assumed to be 50 mm. The routing of different components of runoff was made separately, as discussed below.

10.9 Routing of Different Components of Runoff

(i) Routing of surface runoff

The catchment routing refers to the transformation of input to the basin either in the form of rainfall or melt to the outflow from the basin. Because hydrological response of runoff from SCA and SFA differs, therefore, routing of runoff from these areas was done separately. The linear cascade reservoir approach, which is one of the most popular and frequently used method, was used for routing. When inflow is passed through a linear reservoir, the peak and time base characteristics of the outflow are influenced according to the storage characteristics of the reservoir. In case, the inflow is passed through a series of linear reservoirs with equal storage coefficient, an integrated effect of all the reservoirs will be observed in the outflow from the last reservoir. Each reservoir plays its role in affecting attenuation and lag characteristics of the outflow. Considering n reservoirs in series, the outflow from the second reservoir becomes the inflow to the third reservoir and so on.

The outflow from the n^{th} reservoir represents the response of the basin in terms of outflow. The analytical version of the cascade of equal linear reservoirs is known as the Nash Model. In the case of cascade of reservoirs, the outflow from the n^{th} reservoir is expressed as

$$Q_{n+1,\,j+1} = C_0 Q_{n,\,j+1} + C1\, Q_{n,\,j} + C_2 Q_{n+1,\,j} \qquad (19)$$

where n and j represent the reservoir number and time index, respectively. For a linear reservoir, $C_0 = C_1$, and therefore, the equation representing the outflow from the n^{th} reservoir is simplified as

$$Q_{n+1\,,\;j+1} = 2C_1 \bar{Q}_{\;n\,,\;j+1} + C_2 Q_{n+1\,,\,j} \qquad (20)$$

where

$$\bar{Q}_{n,\,j+1} = \frac{Q_{n,j+1} + Q_{n,j}}{2} \qquad (21)$$

where, $$C_0 = \frac{\Delta t / k}{2 + \Delta t / k} \qquad (22)$$

$$C_1 = C_0 \qquad (23)$$

$$C_2 = \frac{2 - \Delta t / k}{2 + \Delta t / k} \qquad (24)$$

Here C_0, C_1, C_2 are the routing coefficients and the sum of these coefficients equals unity, i.e.

$$C_0 + C_1 + C_2 = 1 \qquad (25)$$

Equation (20) has been applied for the routing of different components of streamflow separately and then the total outflow from the basin was computed by summing the different routed components of runoff. In the present study, SCA and SFA were represented by one and two numbers of linear reservoirs, respectively.

For a basin, which gets runoff from both melt and rainfall, the hydrological response of the basin at a particular time depends upon the areal extent of SCA and SFA in the basin. In the beginning of the melt season, the higher extent of SCA provides much delayed response of snow melt as compared to the later part of melt season. Such delayed response is generated because of time taken by the melt water first to infiltrate through snowpack and then to flow as overland flow under the snowpack. The response of snow melt to streamflow improves with the advancement of the melt season because the areal extent of SCA reduces with time due to the melting of snow. Further, SFA is complimentary to SCA and therefore, as the melt season progresses, the SCA decreases and SFA increases. The extent of SFA is minimum in the beginning of melt season and therefore, rainfall has lowest time of concentration during this period. But, with progress in melt season, the time of concentration for rainfall increases due to increase in SFA. Thus, on the basin scale, the response of snow melt from SCA improves with melt season, whereas for rainfall from SFA it becomes relatively slower.

Keeping in view the different responses of melt and rain and their variations with time, both components were routed separately by splitting the basin into two parts, namely SCA and SFA. Each part of the basin was conceptualized as a cascade of linear reservoirs. To account for variation in response of these components with time, the storage coefficients, k_r for SFA and k_s for SCA, were assumed as the functions of total snow free area (A_{sfa}) and total effective snow covered area (A_{esca}) of the basin, respectively. A_{esca} is defined as extent of SCA, which contributes to the melt. In other words, it represents the extent of SCA which has temperature above 0°C. Depending upon the distribution of temperature in the snow covered area, like in the beginning and end of the melt season, the whole SCA does not contribute to the melt because temperature in the upper part of the basin may be 0°C or < 0°C during this period. Under such a condition, only melt contributing part of SCA will influence the response of melt runoff. Therefore, k_s is considered function of A_{esca} instead of A_{sca}. The ratio of A_{esca} and A_{sca} varies between 0 and 1, being minimum in the beginning and end of melt season, and maximum during summer when melting takes place from the whole SCA. Thus, at a particular point of time, A_{esca} may be either less than or equal to the total $A_{sca.}$ The value of A_{esca} can be easily obtained for each time step by subtracting the area of elevation zones, which do not contribute to melt from A_{sca}. The storage coefficients were related to SCA and SFA in the nonlinear form as follows.

$$k_r = a_r (A_{sfa})^{br} \quad (26)$$

$$k_s = a_s (A_{esca})^{bs} \quad (27)$$

where,

k_r = storage coefficient for SFA

k_s = storage coefficient for SCA

A_{sfa} = total snow free area in the basin

A_{esca} = total effective snow covered area in the basin

a_r and b_r = model parameters for SFA

a_s and b_s = model parameters for effective SCA

The nonlinear relationship between storage coefficients of melt and rainfall with their respective area was adopted considering the nonlinear trend of removal of snow from the basin. The depleting trend of snow from the basin is controlled by the snow depth and prevailing climatic conditions. In the Himalayan region, the altitudinal distribution of snow generates thicker snowpack in the high altitude area as compared to the lower altitudes. The depth of snow increases with increase in altitude. The variation in depth of snow with altitude also controls the depletion trend of snow. In the initial stage of melt season, as the temperature increases, snow from the lower part of the basin depletes at faster rate because of shallow snow depth in the area. In other words, SCA is converted into SFA at a faster rate. While in the later part of the melt season, snow line moves up in the basin where the depth of snow is more and, therefore, the SCA converts into SFA at reduced rate as compared to the rate of beginning of melt season. Thus, conversion of SCA to SFA follows a nonlinear trend with time. Because k_s and k_r are dependent on SCA and SFA, respectively, therefore above relationship was considered. Model parameters (a_r, b_r, a_s and b_s) were optimized using given data sets.

(ii) Routing of subsurface runoff

The movement of subsurface runoff to channel is very slow in comparison to the direct surface runoff. The model routes the subsurface runoff similar to surface runoff with a given value of subsurface storage coefficient, k_b, which is determined using streamflow records of the recession period. There are many methods available for representation of recession of baseflow, but the following exponential type is most widely used and adopted for the model.

$$Q(t) = Q_0 e^{-t/k} \qquad (28)$$

where, $Q_{0\,is}$ the discharge at time t = 0. The parameter k is known as recession constant, or the depletion factor. In the logarithm form this equation can be written as,

$$\ln Q = \ln Q_0 - \frac{t}{k} \qquad (29)$$

In order to determine the storage coefficient for the baseflow, the streamflow of the recession period was plotted against time on the semi-log paper and a straight line was fitted. The slope of the fitted line gives the value of k_b.

11.0 SIMULATION OF DAILY FLOW AT BHOJWASA SITE OF GANGOTRI GLACIER

Institute has monitored hydro meteorological and hydrological data for Gangotri glacier at Bhojwasa. The data collected for the years 2005, 2006 and 2007 are used for hydrological modeling studies. For this purpose SNOWMOD model has been considered. The model requires the following data for its application.

1. Daily mean temperature
2. Daily precipitation
3. Daily flow
4. Degree day Factor
5. Daily snow covered area
6. Division of the study basin into different elevation zones

The processing of the required data and their preparation in the desired format of the model are discussed in the subsequent section.

11.1 Data Processing and Data Preparation

a. Daily mean temperature

The daily maximum and minimum temperature monitored at the site have been computerized and preliminary processing has been carried out for the consistency and the reasonable accuracy of the measurement. Subsequently the daily mean temperature has been computed for the ablation season of each year by averaging the values of daily maximum and minimum temperature.

b. Daily precipitation

The daily rainfall data recorded at the gauging site has been computerized and processed. There is a wide variation in the temperature during the ablation season. Sometimes snowfall has been received in the catchment However, as such there is no snow gauge installed at the observatory for the measurement of the snowfall. In this regard a provision has been made in the model to consider the

precipitation as rain whenever the daily mean temperature is more than 2°C whereas precipitation is considered to be snow if the temperature is less than 0°C. Further more the precipitation is considered as mixture of snow and rain when the temperature is between 0°C and 2°C.

c. Daily Flow

The flow data are generated for three times in a day utilizing the measurements of velocity, gauge and river cross sections using the velocity area method. Subsequently daily flow values are computed taking the average of the three flow values. The daily flow values have been computerized and processed before considering for the modeling.

d. Degree Day Factors

For the computations of snow melt, normal range of degree day factor varies between 1 to 4. It depends upon the exposure of the main body of the glaciers. Since Gangotri Glacier is debris covered glacier, higher values of degree day factor can be used for the computation of glacier melt. The different values of the degree day factors are used in the model for each month of the ablation season. These values are determined through the calibration of the model. These values are kept the same during the simulation of flows for different years.

e. Daily snow covered area

In order to compute the daily snow covered area the satellite imageries for the cloud free days during the ablation seasons for the three years have been procured from NRSA Hyderabad. These satellite imageries have been analysed utilizing the ERDAS Imagine which is a remote sensing analysis and application software. From the analysis it has been observed that the snow covered areas are observed during the month of May for the ablation season. However, there is no snow covered area remaining in the subsequent months of the ablation season. The snow depletion curve has been prepared for the entire ablation season interpolating the snow covered areas. For the months of snow free areas, the glaciated area has been fixed as snow covered area during the modeling.

f. Division of the study basin into different elevation zones

In order to divide the study basin different elevation zones, Digital Elevation Model (DEM) has been prepared using the ILWIS GIS Package. The study basin has been divided in nine elevation zones considering the different ranges of the elevations as given below (Table 8).

Table: 8 Area of elevation zone derived from Digital Elevation Model (DEM) for Gangotri Glacier up to Bhojwasa.

Elevation Zone	Elevation range (m)	Area of Different zones (km^2)
1.	>3800	0.40
2.	3800-4200	8.84
3	4200-4600	31.93
4	4600-5000	90.65
5	5000-5400	122.72
6	5400-5800	141.45
7	5800-6200	109.60
8	6200-6600	43.92
9	6600-7000	5.98

11.2 Results of Flow Simulation and its comparison with the observed flow values.

The SNOWMOD model has been applied for simulating the daily flows of the ablation season for three years. The flow data for the year 2005 has been considered for calibrating the model whereas the year 2006 and 2007 have been considered for validating the model for simulating the daily flows. The efficiency of the model has been computed based on the daily simulated and observed flow values for three years. The values of the model efficiencies are 90%, 95% and 93% respectively for the years 2005, 2006 and 2007. The performance of the model in preserving the runoff volume of entire ablation season has been tested based on the criteria computed as percentage difference in observed and simulated runoff

(D_v) during the ablation season. Their values computed for the year 2005, 2006 and 2007 are –4.01%, -1.61% and 0.29% respectively. The comparison of the daily simulated and observed flow hydrographs for the year 2005 is shown in Figure 23. The model has capability to separate out the contributions of rainfall, snow and glacier melt and base flow from the simulated flows. Daily hydrographs of these contributions are shown in Figure 24 for the year 2005. The simulated and observed daily flow hydrographs along with the contributions of the different components are shown given in Figure 25 and Figure 26 for the year 2006 and 2007 respectively. From these figures, it has been observed that the model has simulated the daily flows reasonably well showing generally a good matching with the daily observed flows. The trends and peaks of the daily flow hydrographs for the ablation period are very well simulated by the model. Percentage difference in volume, model efficiency and contributions of rain snow and base flow computed by the model are summarized in Table 9 for the year 2005 to 2007. From the Table it is observed that in general

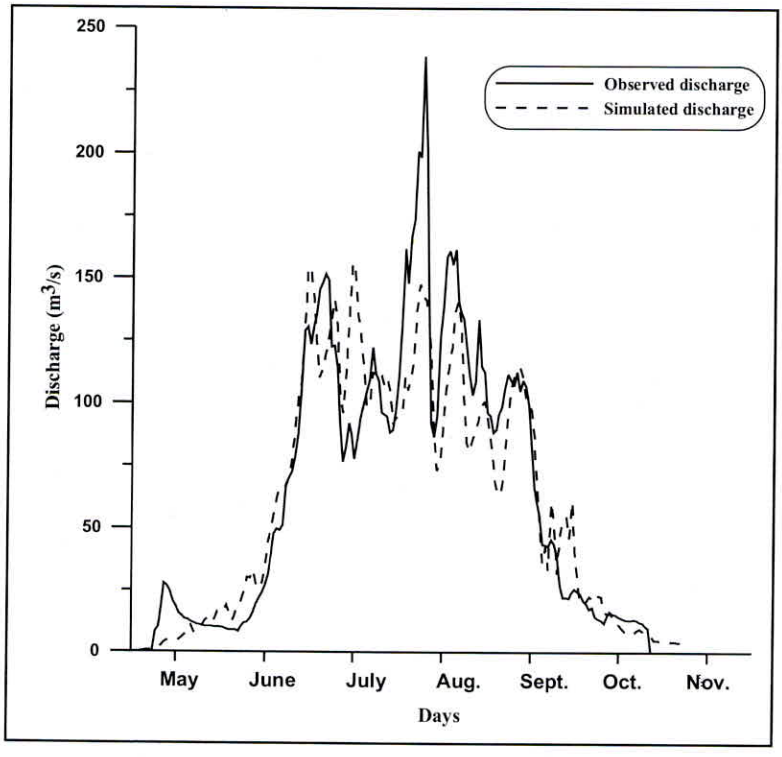

Figure 23 : Comparison of observed and simulated discharge for the calibration year 2005.

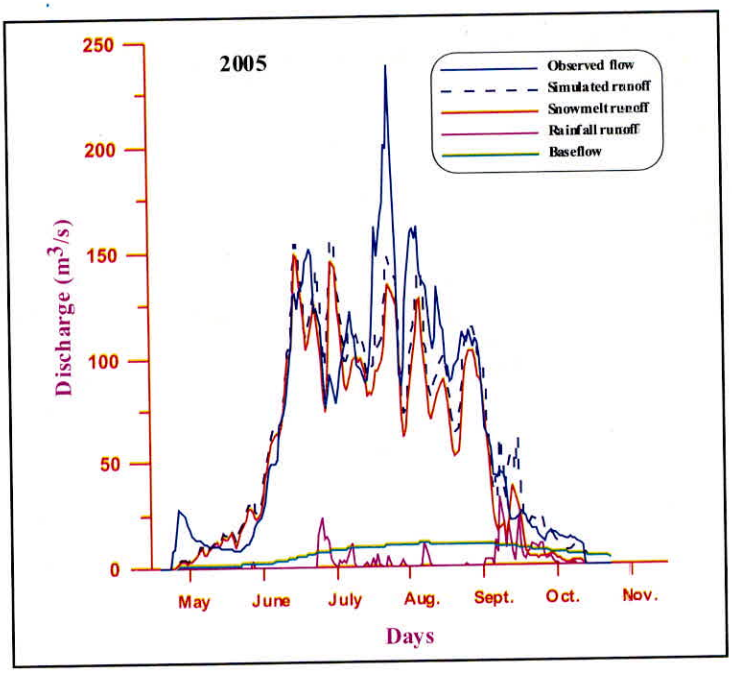

Figure 24 : Different components of simulated runoff for summer season 2005 for the Gangotri Glacier.

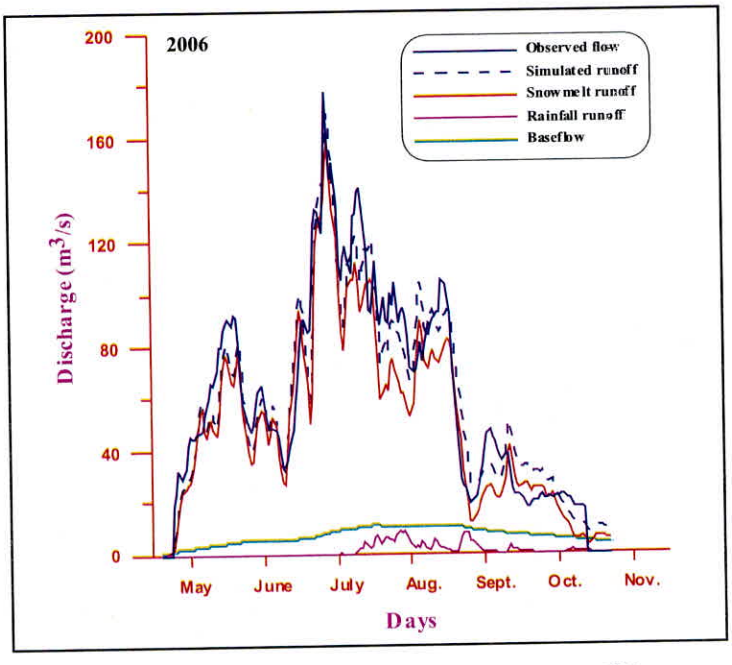

Figure 25 : Different components of simulated runoff for summer season 2006 for the Gangotri Glacier.

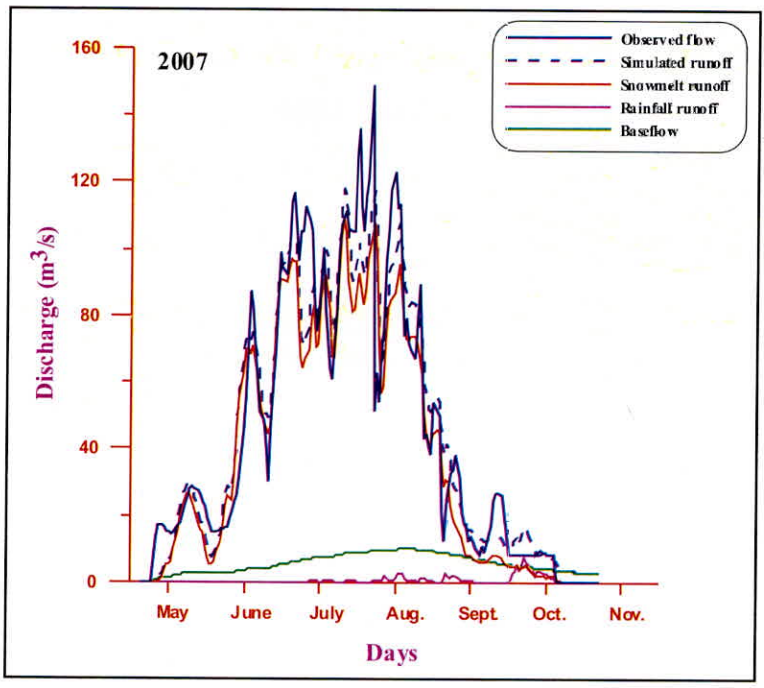

Figure 26 : Different components of simulated runoff for summer season 2007 for the Gangotri Glacier.

Table 9: Percentage difference in volume, model efficiency and contributions of rain snow and base flow computed by the model.

Year	Model	Percentage Diff. in Vol.	Model efficiency (%)	Rain %)	Snow (%)	Base flow (%)
2005	Snowmod	-4.01	90	4.00	85.10	10.90
2006	Snowmod	-1.61	95	2.06	86.34	11.60
2007	Snowmod	0.29	93	1.30	86.39	12.31

rain has very little contribution to flow in comparison to snow and glacier melt contribution. Moreover, the contribution of rain varies significantly because of variation in its intensity and volume over the years during the ablation season. Most of the high peaks observed in the daily flow hydrographs are generally during the months of July and August attributed to the glacier melt. Thus these months are considered as the peak melting season in the western Himalayan region. However, sometimes

the flow resulting due to high intensity rainfall also reflects the peaks in the daily flow hydrographs. For example, in June 2005 the rainfall occurred for 3 days (5–7 July, 2005) and provided total rainfall 106.3 mm. This event generated a peak in the flow in the early part of melt season. Further, a storm in September 2005 which sustained for 4 days (23–26 September, 2005) and provided total rainfall of 63.8 mm, generated peak in the later part of melt season. The simulation of baseflow indicates that the baseflow contribution to the streamflow increases as the season advances, being at maximum during the peak season and then starts decreasing.

The model has been applied to simulate the daily flow hydrographs considering the records of three ablation seasons together. It has been found that the overall efficiency of the model over the study period of three years was about 0.92 and overall percentage difference in volume of simulated and observed flows (D_v) was about –1.77%. It was also observed that the model is capable of simulating the daily flows very well except few peaks for the year 2005. It may be attributed to some factors which have not been considered in the model. Thus it requires further investigations to understand the reason and suitably modify the structure of the model to cater such an event.

12.0 ISTOPIC INVESTIGATION AND DATA ANALYSIS

12.1 Introduction

Isotope Hydrology deals with the application of isotopes as tracers in water resources development and management. Applications of isotopes in hydrology are based on the general concept of "tracing", in which either intentionally introduced isotopes or naturally occurring (environmental) isotopes are employed. Environmental isotopes (either radioactive or stable) have a distinct advantage over injected (artificial) tracers in that they facilitate the study of various hydrological processes on a much larger temporal and spatial scale through their natural distribution in a hydrological system. Thus, environmental isotope methodologies are unique in regional studies of water resources to obtain time and space integrated characteristics whereas the artificial tracers generally are effective for site–specific, local applications. Generally isotope tracers are not used as independent tools but to supplement hydrogeological, geophysical and geochemical information and for a better understanding of the processes taking place in a hydrological system. As all isotopic, hydrogeological, hydrochemical, and hydrodynamic interpretations are space and time related, it is imperative that one should consider all the related aspects of water sampling and prevailing hydrogeological conditions in a study area. Specifically, the isotope can be used for tracing the source, movement, and pollution of ground water. Similarly, the isotopes can be used for a number of investigations related to surface water studies. For example, isotopes are used for stream flow measurement in mountainous area, contribution snow/ice melt in river/ stream, hydrograph separation, water balance and lake dynamic studies, surface water and groundwater interactions studies. Further, Global Network for isotopes in Precipitation (GNIP) program has revealed the linkages of regional climates with isotope ratios in precipitations. River basins constitute major receptors and short term integrators of precipitations over sizeable spatial scales. Consequently, time variation of isotopic ratios in rivers may be useful in tracing magnitude of recent climate change.

As mentioned in earlier chapter, a hydrometeorological observatory is set-up near Gomukh for monitoring the meltwater discharge and meteorological data during the ablation period and to develop the snowmelt discharge model for river Bhagirathi. Since isotopes have potential to estimate the snowmelt and rainfall

contribution in rivers/stream and widely used in developed countries. An attempt has also been made in this project to determine the contribution of snow, glacier/ice and runoff in stream discharge using environmental isotopes.

12.2 Basic Information about Isotopes

A large variety of environmental stable and radioactive isotopes are employed for hydrological studies (e.g., ^{2}H, ^{3}H, ^{3}He, ^{4}He, ^{6}Li, ^{11}B, ^{13}C, ^{14}C, ^{15}N, ^{18}O, ^{34}S, ^{36}Cl, ^{37}Cl, ^{81}Br, ^{81}Kr, ^{87}Sr, ^{129}I, ^{137}Cs ^{210}Pb etc.). However, the stable isotopes have the distinct advantage over injected (artificial) tracers (^{3}H, ^{46}Sc, ^{60}Co, ^{82}Br, ^{131}I, ^{198}Au, etc.) in that they facilitate the study of various hydrological processes on a much larger temporal and spatial scale through their natural distribution in a system. The use of artificial tracers generally is effective for site-specific, for local applications. Among the stable isotopes, oxygen and hydrogen have wide application in hydrology because, as part of the water molecule itself, they act as natural tracers.

Oxygen has six isotopes viz., ^{14}O, ^{15}O, ^{16}O, ^{17}O, ^{18}O and ^{19}O. Since, ^{14}O, ^{15}O and ^{19}O are radioactive with very short half-lives, they are not useful for any meaningful hydrological study. Among the remaining three isotopes the mass abundance of ^{16}O (99.759%) and ^{18}O (0.204%) are higher than ^{17}O (0.037%). Therefore, the ratio of $^{18}O/^{16}O$ is important for hydrological studies (Gat, 1981). Hydrogen has three isotopes viz., ^{1}H (Protium), ^{2}H or D (Deuterium) and ^{3}H (Tritium). ^{1}H is the most abundant hydrogen isotope (99.9855%) followed by (0.0145%). Tritium is a radioactive isotope with a half-life of 12.43 years. In isotope hydrology, among various species of water molecules only $H_2{}^{16}O$, $H_2{}^{18}O$ and $HD^{16}O$ are generally considered. The river water, ice samples and precipitation samples were collected for measuring $d^{18}O/d^{16}O$, $dD/d^{1}H$) in order to understand the hydrological processes.

The stable isotopic ratios are expressed as deviation with respect to a standard such as V-SMOW (Vienna - Standard Mean Oceanic Water), denoted by

δ and expressed in permil (‰). where, R_x denotes the ratio of rarer to the common isotope ($^{18}O/^{16}O$ or D/H). The δ notations have better resolution over the absolute ratios and facilitate intercomparison of results and aid

12.3 Methodology

12.3.1 Collection of Rainfall Sample

Rain samples were collected in plastic containers using an ordinary raingauge with a metal funnel having effective catch-diameter of 210 mm. The daily precipitation collected during each calendar month was thoroughly mixed to yield a representative integrated sample. All necessary precautions were taken to avoid evaporative enrichment during collection and storage.

Rainwater sampling were carried out for ablation period of 2004, 2005, 2006 and 2007. A monthly sample represents rain collected over the period beginning on the first day of a month and continuing until the end of the month. The rainwater from the rain gauge is collected daily into a large capacity (~ 5 litres) container having tight inner lid and a screw cap. This process continues for a month. At the end of the month, the integrated monthly rainwater sample is drawn from this volume of water collected over the entire month. From the integrated samples 20 ml water sample was collected for stable isotopes and 500 ml for environmental tritium. Diffusive and evaporative losses from rain gauges and storage containers are avoided by use of liquid paraffin or silicon oil. The process described above was repeated every month for rainfall during study period. For hydrograph separation purpose ten daily integrated and daily sampling of precipitation were also carried out.

12.3.2 River Water Sampling

River samples were collected from the mid-stream sections or flowing portions. Standing water should was avoided because the isotopic composition might have been affected by evaporation of standing water. Sampling at the confluence of Bhagirathi and Alaknanda was done downstream of confluence with great care due to problems of incomplete mixing. River water samples were collected from each site on fortnightly, weekly and daily basis.

12.3.3 Snow and Ice Sampling

Snow and ice samples were collected from the Gangotri glacier. Few snow samples were collected in sealable plastic bags or containers. In order to avoid sublimation, re-crystallization, redistribution, melting and rainfall on snow, which alter the isotopic composition of snow and ice, the snow sampling was carried out shortly after every snowfall. Once, the snow was melted in containers, the water samples were transferred to plastic bottles as described in case of rain samples for ^{2}H, ^{18}O and ^{3}H analyses. Since it was not possible to stay during the winter period at Gomukh site, so representative samples of snow could not be collected during the winter season. But the snow fall occurring during May to June and stream discharge initially generated by snow melt has been taken as representative of snow. Few ice samples were collected using a hand auger from the upper part of the glacier. For collection of deep ice cores or depthwise samples, the required power drill was not available.

12.3.4 Measurement of Isotope Ratio

The collected samples were analysed by Stable Isotope Ratio Mass Spectrometer (SIRMS) at the Nuclear Hydrology Laboratory, Roorkee. Particularly, the Dual Inlet Isotope Ratio Mass Spectrometer was used for oxygen and hydrogen isotopes ratio analyses using the CO_2 equilibration method in order to determine $d^{18}O$ (Epstein and Mayeda, 1953) and Hokko beads were used for determining dD (Coleman et al., 1982). The measurement precision for $d^{18}O$ was ±0.1 ‰ and for dD was ±1‰. All the dD and $d^{18}O$ isotope data reported in this article correspond to VSMOW. The detailed steps followed in analysis are mentioned below:

12.3.5 Equilibration procedure for D/H analysis

Measurement of D/H ratio in water requires preparation of a representative hydrogen gas from the water sample because normally a mass spectrometer cannot analyze water directly. At present, there are two basic procedures to prepare representative hydrogen gas: (i) reduction of water to hydrogen gas by reaction with hot metal, and (ii) isotopic equilibration of tank hydrogen with the water sample to reflect its isotopic composition. In the present case, equilibration method has

been followed. In this method, some amount of tank hydrogen gas is equilibrated with the water sample in a closed bottle with the help of Hokko beads where by isotopic exchange takes place and the D/H ratio of the hydrogen gas is changed to a value determined by that of the water, but being off-set by a certain amount of fractionation which is determined by the temperature of equilibration. At 25 °C the fractionation is large – the hydrogen gas is depleted by about 737.5 ‰ relative to water. The temperature coefficient is also large (about -6 ‰ per °C) and that makes it essential to keep the temperature constant precisely. This is one of the simple viable methods at present that allow for fully automatic determination of D/H ratio in water samples.

In SIRMS available at NIH, Roorkee a set of 60 samples are loaded in small vials (~ 2 ml) provided with rubber septum to make the bottle airtight. In each bottle 400ml water with a few beads of platinum catalyst (Hokko beads) are put which are light and being hydrophobic stay on top of the water surface. Alternatively, Pt-sticks can also be used to act as catalyst. In principle, the catalyst is re-useable. The set of bottles is put in 60 holes in an aluminum block arranged in the form of x-y matrix with each hole having a set of precise x-y value addressable by the control program. Initially, the each bottle is evacuated by an arrangement using Gilson hypodermic needle which is inserted into the rubber septum through a computer controlled device. Then all the 60 bottles are flushed one after another with pure tank hydrogen and filled with the tank hydrogen gas at a pressure slightly above the atmosphere. The temperature of the aluminum block is accurately maintained at 40°C since the fractionation is highly temperature sensitive (decreases by 6 ‰ for 1 °C rise). The flushing of the space above the water removes little amount of water along with the air but does not impact the analysis since standards are also treated in exactly the same way. In general, several standards are placed in the array to take care of minor temperature variations across the block. For calibration, IAEA standards (VSMOW, VSLAP and GISP) are occasionally used against the internal water standards. The precision of the measurements can be optimized by choice of an appropriate sample size. Normally, laboratories require amounts between 1 to 5 ml for dD and $d^{18}O$ analyses. After a few hours, the equilibration is complete and the gas can be extracted by expanding to the inlet of the mass spectrometer after scrubbing the moisture by –75°C trap.

12.3.6 Measurement of $^{18}O/^{16}O$ ratio in water

The most common method to measure the $^{18}O/^{16}O$ ratio in a water sample is to equilibrate tank carbon dioxide with the water sample at a certain temperature and to measure subsequently the isotopic composition of the carbon dioxide. The equilibrated CO_2 gas is isotopically representative of the water sample because after equilibration, it attains a specific isotope ratio relative to the water. At 25°C, the CO_2 gas is enriched by 41.2 ‰ relative to water. In practice, standard water whose isotopic ratio is known is analyzed in parallel with the samples. The raw data are converted using the isotopic ratio of the standard

The principle of the method is similar to that of D/H ratio described before and is normally done using the same water sample if commercial system is used. However if only oxygen isotope ratio is to be determined and a separate extraction system is envisaged, following method can be used. A glass bottle with the water sample is evacuated through a capillary for a period of time short enough to pump only air. The resistance in a capillary for pumping water vapour is higher than that of air and, therefore, only very small water vapour is pumped out without any significant change in the isotopic content of the water sample. Further, as internal standards are also run in parallel, correction for change of isotopic content, if any, would automatically be taken care of. Tank carbon dioxide is then admitted to the bottle at close to atmospheric pressure which dissolves in water to form bicarbonate. Dissolution rate is enhanced if the water is agitated by shaking the bottle. The oxygen isotopes are exchanged between CO_2 and H_2O through bicarbonate formation and dissociation until equilibrium is reached. At equilibrium, the CO_2 gets enriched in heavy isotopes relative to water and the enrichment is dependent on temperature of equilibration. The amount of CO_2 being very small compared to water, its initial composition is not important. Since, in general, several samples and standards are prepared simultaneously, it is important that the temperature for all bottles is same within close limits. This can be done by immersing the bottles in a water bath or in an air thermostat. After equilibration, the CO_2 gas is extracted from water, purified from water vapour and non-condensable and put into the mass spectrometer through inlet system. A detailed description of the technique is given in the IAEA Isotope Hydrology Laboratory Technical Procedure Note no. 29. As mentioned before, the preparation system is commercially available (from several sources) and can process large number of samples simultaneously (~ 60 to 80). Modern isotope

ratio mass spectrometers are able to measure the samples automatically after equilibration. The same system that measures the D/H ratio in water can be used to measure $^{16}O/^{18}O$ ratio. This facility to measure both the isotope ratios is useful since better insight in hydrological processes can be obtained if both the ratios are known. In practice, the samples are placed in the preparation line in the afternoon and after a typical equilibration time of 4 hours, measured overnight. An experienced technician can therefore easily measure 60 samples per day. For higher accuracy, 3 to 4 internal standards are run in parallel on routine basis. For calibration, IAEA standards (VSMOW, VSLAP and GISP) are occasionally used against the internal standards. The precision of the measurements can be optimized by choice of an appropriate sample size. Normally, laboratories require amounts between 1 to 5 ml, but about 2 ml sample is a good size that also helps to extend the availability of the standards over a longer period.

12.4 Result and Discussion

12.4.1 Isotopic Composition of Precipitation

Isotopic values of rainfall measured for year 2004, 2005, 2006 and 2007 reveal similar trend in which enrichment in both $\delta^{18}O$ and δD during premonsoon rain and depleted values measured for the monsoon rain (Fig.27). The $\delta^{18}O$ peaks in monsoonal precipitation of 2004, 2005, 2006 and 2007 occur in July, August and September months. This depletion of $\delta^{18}O$ and δD in July and August months (Fig.28) may be due to amount effect of isotopes in precipitation while the minimum depleted value of $\delta^{18}O$ in September month shows the September rain may have the moisture remaining after the condensations of July and August due to which small precipitation that occurs in September month becomes more depleted. The source of water vapours can only be oceanic.

For example the minimum depleted values of $\delta^{18}O$ in September months in years 2004, 2005, 2006 and 2007 are -23.8‰, -30.3‰, -23.2‰, -22.9‰, respectively. The maximum enriched values of $\delta^{18}O$ in precipitation observed during the summer months in the year 2004, 2005, 2006 and 2007 are -1.7‰ (June), -3.6‰ (June), -4.7‰ (June), and 0.05‰ (June) respectively. This reveals that source of moisture for precipitation in the months of July, August and September are different from May and June. The depleted value of July August and September confirm that precipitation

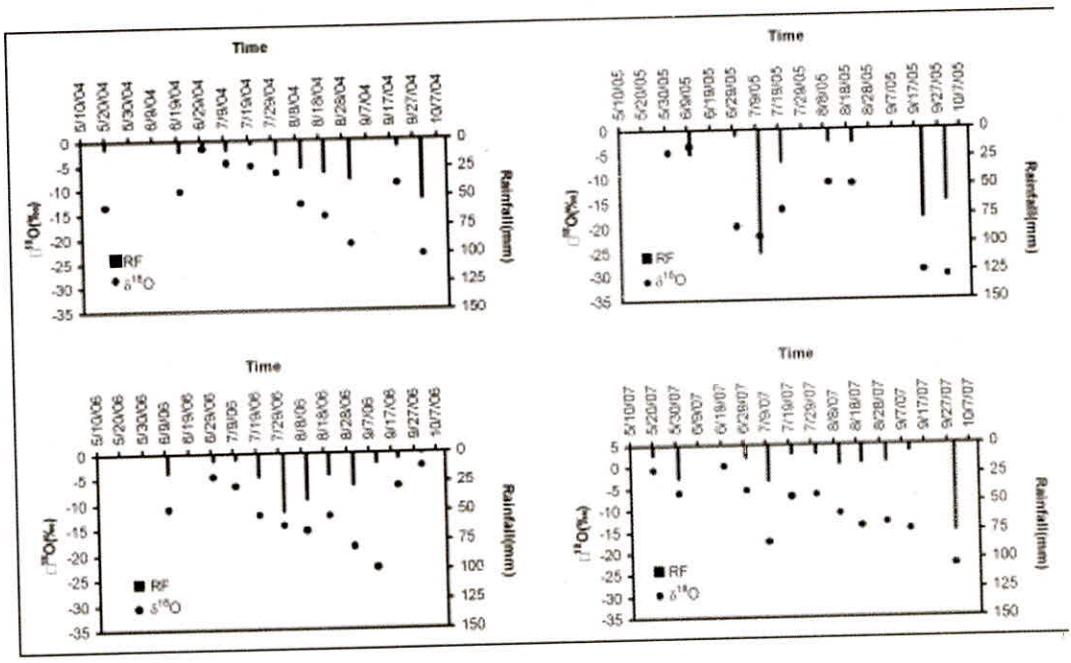

Figure 27: Variation of $\delta^{18}O$ values in precipitation during ablation period in year 2004-2007

if from Monsoon vapour. The source of moisture during summer months may be local evapotranspiration. The isotopic enrichment of premonsoon rain may also be due to the secondary evaporation of rain during fallout process.

Meteoric water line is the best fit line of the $\delta^{18}O$ and δD content of the fresh waters and it indicates the source/origin. Craig (1961) after a global survey of stable isotope contents in freshwaters proposed a Global Meteoric Water Line (GMWL), which was later modified by Rozanski et al. (1993). The equation (30) for the GMWL on the basis of exhaustive isotope data collected through the IAEA/WMO world wide network is given by Rozanski et al., 1993. The GMWL is essentially a global average of several Local Meteoric Water Lines (LMWL). The LMWL is controlled by the local climatic conditions and the source of the vapour mass, particularly the slope of the line is influenced by the secondary evaporation. The knowledge of LMWL is essential for regional or local hydrological studies.

$$\delta D = (8.2 \pm 0.1)\delta^{18}O + (11.3 \pm 0.6) \text{ GMWL}$$

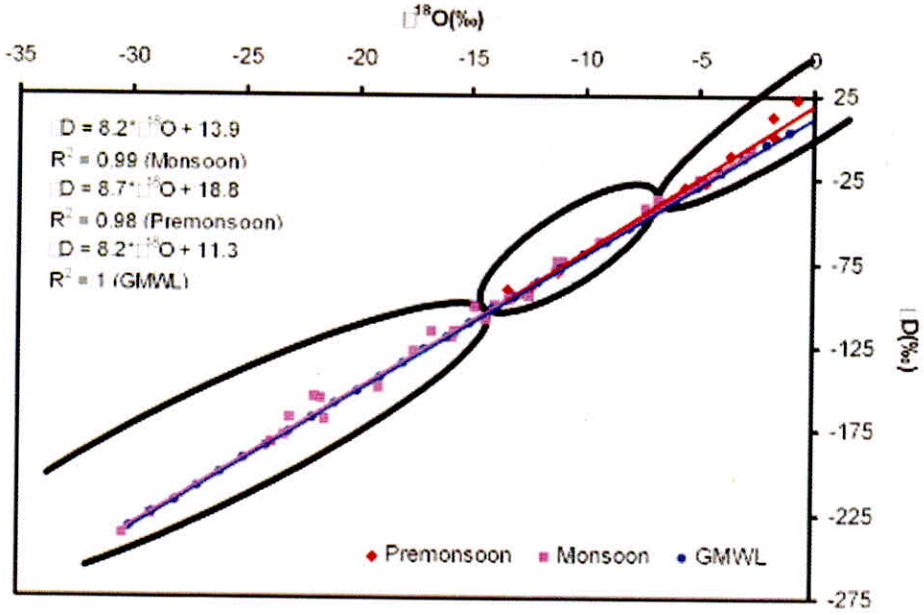

Figure 28: Isotopic composition of premonsoon and monsoon precipitation.

The best fit line developed for the Gomukh using ten daily $\delta^{18}O$ and δD data for monsoon season is very close to the GMWL (equation 3.1) while for Bhagirathi basin, the LMWL is $\delta D=8.0 \pm 0.1*\delta^{18}O + 11.5 \pm 1.1$ (Fig. 29). The similarity in slope and intercept between LMWL and GMWL indicates that the precipitation at Gomukh did not suffer any kinetic effect during and after the rainfall. However, if we analyse the isotope in two parts i.e. premonsoon and monsoon period. It is found that comparatively higher slope and intercept of LMWL developed using the isotopic composition of premonsoon precipitation which indicates kinetic fractionation. The higher than 8 slope at Gomukh appears to be mainly due to low air temperature and snow precipitation. Rozanski et. al. (1993) noted that for stations with substantial contribution of snow precipitation, higher deuterium excess values during winter may result from additional kinetic fractionation during snow formation.

The best fit line (LMWL) developed for four years using all $\delta^{18}O$ and δD ten

daily data collected during 2004-2007 are given below:

$\delta D = 8.4 \pm 0.16 * \delta^{18}O + 15.4 \pm 2.2$, $R^2 = 0.98$, n = 16 (2004) (31)

$\delta D = 8.2 \pm 0.2 * \delta^{18}O + 17.4 \pm 2.6$, $R^2 = 0.99$, n = 10 (2005) (32)

$\delta D = 8.5 \pm 0.1 * \delta^{18}O + 13.4 \pm 1.6$, $R^2 = 0.99$, n = 10 (2006) (33)

$\delta D = 8.3 \pm 0.2 * \delta^{18}O + 18.2 \pm 2.5$, $R^2 = 0.99$, n = 14 (2007) (34)

$\delta D = 8.3 \pm 0.1 * \delta^{18}O + 15.6 \pm 1.4$, $R^2 = 0.99$, n = 50 (2004-2007) (35)

Slope and the intercept of LMWL for Gomukh (Eq. 31 to 34) are comparatively higher to those of Global Meteoric Water Line (GMWL) and LMWL for Bhagirathi basin. However LMWL for Gomukh and GMWL are almost parallel lines. The similarity in slope and intercept between LMWL and GMWL indicates that the precipitation at Gomukh comprise of vapours from the higher altitude (colder parts). The similarity in monthly trend of d-excess for three consecutive years indicates that origin of vapour sources and other climatic parameters (temperature, humidity etc) did not significantly vary during these three ablation period. Hence ten daily weighted averages of $\delta^{18}O$ and δD can be considered as reasonable representative of Bhagirathi river at Gomukh.

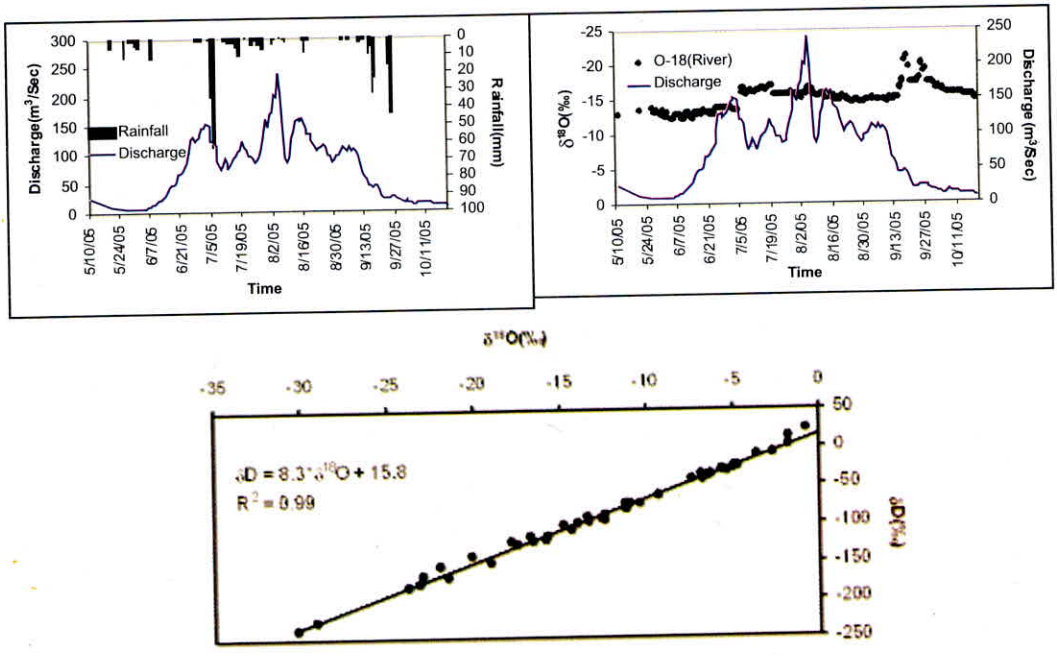

Figure 29: Meteoric Water Line for Bhagirathi river at Gomukh based on 2004-2007 data.

12.4.2 Isotopic Composition of Stream Water

The spatial and temporal variations in the isotopic composition of river waters mainly depend upon the number and type of its sources, and to some extent on the evaporation from river surface. The variations in the observed δ_R, reflect the variable contributions from isotopically different sources, which can be evaluated if isotopic indices of the sources are known. However, the river water isotopic characterisation and its utility in studying hydrograph separation and river-aquifer interactions depend greatly on the spatial and temporal variations of isotopic ratios.

To study the isotopic variations in stream discharge at Gomukh site the stream samples were collected on ten daily basis for the period from May to October during year 2004 and 2006. In year 2005 daily sampling was carried out for analyses rainfall contribution in river discharge. The δD and $\delta^{18}O$ variation in stream water (Bhagirathi River) and precipitation at site Gomukh are shown in figure 4. The isotopic data reveals the systematic variation in $\delta^{18}O$ and δD values with time (Fig. 30). Discharge of Bhagirathi stream at Gomukh start increases in May month and maximum in July/August depending upon air temperature variation. The maximum discharge occurs during July and August when temperature reaches maximum.

The isotopic signatures of stream water at Gomukh also changes with time. As discharge start increases during the months of May and June, the enriched isotopic values are observed. The maximum isotopically enriched values observed in the stream water in the years 2004, 2005, 2006 and 2007 are -12.4‰, (May), -12.8‰ (June), -12.4‰ (April), -12.7‰ (June), respectively show that discharge is dominated by snow melt in May and June months. This $\delta^{18}O$ values depleted in July and August and reaches to -1.5‰. This difference in isotopic value clearly indicates variation in contribution during different month or melting. These enriched values of river water are closed to $\delta^{18}O$ value of snow ranges in the month of May and June between -9.7‰ to -14.4‰ reveal that snow is the main source of stream discharge during summer months (May and June). After third week of June, $\delta^{18}O$ and δD values of stream water start depleting, which reveals that contribution of snow component is decreasing and ice melt component is increasing. Due to the melting of snow in these months the glacier becomes exposed and comes directly in contact with solar radiation comparatively at lower altitudes. Depletion in $\delta^{18}O$ and δD value of stream discharge in July and August reveals that stream peak discharge at Gomukh

results of ice melt as a major component. However the melting of snow at higher altitudes having slightly depleted of isotopic values also contributes to stream discharge. But in the absence of isotopic index of higher altitude snow, it is not possible to distinguish contribution of higher altitude snow. As precipitation takes place in the months of July, August and September, the $\delta^{18}O$ and δD values of stream discharge become deplete sharply. Because the measured isotopic value of rains more than 10mm in the month of July, August and September are more depleted than snow/ice melt of stream discharge. Obviously the depleted value of rain generated runoff of depleted value. This depleted value of runoff as join the stream depletes the stream water. Due to this the sudden fall in ^{18}O and δD is observed in Fig. 30 clearly indicates the contribution of rain as runoff is significant in quantity.

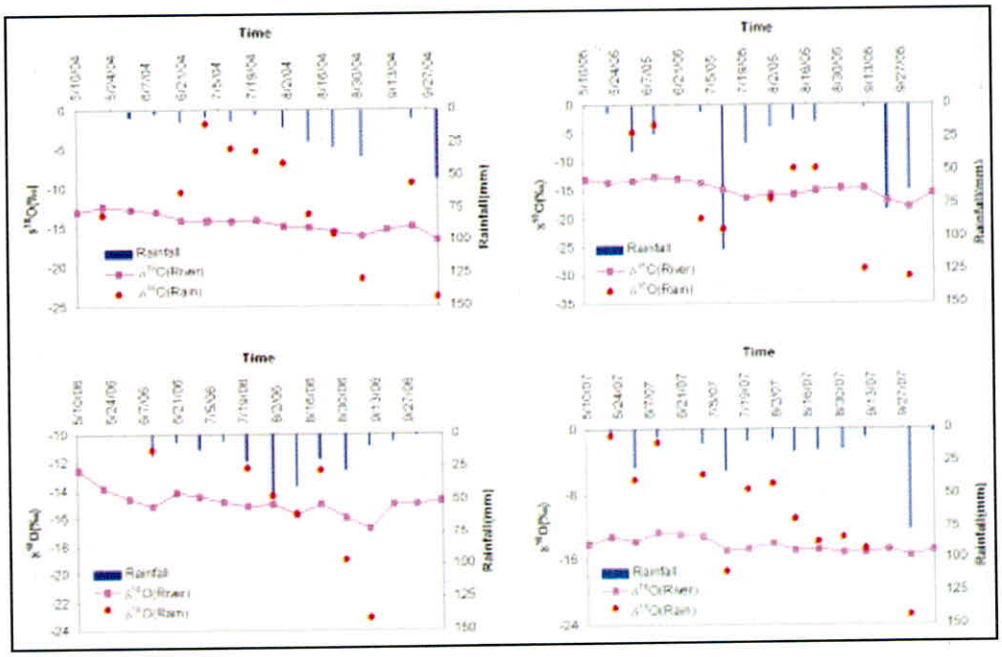

Figure 30: $\delta^{18}O$ and δD variations in Bhagirathi River stream and precipitation with time at Gomukh.

The δD vs $\delta^{18}O$ plots for stream discharge at site Gomukh is shown in figure 31 separately for premonsoon and monsoon periods during the years 2004 to 2007 along with LMWL for Bhagirathi basin. Based on 2004- 2007 data the δD vs $\delta^{18}O$ plots of stream discharge gives the average isotopic composition which will be used for further study as base line (Fig. 32). A large variation in isotopic composition is visible that ranges between -84‰ and -145‰ in case of δD while between -12.3‰ to -20‰ in case of $\delta^{18}O$. However, carefully segregation of isotopic data reveals that stream water is enriched in δD or $\delta^{18}O$ values during premonsoon period and comparatively highly depleted during the monsoon period. However, there is an overlap in isotopic values belonging to premonsoon and monsoon. The comparatively enriched isotopic value during premonsoon period seems to be justified as the premonsoon rains are enriched in isotopic composition due to evaporation of rain drops during fall out process. However, the snowmelt contribution that is also comparatively enriched than ice melt and monsoon rain in isotopic composition. But a depleted summer rain keeps the isotopic composition between -12‰ and -15‰ with certain component of ice melt. This makes the overlap between premonsoon and monsoon isotopic composition of stream discharge as monsoon rains are mostly depleted due to different sources i.e. oceanic vapours that reaches after moving a long distance and rainout process. It further depleted due to altitude effect in mountain region. However, the amount effect also plays significant role in depleting isotopic composition of rainfall.

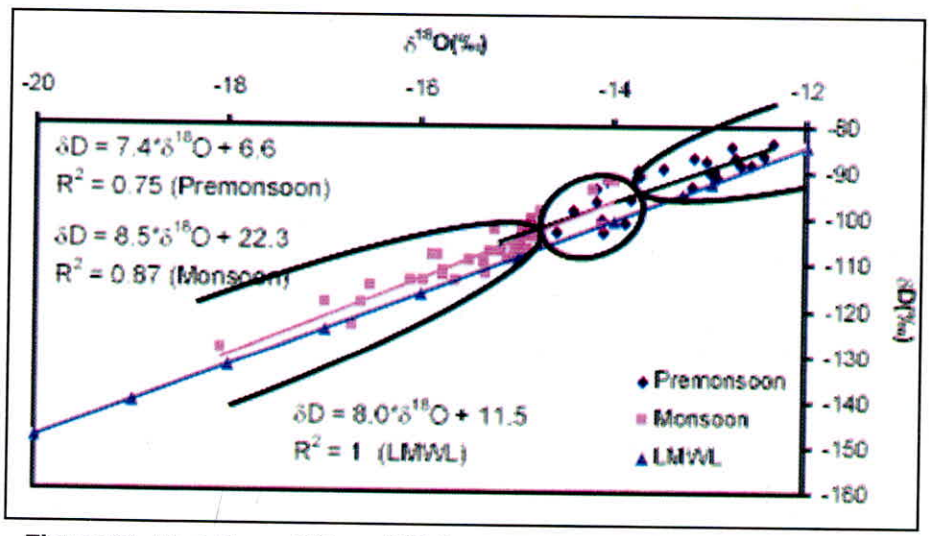

Figure 31: Variation of δD vs $\delta^{18}O$ for stream discharge at site Gomukh

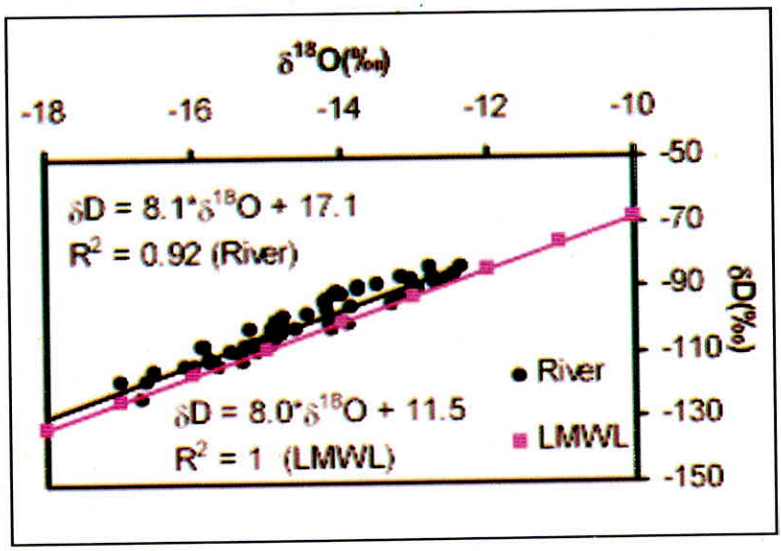

Figure 32: Composition of δD and $\delta^{18}O$ of Bhagirathi stream at Gomukh site

$\delta D=8.3 \pm 0.6*\delta^{18}O + 21.2 \pm 8.2$, $R^2 = 0.94$, n = 16 (2004) (36)

$\delta D=8.5 \pm 0.3*\delta^{18}O + 25.4 \pm 3.9$, $R^2 = 0.99$, n = 16 (2005) (37)

$\delta D=8.3 \pm 0.4*\delta^{18}O + 18.3 \pm 5.9$, $R^2 = 0.96$, n = 18 (2006) (38)

$\delta D=8.0 \pm 0.4*\delta^{18}O + 11.9 \pm 5.1$, $R^2 = 0.97$, n = 16 (2007) (39)

$\delta D=8.1 \pm 0.3*\delta^{18}O + 17.1 \pm 4.5$, $R^2 = 0.92$, n = 66 (2004-2007) (40)

12.4.3 Hydrograph Separation

The hydrograph of Bhagirathi River at Gomukh site comprise of multiple peaks (Fig. 33). The variation in discharge occurs due to variations in climatic conditions which affect the contribution of different components in stream discharge. The first peak in discharge mainly consists isotopically enriched values ranging between -12.4‰ and -13.5‰ which compares well with the isotopic signatures of snow, thereby reveals that major contribution in stream discharge is due to the melting of snow at lower altitudes during May and June months. The second highest peak in stream discharge consists depleted isotopic values in the range of -15‰ to -16‰ which resembles with the isotopic signatures of ice at the lower altitude thereby confirms major contribution of ice and glacier melts. It has been observed that

whenever precipitation occurs at the Gomukh, the stream discharge declines sharply instead of increasing trend. This leads to the confusion that precipitation has the negative effect on stream discharge. But the variation in isotopic signatures of the stream water before and after the rainfall clearly indicates significant contribution of rainfall runoff to the stream discharge. This variation in isotopic composition of stream water clearly reveals the hidden cause of reduction in discharge during the precipitation. Due to cloudy weather conditions during precipitation results in sudden decline the air temperature. This decline in temperature decreases the melting of snow and ice. The reduction in the snow and ice melt water quantity causes sharp recession in hydrograph instead of rising as the runoff generated by precipitation is not enough to compensate the reduction in melt water discharge.

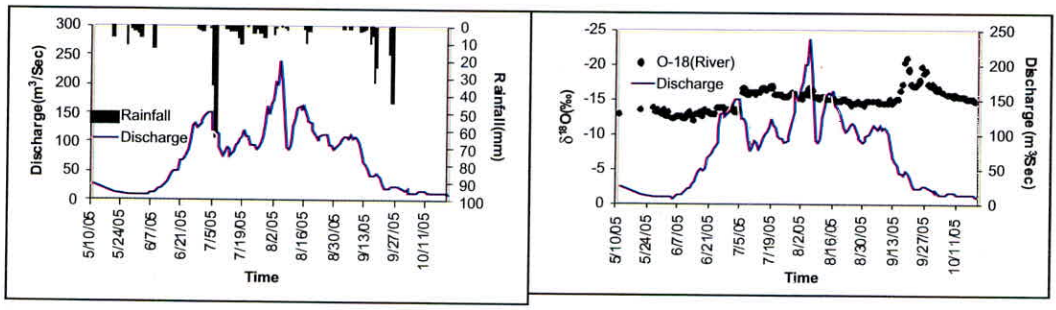

Figure 33: Variation of stream discharge and its $\delta^{18}O$ composition with rainfall during ablation period in the year 2005.

But it has been observed that precipitation and stream discharge before and after the precipitation are isotopically different. The extent of change in isotopic composition of stream water is a function of proportion of rainfall contribution to the meltwater at discharge measurement site. The proportion of two components in total discharge could be separated out using two components model. This can be expressed by the following equations which conform to the law of mass conservation:

$$Q_t = Q_{sm} + Q_r \qquad (i)$$

Where Q is discharge component, and subsripts t, sm and r represent total stream flow, prestorm snow/ice melt and storm runoff respectively. With sampling

of the prestorm stream flow, rain itself, and the total discharge during a storm, the isotopic compositions of these components were established. Then an isotopic mass balance equation can be written as

$$\delta_t Q_t = \delta_{sm} Q_{sm} + \delta_r Q_r \qquad \text{(ii)}$$

Where $d = [(R_{sample}/R_{std}) - 1] * 10^{3}‰$

By substituting $Q_r = Q_t - Q_{sm}$ and rearranging equation (ii), we get

$$Q_{sm} = Q_t (\delta_t - \delta_r)/(\delta_{sm} - \delta_r) \qquad \text{(iii)}$$

Using the equation (iii) the runoff component can be separated out.

In order to separate out the runoff component, different event of precipitation were selected from hydrograph. The rainfall events above 10mm are considered for computing the runoff component. In year 2004, sampling was carried out on ten daily intervals, so only one event is used for this purpose where the isotopic values are varying significantly. To observe isotopic variations for all the rainfall events in stream water daily sampling was carried out during the year 2005.

Isotopic signature ($\delta^{18}O$) of rainfall events occurred between 21st August to 31st August 2004 is -21.5‰, for prestorm snow/ice melt -13.0‰ and mixture of both during total discharge -16.1‰. Thus by using two component model (Eq iii) the maximum runoff contribution comes out to be 35% in stream discharge. Similarly, the maximum runoff contribution three events were monitored in year 2005. The isotopic variations for these events are depleted in figure 34a and 34b. The maximum contribution has been found between 35% to 44% of the total discharge for the rainfall events that occurred during in month July or September in the year 2005. The maximum runoff contribution on particular date not meets out the objective. Therefore due to availability of daily based data contribution of rainfall computed in daily bases. In the year 2005, daily isotopic signatures of stream water were measured therefore, hydrographs have been separated out on daily basis (Fig. 35). The results reveal that 14% to 15% contribution of precipitation in stream discharge has been found out of total stream discharge in these storm periods. If one compares with total melt discharge in ablation period of 2005, it comes about only 3% of the total discharge.

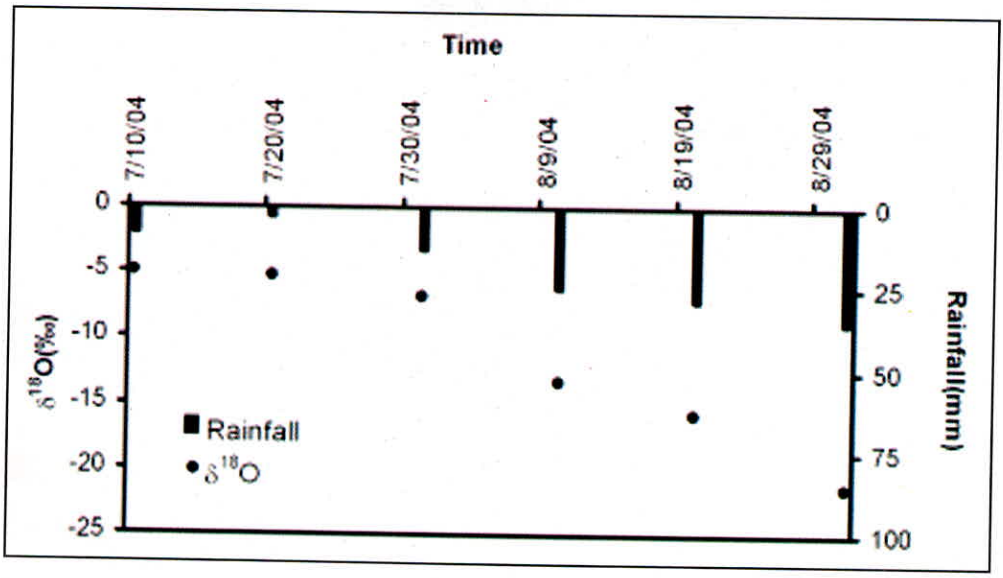

Figure 34a: Rainfall events and variation of $\delta^{18}O$ composition in precipitation at site Gomukh during the year 2004

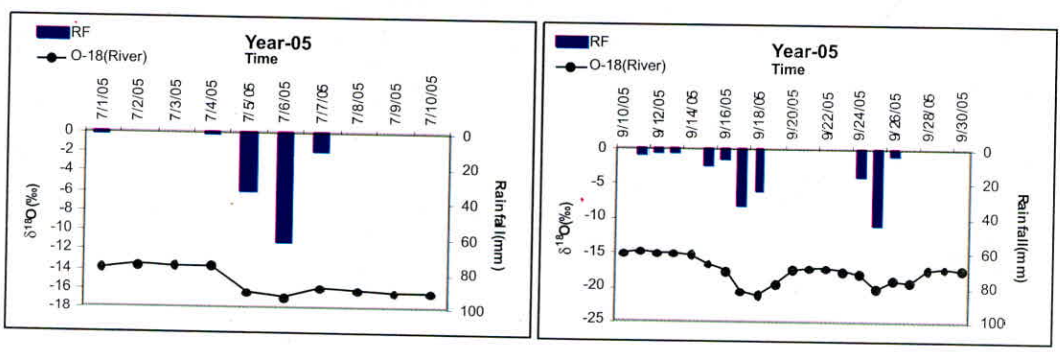

Figure 34b: Variation of $\delta^{18}O$ values in stream discharge due to rainfall of depleted $\delta^{18}O$ in year 2005

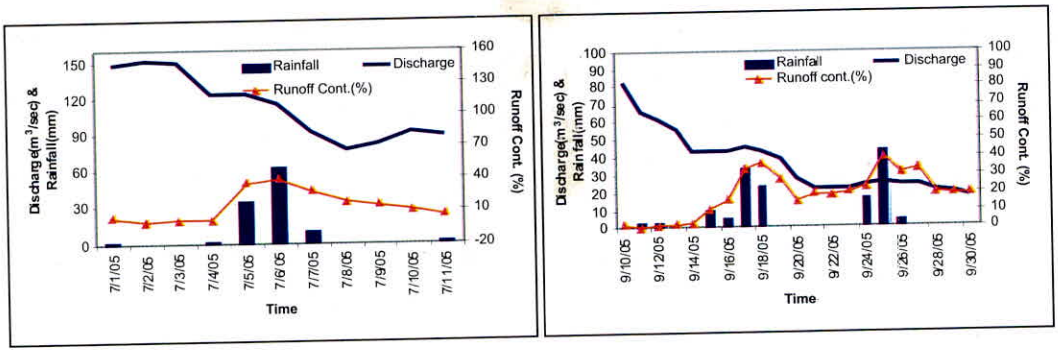

Figure 35: Runoff component separated out using isotopic signatures of stream water and precipitation on the basis of daily sampling data during the year 2005 at site Gomukh

13.0 DISCUSSION OF RESULTS AND CONCLUSIONS

a) Hydrometeorology of the study basin

Hydrometeorological data for the Gangotri Glacier was collected under the project by establishing a standard meteorological observatory and a gauging site near the snout of the glacier. The required data were collected for 3 ablation seasons (May-October) during 2005 to 2007 and analysis was made to understand the weather conditions and melting pattern of the glacier. Daily rainfall hardly exceeds 15 mm in the study area. About 78.74% rain events recorded daily rainfall of less than or equal to 5 mm. Average monthly rainfall for May, June, July, August, September and October has been computed to be 24, 20.8, 94.8, 53, 80.3 and 2.4 mm, respectively. The total rainfall and its distribution over the summer season are found to vary from year to year. For example, the total rainfall for the summer season (May to October) for 2005, 2006 and 2007 was recorded to be 380.5, 208.1 and 237.6 mm. Based on 3 years data average seasonal rainfall for the Gangotri Glacier was observed to be about 275.4 mm. For the first year 2005, it was computed maximum in the month of July, while for the year 2006 it was observed to be maximum in the month of August and during last year 2007 it was maximum in the month of September. Analysis of rainfall intensity shows that about 41% hourly rainfall events represented the rainfall intensity between 0.1 and 0.5 mm/hr, showing that mostly light intensity rain (drizzle type) occurs in the study area. Maximum rainfall events occurred either in the evening period or in the early morning.

The average daily maximum and minimum temperatures over the summer season were computed to be 14.9 °C and 3.7 °C, respectively, whereas average mean temperature was 9.3 °C. Diurnal variations in temperature indicate that generally maximum temperature is observed sometimes around 1400 hours while the minimum at the early morning. Mean monthly temperatures for May, June, July, August, September and October were 13.9, 16.3, 15.9, 15.7, 14.4 and 12.0°C, respectively, suggesting that July was the warmest month. Diurnal range of temperature was found to be higher in May and October due to relatively cloud free weather conditions, while it was lowest in August due to generally cloudy conditions. Results indicate that changes in minimum temperature are more significant than the changes in maximum temperature.

Analysis of wind data shows that on an average the daytime wind speeds are much stronger (4 times) than the nighttime winds. The records of wind direction show that during the daytime mostly wind blew from northwest. In the beginning and end of summer season, the relative humidity was about 69%, but during rainy months (June-September) it was about 82%. Average relative humidity over the different summer seasons varied between 77-83%, respectively, which shows reasonably high humidity. Generally, the duration of daily mean sunshine hours becomes maximum in May and minimum in August. On the seasonal scale daily mean sunshine hours were 5.5 hours. Monthly total pan evaporation was 81.5, 119.0, 92.7, 91.4, 81.6 and 44.4 mm for the month of May, June, July, August, September and October, respectively. The total pan evaporation during the summer season varied between 492 and 521 mm. Mean daily evaporation for the summer season as a whole is found to be 3.4 mm, which is comparable to the pan evaporation data observed at foothill station of the Himalayas. The combination of weather conditions like longer sunshine duration, little rainfall, low humidity and high wind speed could have attributed to higher evaporation in the month of May. On the other hand, weather conditions allowed for lower evaporation in October.

b) Hydrology and glacio-fluvio sediment transfer in the basin

The discharge showed increasing trend from May onward, reached to its highest value in July and then started reducing. The maximum and minimum daily mean discharge observed during study period was 8 to 239 m^3/s. The mean monthly discharge observed for May, June, July, August, September and October was 28.7, 56.3, 110.9, 95.8, 34.8 and 12.7 m^3/s, respectively. The distribution of observed runoff indicates maximum runoff in July (33.39%) followed by August (29.46%). These two months contribute about 63% to the total melt runoff. Almost similar trend of distribution of runoff is observed for all the years. The melt water yield during May, June, July, August, September and October was 0.12, 0.26, 0.52, 0.46, 0.16 and 0.04 m respectively. The melt water yield over the melt season is about 1.56 m. The strong storage characteristics of the Gangotri Glacier are reflected by the comparable magnitude of runoff observed during daytime and nighttime.

Suspended sediment concentration in the observed discharge was very high. More over it was very much variable over the melt season. Daily mean concentration varied between 34 to 11093 ppm. Mean monthly suspended sediment

concentration for May, June, July, August, September and October during the study period was 1628, 1753, 3262, 2231, 892 and 225 ppm respectively. Mean monthly total suspended sediment loads for May, June, July, August, September and October during the study period was found to be 162, 220, 1016, 603, 81 and 5×10^3 tonnes respectively.

c) Modelling of streamflow for the upper Bhagirathi river basin

A simple conceptual hydrological model was developed for simulating daily discharge from the Gangotri Glacier. The melting was computed using temperature index method. The routing of the melt water and rainfall-runoff was made using cascade reservoir approach. The model simulated daily streamflow satisfactorily for all the years, providing coefficient of determination (R^2) above 0.92, and average volume difference (D_v) about 1.8 %. There is need to test the model using a longer hydro meteorological database. To improve the model, a better representation of melt rate in the accumulation and ablation zones and its variation with time, has to be incorporated. Results also strengthen the view of strong storage and drainage characteristics of the glacier, which need further investigation.

d) Isotopic study of Melt Runoff

The isotopic signatures of stream water changes with time. As discharge start increases during the months of May and June, the enriched isotopic values are observed. The maximum isotopically enriched values observed in the stream water in the years 2004, 2005, 2006 and 2007 are -12.4‰, (May), -12.8‰ (June), -12.4‰ (April), -12.7‰ (June). This $d^{18}O$ values depleted in July and August and reaches to -15‰. This difference in isotopic value clearly indicates variation in contribution during different month or melting. These enriched values of river water are closed to $d^{18}O$ value of snow ranges in the month of May and June between -9.7‰ to -14.4‰ reveal that snow is the main source of stream discharge during summer months (May and June). After third week of June, $d^{18}O$ and dD values of stream water start depleting, which reveals that contribution of snow component is decreasing and ice melt component is increasing. As precipitation takes place in the months of July, August and September, the $d^{18}O$ and dD values of stream discharge become deplete sharply. Obviously the depleted value of rain generated runoff of depleted value.

Rain contributions to stream discharge have been computed using two component model. The maximum contribution has been found between 35% to 44% of the total discharge for the rainfall events that occurred during in month July or September in the year 2005. 14% to 15% contribution of precipitation in stream discharge has been found out of total stream discharge in these storm periods. If one compares with total melt discharge in ablation period of 2005, it comes about only 3% of the total discharge.

14.0 RECOMMENDATIONS & SUGGESTIONS FOR FURTHER WORKS

The snow & glacier melt contributes significantly to the Himalayan river systems particularly during the summer months. For hydropower generation and meeting the conservative demands, the long term sustainability of the snow & glacier melt is required. However, it is being reported world over that the glaciers are retreating because of climate change. In order to provide the explanations for various issues emerging from global warming, there is a need to take up some scientific studies of glaciers of Indian Himalayas. For such studies better data base of climatological & hydrological variables are required. .Gangotri Glacier is one of the largest glaciers of Himalayas and significantly contributes to the water resources of the region. Thus, there is a strong need for creating a larger hydro meteorological database for this glacier. So far Institute has monitored the hydrological and hydro-meteorological variables at Bhojbasa site of Gangotri glacier during the ablation season since last eight years. However, the data base created so far are not adequate to study the storage and melting characteristics of the Gangotri glacier considering the phenomenon of climate change. Thus, it is required to continue such monitoring activities in future as well on long term basis. For better understanding of the storage & melting characteristics of glaciers, it would be essential to monitor the climatic variables throughout the year. In this regard, an automatic weather station needs to be installed at the site to provide the climatological data at the desired time interval. At present, the river flow velocity is measured using the float method. Efforts must be made to procure an advanced velocity measuring instruments which should be very effective and useful under turbulent flow conditions. During this project, an effort has been made to apply the nuclear techniques for analyzing the water samples collected from the site. However, the applications of nuclear techniques are required to be further investigated with the different types of water & ice core samples in order to provide the better compositions of the environmental isotopes. This may be utilized for determining the contributions of different components of melt & rain in the flow. The Gangotri glacier is a debris covered glacier. Hence the river flow carries a huge amount of suspended sediments. At present water samples are taken near the bank of the river to analyze for the sediment concentrations. It does not reflect the distribution of the suspended sediment across the river cross sections. In order to have a better estimate of the suspended sediment, some mechanism needs to be evolved for taking the samples across the river cross section.

In this study hydrological modeling has been carried out using SNOWMOD model. The model computes the melt using temperature index method. In literature, the energy balance method is recommended for the computation of melt more accurately as compared to the temperature index method. For energy balance method, the data requirement is very much exhaustive. Hence, for the application of energy balance method, all the required variables need to be monitored. In this model snow & glacier melts are being computed together. Necessary modifications are need in the structure of the model to provide the snow & glacier melt contributions separately. The high resolution remote sensing data can be used to study the movement of snowline, which can provide the information on glacier ice exposing trend with time for better hydrological modelling. The glacier retreats are being measured by other organizations for Gangotri Glacier. Institute has the data of the runoff volumes of eight years for ablation seasons. A study must be undertaken correlating the retreat rates with the runoff volumes of the respective years.

15.0 PUBLICATIONS

Manohar Arora, R. D. Singh, Pratap Singh and Amit Kumar (2006): "Melt –Runoff Delaying Characteristics of Gangotri Glacier". Submitted to International Conference WEES-2009

Manohar Arora, R. D. Singh and Amit Kumar (2007): "Status of Climate change in India". National Seminar on "Threats: Global Warning to Global Warming". 31st March 2007 at KLDAV College Roorkee. Pp 29 – 44.

Manohar Arora, R. D Singh, Amit Kumar (2008): "Application of Snow Cover Estimation in Snow Melt Runoff Modeling": A case study of Gangotri glacier Basin Himalayas. Proceedings International Workshop on Snow, Ice, Glacier and Avalanches, 26-33.IIT, Bombay

Manohar Arora, R. D Singh, Amit Kumar (2008): "Estimates and analysis of suspended sediment from a glacierized basin in the Himalayas". National Snow Science Workshop 2008, (NSSW-2008).

Some more research papers are under preparation for submission to the International Journals.

16.0 REFERENCES

Bahadur, J. (1987).Himalayan water from snow, ice and glaciers.*Proc.1st National Water Convention* (vol II), CBIP, New Delhi, 1-32.

Bollasina,M.,Bertolani,L. and Tartari,G.(2002) .Meteorological observations at high altitude in the Khumbu Valley, Nepal Himalayas,1994-1999.Bull.Glaciol.Res.,**19**, 1-11.

Geological Survey of India. (1999) *Inventory of the Himalayan Glaciers.* Special Publication No.34; 165 pp.

Hodgkins, R.1996. Seasonal trend in suspended-sediment transport from an Arctic glacier, and implications for drainage-system structure. *Annals of Glaciology* 22: 147-151.

Hodgkins, R. (2001). Seasonal evolution of melt water generation, storage and discharge at a non-temperate glacier in Svalbard.*Hydrol. Processes*, **15**, 441-460

Kanwar Sain (1946). The Role of Glaciers and Snow Hydrology of Punjab Rivers,Central Board of Irrigation and Power, Aug 1945 Publn No.36 pp 144.,New Delhi,pp.29.

Karpov, A.P and S.S Kirmani (1968): The part of Indus valley in Himalayas-The largest known concentration of glacier, 49 annual meeting of the American Geophysical Union, pp 1-19.

Kasser, P. (1959). Der Einfluss von Gletscherruckgang und Gletschervostoss auf den wasserhaushalt, *Wasser und Energiewirt.* **6,155**-168

Kotlyakov, V.M. (1996). Variations of Snow and Ice in the past and at present on a global and regional scale. IHP-V. *Technical Documents in Hydrology No.1* UNESCO,Paris. Krenek, L and Bhawani, V.1945.Recent and Past glaciation of Lahul, Indian. *Geog.J.*20 (3), 93-102.

Kotlyakov, V.M. and Lebedeva, I.M. (1998). Melting and Evaporation of Glacier Systems in Hindukush-Himalayan Region and their Possible Changes as a result of Global Warming ,Proc.International Conf. on Ecohydrology of High Mountain Areas,Kathmandu,Nepal,24-28 March 1996,ICIMOD,pp 367-375.

Kulkarni, A.V. (1989) 'Application of remote sensing for glacier inventory and mass balance' Proc. Of national symposium on engineering Application of Remote Sensing and Recent Advances, Indore, pp. 26-30.

Lang, H. (1973): Variations in the relation between glacier discharge and meteorological elements. Symposium on the Hydrology of Glacier (Cambridge, UK, 1969), 79-84. IAHS Publ.no.95.

Lang, H. and G. Dayer (1985): Switzerland case study: water supply in proc: Techniques for prediction on Runoff Glacierized Areas. IAHS Publ. no. 149, pp 45-57.

Meier, M.F (1973): Evalution of ERTS imagery for mapping of changes of snow cover on land and on glaciers, Symposium on significant results obtained from the Earth Resources Technology Satellite 1,New arrollton,Maryland,NASA,Vol.1,pp.863-875.

Meier, M.F. and Roots, E.F. (1982). 'Glaciers as a Water Resource', Nature and Resources, Vol. xviii No. 1 July-Sept, pp. 7-14.

Menzies, J. (1995). Hydrology of glaciers. In Modern Glacial Environments, Processes, Dynamics and Sediments . Menzies, J. (ED.), Butterworth-Heinemann, London, pp.621.

Milller, K.J. (ed) (1994) International Karakoram Project (IKP), Vol. I and II, Cambridge University Press.

Muller. (1970). Inventory of glaciers in Mount Everest region, UNESCO, Technical Papers in Hydrology.

Nainwal,H.C.,A.K.Naithani,D.Kumar,B.D.S.Nagi andC.Prasad(2003): Glacial morphology of the Gangotri glaciers in Garhwal Himalaya , Uttaranchal ,Abstract Volume of the Workshop on Gangotri Glacier, 26-28 March 2003, Geological Survey of India , Lucknow,pp26-27.

Rothlisberger, H. 1972. Water pressure in intra-and subglacial channels, J. Glaiol., 11, 177-203.

Rothlisberger, H and Lang, H. 1987. Glacial hydrology. In: Glacio-Fluvial Sediment Transport- An Alpine Perspective. Gurnell, A.M. and Clark, M.J. (Eds). John Wiley, Chichester, U.K., 207-284.

Sharma, M.C. and Owen, L.A. (1996) 'Quaternary glacial history of NW Garhwal, Central Himalayas' Quaternary Science Reviews 15, pp. 335-65.

Sharp, R.P. (1988): Living Ice: Understanding Glacier and Glaciation, Cambridge University press Cambridge,pp 225.

Stenborg, T. (1970). Delay of runoff from a glacier basin. *Geogr.Ann.* **52A** (1), 1-30.

Tangri, A.K.(2000) . Integration of remote sensing data with conventional methodologies in snowmelt runoff modeling in Bhagirathi river basin-U.P.Himalaya, Remote Sensing Application Centre, U.P., India, pp601.

Tangborn, W.V., Krimmel, R.M and Meier, M.F. (1975): A comparison of glacier mass balance by glaciological hydrological and mapping method, South Cascade Glacier, Washington.In: Proceeding of the snow and ice symposium, Moscow, August 1971.IAHS publ., 104,185-196.

Vohra, C.P.(1978) Glacier resources of the Himalayas and their importance to environmental studies, Proceedings of National seminar of resources development in the Himalayan region, N.Delhi,April 10-13,pp 441-459

Vohra, C.P. (1980): Some problems of glacier inventory in the Himalayas. In: *World*

Glacier Inventory (Proc. Riederalp Workshop, September 1978), 67-74.IAHS Publ.no.126.

Young, G.J. and Hewitt, H. (1990): Hydrology research in the upper Indus basin, Karakoram Himalaya, Pakistan.

ACKNOWLEDGEMENTS

Principal Investigator (PI) of the Gangotri Glacier project is very grateful to the Department of Science and Technology (DST), Govt. of India, New Delhi, for providing funds to carry out the hydrological study on the Gangotri Glacier. The technical support and suggestions helped in the successful completion of the project. Results of the project were presented before Programme Advisory and Monitoring Committee for Himalayan Glaciology (PAMC-HG) of DST from time to time. Their valuable suggestions improved the output of the technical study. PI is thankful to all the PAMC members.

Director, National Institute of Hydrology took keen interest in planning, management and execution of the project and provided constant encouragement throughout the period of the project. His guidance and continuous support is gratefully accredited. Dr. R. D. Singh, Scientist F and Head, Surface Water Hydrology Division guided in execution of the project. Technical support provided by Shri. R. D. Singh is very much acknowledged. Dr Bhishm Kumar, Scientist F and Head, Hydrological Investigation Division was kind enough in granting permission for isotope analysis in the Nuclear Laboratory. Shri S. P. Rai Scientist C has carried out the isotope analysis and was a very active member of the project team.

PI is also thankful to the Chairman and members of Technical Advisory Committee (TAC) and Surface Water Working Group of NIH, Scientists of NIH who always actively participated in technical discussions related with Gangotri Glacier studies. Thanks are also due to the scientific staff of the Soil Water Laboratory of NIH for their help in analyzing the suspended sediment data.

Shri Naresh Kumar, PRA, Shri Yatveer Singh, SRA, Shri N. K. Bhatnagar, SRA, Shri R. K. Nema, SRA, and Shri Ved Pal, Technician assisted in field investigations and analysis of the data. The project staff, Shri Amit Kumar, Project Officer, Shri Peeyush Kumar Sharma, Project Assistant also participated in the project related field activities and analysis. They all worked very hard as team members of the project and all of them deserve thanks for their keen interest in the work.

April 30, 2008
Roorkee

(Manohar Arora)
Principal Investigator

Appendix - I
DETAILS OF THE PROJECT

Title of the Project	:	Seasonal characterization of ablation, storage and drainage of melt runoff and simulation of streamflow for the Gangotri Glacier.
Principal Investigator	:	Dr. Manohar Arora, Scientist B, Surface Water Hydrology Division, National Institute of Hydrology, Roorkee
Co-Principal Investigator	:	Dr. S. P. Rai, Scientist C, National Institute of Hydrology, Roorkee
Sponsoring Authority	:	Department of Science and Technology, Govt. of India, New Delhi. (DST Ref: Sanction Letter No. ESS/91/05/2002)
Project Duration	:	3 years (January 2005 – 31st March, 2008)
Main Scope of the Work	:	Collection of meteorological and hydrological data for the Gangotri Glacier and development of a hydrological model for simulating the glacier melt runoff. Study of the meltwater storage and drainage characteriscics of the glacier. Identification of different component of runoff using isotopic method. Estimation of suspended sediment concentration and load.
Total Cost of the Project	:	Rs. 21, 52,000/-

Table 3(a): General statistics of daily air temperature (°C), Rainfall (in mm), discharge (in m^3/s), suspended sediment concentration (in ppm), Evaporation (in mm) and wind speed (in km/hr) for the summer 2005 on monthly basis.

Period	Variable	Maximum	Minimum	Mean	STD	CV
May, 2005	Temperature	7.5	2.5	5.3	1.22	0.23
	Rainfall	11.4	0.0	1.4	2.82	2.01
	Discharge	27.7	8.1	13.8	5.65	0.40
	SSC	4570	110	852.5	1145.7	1.34
	Relative Humidity	89	43.0	67	13.51	0.20
	Sunshine Hours	10.41	0.0	5.48	2.90	0.52
	Evaporation	5.3	0.9	2.8	1.01	0.36
	Wind speed	12.4	3.3	8.1	2.41	0.29
June, 2005	Temperature	16.3	5.0	9.8	2.74	0.28
	Rainfall	12.0	0.0	0.9	2.47	2.74
	Discharge	145.2	8.1	57.6	45.97	0.79
	SSC	6030	120	1631	1479.9	0.90
	Relative Humidity	95	47	72	12.23	0.17
	Sunshine Hours	10.72	0.0	5.91	2.93	0.49
	Evaporation	7.1	2	4.27	1.18	0.27
	Wind speed	10.6	4.5	7.4	1.38	0.18
July., 2005	Temperature	13.7	5.8	10.4	1.66	0.16
	Rainfall	62.6	0.0	5.0	12.4	2.48
	Discharge	166.8	76.5	110.8	25.72	0.23
	SSC	5340	1050	2321.6	1074.2	0.46
	Relative Humidity	98	81	93	4.79	0.05
	Sunshine Hours	10.17	0.0	3.45	3.09	0.89
	Evaporation	5.1	0.0	2.70	1.50	0.55
	Wind speed	8.5	0.7	6.2	1.94	0.31
Aug., 2005	Temperature	14.0	8.5	10.7	1.39	0.13
	Rainfall	9.2	0.0	0.8	1.91	2.38
	Discharge	238.5	86.6	132.0	39.60	0.3
	SSC	4880	670	2032.5	975.14	0.47
	Relative Humidity	98	72	86	7.15	0.08
	Sunshine Hours	9.75	0.23	6.44	3.04	0.47
	Evaporation	5.2	0.7	3.44	1.15	0.33
	Wind speed	8.3	3.8	6.5	1.09	0.16
Sept., 2005	Temperature	12.7	2.9	8.9	2.69	0.30
	Rainfall	43.6	0.0	4.8	10.59	2.20
	Discharge	112.6	17.7	57.9	36.15	0.62
	SSC	1900	160	621.5	505.4	0.81
	Relative Humidity	94	58.0	78	9.97	0.12
	Sunshine Hours	9.0	0.0	4.29	3.30	0.76
	Evaporation	4.80	0.0	2.37	1.48	0.62
	Wind speed	7.6	0.3	5.1	1.87	0.36

Oct., 2005	Temperature	8.3	1.8	5.5	2.04	0.37
	Rainfall	0.0	0.0	0.0	0.0	0.0
	Discharge	18.3	9.8	13.6	2.04	0.15
	SSC	60	20	24	11.2	0.46
	Relative Humidity	76	45	64	9.73	0.15
	Sunshine Hours	8.07	4.72	6.95	1.04	0.15
	Evaporation	4	1.7	2.84	0.69	0.24
	Wind speed	11.1	4.5	6.6	1.71	0.25
May to October 2005	Temperature	16.3	1.8	8.61	2.97	0.3
	Rainfall	62.6	0.0	2.14	7.07	3.3
	Discharge	238.5	8.1	69.18	54.29	0.8
	SSC	6030	20	1380.6	1270.6	0.9
	Relative Humidity	98.3	42.6	77.47	13.97	0.2
	Sunshine Hours	10.7	0.0	5.33	3.10	0.6
	Evaporation	7.1	0.0	3.09	1.38	0.4
	Wind speed	12.4	0.3	6.60	1.98	0.3

Table 3 (b): General statistics of daily air temperature (°C), Rainfall (in mm), discharge (in m^3/s), suspended sediment concentration (in ppm), Evaporation (in mm) and wind speed (in km/hr) for the summer 2006 on monthly basis.

Period	Variable	Maximum	Minimum	Mean	STD	CV
May,2006	Temperature	12.25	5.05	9.433	1.773	0.18
	Rainfall	0.0	0.0	0.0	0.0	0.0
	Discharge	92.66	18.65	56.53	22.70	0.40
	SSC	102.00	1.90	2821.3	2123.3	0.75
	Relative Humidity	85.50	48.00	69.95	9.84	0.14
	Sunshine Hours	9.7	0.8	6.16	2.61	0.42
	Evaporation	6.0	1.5	4.53	1.91	0.26
	Wind speed	9.85	5.29	7.94	1.31	0.16
June,2006	Temperature	13.5	9.5	9.6	2.4	0.2
	Rainfall	8.6	0.0	0.9	2.0	2.2
	Discharge	91.9	33.2	58.0	17.1	0.3
	SSC	4560.0	220.0	1250.3	1078.0	0.9
	Relative Humidity	92.8	54.0	75.6	9.7	0.1
	Sunshine Hours	9.3	0.1	5.1	2.9	0.6
	Evaporation	6.0	0.2	3.6	1.7	0.5
	Wind speed	9.1	3.3	6.3	1.4	0.2
July,2006	Temperature	15.4	8.9	11.8	1.7	0.1
	Rainfall	10.5	0	2.4	3.2	1.3
	Discharge	177.6	86.7	121.6	21.8	0.2
	SSC	8590.0	2180.0	4293.5	1501.2	0.3
	Relative Humidity	97.2	65.8	85.3	8.9	0.1
	Sunshine Hours	10.2	0.1	4.6	3.2	0.7
	Evaporation	5.6	0.6	2.8	1.6	0.6
	Wind speed	10.2	2.9	5.8	1.6	0.3
August,2006	Temperature	12.25	6.0	10.68	1.30	0.12
	Rainfall	23.60	0	2.77	4.48	1.62
	Discharge	105.23	28.15	84.61	16.47	0.19
	SSC	2670.0	110.0	1707.10	604.24	0.35
	Relative Humidity	96.88	73.88	87.72	5.03	0.06
	Sunshine Hours	8.75	0.92	3.88	2.28	0.59
	Evaporation	5.10	0.30	2.28	1.15	0.51
	Wind speed	7.60	3.26	5.75	1.13	0.20
September ,2006	Temperature	11.70	6.25	9.11	1.55	0.17
	Rainfall	6070	0	0.49	1.34	2.73
	Discharge	47.98	17.80	29.12	9.71	0.33
	SSC	840.0	300.0	529.33	161.41	0.30
	Relative Humidity	94.08	58.67	77.52	9.03	0.12
	Sunshine Hours	8.92	0.50	6.51	2.12	0.33
	Evaporation	4.40	0.20	3.13	1.04	0.33
	Wind speed	7.52	3.63	6.16	0.83	0.14

October,2006	Temperature	8.75	2.7	6.47	1.42	0.21
	Rainfall	3	0	0.29	0.84	2.88
	Discharge	22.48	17.32	20.97	1.54	0.07
	SSC	340	180	292.66	47.12	0.16
	Relative Humidity	74.95	56.95	64.85	5.56	0.08
	Sunshine Hours	8.16	5.66	7.24	0.54	0.07
	Evaporation	5	1.7	3.21	0.97	0.30
	Wind speed	9.32	3.86	6.80	1.19	0.17
May to October 2006	Temperature	15.4	2.7	9.59	2.30	.2
	Rainfall	23.6	0	1.25	2.79	2.2
	Discharge	177.6	16.8	65.66	37.68	0.6
	SSC	10200.0	110.0	1971.79	1831.65	0.9
	Relative Humidity	97.2	48.0	78.05	11.20	0.1
	Sunshine Hours	10.2	0.1	5.43	2.72	0.5
	Evaporation	6.0	0.2	3.20	1.48	0.5
	Wind speed	10.2	2.9	6.40	1.47	0.2

Table 3 (c): General statistics of daily air temperature (°C), Rainfall (in mm), discharge (in m^3/s), suspended sediment concentration (in ppm), Evaporation (in mm) and wind speed (in km/hr) for the summer 2007 on monthly basis.

Period	Variable	Maximum	Minimum	Mean	STD	CV
May, 2007	Temperature	11.25	0.50	7.52	2.42	0.32
	Rainfall	22.6	0.0	1.5	4.5	3.03
	Discharge	28.8	12.8	19.7	5.14	0.26
	SSC	1956.4	697.9	1201.5	358.4	0.29
	Relative Humidity	93.4	47.5	72.3	9.69	0.13
	Sunshine Hours	9.0	0.0	5.4	2.38	0.44
	Evaporation	5	0.4	3.13	1.3	0.42
	Wind speed	10.8	4.7	7.5	1.44	0.19
June, 2007	Temperature	14.10	6.50	10.86	2.42	0.22
	Rainfall	7.3	0.0	0.6	1.52	2.53
	Discharge	114.4	14.9	53.4	30.63	0.57
	SSC	6095.8	220.0	2214.7	1425.8	0.64
	Relative Humidity	94.9	55.4	76.4	10.31	0.13
	Sunshine Hours	10.2	0.0	6.4	2.91	0.45
	Evaporation	6.8	1.2	4.37	1.26	0.29
	Wind speed	10.0	5.3	7.9	0.99	0.12
July, 2007	Temperature	13.35	6.20	11.21	1.53	0.13
	Rainfall	13.0	0.0	1.6	2.79	1.7
	Discharge	136.3	60.7	100.4	17.9	0.17
	SSC	5138.3	1562.7	3005.9	864.03	0.28
	Relative Humidity	-	-	-	-	-
	Sunshine Hours	10.1	0.0	5.5	3.02	0.54
	Evaporation	8.8	0.8	3.6	1.7	0.47
	Wind speed	8.9	4.2	6.9	1.27	0.18
Aug., 2007	Temperature	13.50	8.75	11.36	1.43	0.12
	Rainfall	8.10	0.0	1.59	2.28.	1.43
	Discharge	149.0	12.1	70.8	32.13	0.45
	SSC	5286.6	1053.9	2799.2	1127.5	0.40
	Relative Humidity	100.0	66.7	90.7	7.08	0.07
	Sunshine Hours	8.5	0.0	4.1	3.16	0.77
	Evaporation	5.1	0.6	3.18	1.33	0.42
	Wind speed	9.3	2.8	6.1	1.82	0.29
Sept., 2007	Temperature	12.0	3.25	8.83	2.49	0.28
	Rainfall	30.60	0.0	2.79	7.08	2.53
	Discharge	38.2	7.9	17.5	9.16	0.52
	SSC	2513.2	806.8	1372.6	407.8	0.29
	Relative Humidity	96.3	50.9	81.8	9.55	0.11
	Sunshine Hours	8.5	0.0	5.0	2.63	0.52
	Evaporation	5.3	0.0	2.66	1.23	0.46
	Wind speed	10.5	3.8	6.3	1.36	0.21

Oct., 2007	Temperature	6.50	3.75	5.07	0.88	0.17
	Rainfall	2.20	0.0	0.17	0.61	3.58
	Discharge	8.4	8.4	8.4	0.0	0.0
	SSC	-	-	-	-	-
	Relative Humidity	92.9	41.5	66.5	13.06	0.19
	Sunshine Hours	8.0	1.0	6.2	2.18	0.35
	Evaporation	4.1	0.4	2.33	1.08	0.46
	Wind speed	14.3	5.3	8.6	2.44	0.28
May to October 2007	Temperature	14.1	0.5	9.65	2.85	0.3
	Rainfall	30.6	0.0	1.48	3.98	2.7
	Discharge	149.0	7.9	50.22	38.89	0.8
	SSC	6095.8	220.0	2172.68	1184.52	0.5
	Relative Humidity	100	41.5	79.07	12.25	0.2
	Sunshine Hours	10.2	0.0	2.87	2.87	0.5
	Evaporation	8.8	0.0	1.48	1.48	0.4
	Wind speed	14.3	2.8	7.04	1.67	0.2